DEVELOPMENT OF ULTRADEFORMABLE LIPID VESICLES COMPRISING POLYOXYETHYLENE OLEYL ETHER FOR TARGETED DRUG DELIVERY ACROSS THE SKIN

D i s s e r t a t i o n

zur Erlangung des akademischen Grades
Doctor rerum naturalium (Dr. rer. nat.)

vorgelegt der

Naturwissenschaftlichen Fakultät I - Biowissenschaften
der Martin-Luther-Universität Halle-Wittenberg

von

Herrn Christian Ulrich Wachter
geboren am 22.04.1977 in Ravensburg

Gutachter /in

1. Prof. Dr. Dr. Reinhard Neubert, Martin-Luther-Universität Halle-Wittenberg

2. Prof. Dr. Karsten Mäder, Martin-Luther-Universität Halle-Wittenberg

3. Prof. Dr. Gregor Cevc, IDEA AG München

Halle (Saale), 15. Oktober 2008

urn:nbn:de:gbv:3-000014488
[http://nbn-resolving.de/urn/resolver.pl?urn=nbn%3Ade%3Agbv%3A3-000014488]

Erklärung

Hiermit versichere ich, dass ich die vorliegende Arbeit selbständig und ohne fremde Hilfe verfasst, keine anderen als die von mir angegebenen Quellen und Hilfsmittel verwendet und die den benutzen Werken wörtlich oder inhaltlich entnommenen Stellen als solche kenntlich gemacht habe.

Halle (Saale), Mai 2008

Christian Wachter

Curriculum vitae

Name:	Christian Ulrich Wachter	
Geburtstag:	22. April 1977	
Geburtsort:	Ravensburg, Deutschland	
Familienstand:	verheiratet	
Bildungsweg:	1987 – 1996	Allgemeine Hochschulreife Welfengymnasium, Ravensburg
	1997 – 2002	Studium der Pharmazie Albert-Ludwigs-Universität, Freiburg
	2002	Pharmaziepraktikum in der Pharma-Industrie IDEA AG, München
	2002 – 2003	Pharmaziepraktikum in der Offizin-Apotheke Isartorapotheke, München
	2003	Approbation zum Apotheker Regierungspräsidium Stuttgart
	2003 – 2008	Promotionsstudium IDEA AG, München und Martin-Luther-Universität, Halle-Wittenberg
Berufliche Tätigkeiten:	2003 – 2007	Apothekenleitung in Vertretung Isartorapotheke, München
	2003 – 03/2008	Wissenschaftlicher Mitarbeiter Basic Research and Formulation Development IDEA AG, München
	seit 04/2008	Manager Pharmaceutical Production IDEA AG, München

Halle (Saale), Mai 2008

Christian Wachter

Danksagung

Mein besonderer Dank gilt meinen Betreuern Prof. Dr. Gregor Cevc von der IDEA AG in München und Prof. Dr. Dr. Reinhard Neubert vom Institut für Pharmazie der Martin-Luther-Universität Halle-Wittenberg.
Prof. Dr. Gregor Cevc möchte ich hierbei für die Bereitstellung des Themas und für die interessante Aufgabenstellung dieser Dissertation danken. Die intensiven und konstruktiven Diskussionen rund um diese Arbeit und seine Geduld und Bereitschaft mir mein pharmazeutisches Wissen mit biophysikalischen Themen zu erweitern werden mir dankbar in Erinnerung bleiben.
Prof. Dr. Dr. Reinhard Neubert danke ich für die universitäre Betreuung und pharmazeutische Förderung dieser extern durchgeführten Promotionsarbeit.

Der IDEA AG bin ich zu tiefstem Dank verpflichtet, sowohl für die finanzielle Unterstützung als auch für die Förderung meiner wissenschaftlichen Arbeit durch die Möglichkeit zur Teilnahme an nationalen und internationalen Kongressen und Fortbildungen.

Den gesamten Kollegen der IDEA AG danke ich für das wundervolle Arbeitsklima, die hervorragende Zusammenarbeit und die vielen Diskussionen über wissenschaftliche und weniger wissenschaftliche Themen, die meine Promotionszeit zu einem besonderen Lebensabschnitt machten.
Herausheben möchte ich dabei meinen Dank an Dr. Ulrich Vierl für seine Unterstützung bei mathematischen und biophysikalischen Fragestellungen, deren Lösung einen maßgeblichen Anteil zum Gelingen der vorliegenden Arbeit beitrug.

Ein besonderer Dank gebührt meinen Eltern, die mich während des Studiums und der Doktorarbeit finanziell und mit viel Verständnis unterstützen.

Der größte Dank gebührt jedoch meiner Frau Sibylle, die während der Erstellung dieser Dissertation sowohl in guten als auch schwierigen Zeiten immer die richtigen Worte fand und mir dadurch unendlich viel Kraft und Unterstützung gab.

1. INTRODUCTION AND OBJECTIVES

Controlled drug delivery into a body is one of the major topics in pharmaceutical research. The pathway through the skin, for example, is a predestined route for the drugs, which undergo degradation and metabolism in the gastro-intestinal tract or the liver after an oral application, or when only a local treatment of dermal and subdermal diseases is desired.

The development of such transdermal pharmaceutical products or applications must consider the skin structure and functionality. The advantages of the skin as an easily accessible organ with a limited metabolic activity is counter-balanced by it's nearly, however protecting, impermeability. Skin permeation, penetration, or poration (Cevc 1997) are therefore key factors for new transdermal drug delivery systems to pass this barrier.

Skin permeability can be influenced chemically by permeation enhancers (Trommer et al. 2006) and microemulsions (Heuschkel et al. 2007), which improve and accelerate the diffusion of drug substances across the skin. Enhanced drug transport can also be achieved by penetrating the skin with acoustic sonophoresis (Bommannan et al. 1992), radio frequency (RF) ablation (Levin et al. 2005), iontophoresis (Singh et al. 1989), electroporation (Prausnitz et al. 1993) or various impact devices (Arora et al. 2007), which typically create long-lasting pores (1 - 100 µm) through the skin. An alternative and gentler skin penetration method is the administration of drug loaded ultradeformable vesicles (Cevc et al. 1998; Honeywell-Nguyen et al. 2002; Cevc et al. 2003b).

The following introducing sections first summarises common knowledge on the skin structure and the possible pathways through the barrier followed by an outline of different amphiphiles forming bilayer membranes and micelles. The present thesis deals with such aggregates, in particular with ultradeformable lipid bilayer vesicles and the development of the latter, based on the bilayer membrane forming lipid soybean phosphatidylcholine and the potentially membrane softening amphiphile polyoxyethylene (20) oleyl ether. The introducing section closes with an overview of the objectives and structure of this thesis.

1.1. The human skin

The skin is the biggest human organ and a protecting barrier that keeps water in and noxious substances out of a body (Hadgraft 2001). The skin controls, together with the kidney, the body's water-electrolyte balance, regulates the body temperature, and represents one of the five human sense organs (Casey 2002).

The skin is composed of three anatomically distinct layers: the epidermis, the dermis and the subcutis (Neubert et al. 2001). The overlying epidermis can be subdivided into four layers: the viable stratum basale, stratum spinosum, stratum granulosum and the biologically dead superficial stratum corneum, which all contain keratinocytes (right graph in Figure 1).

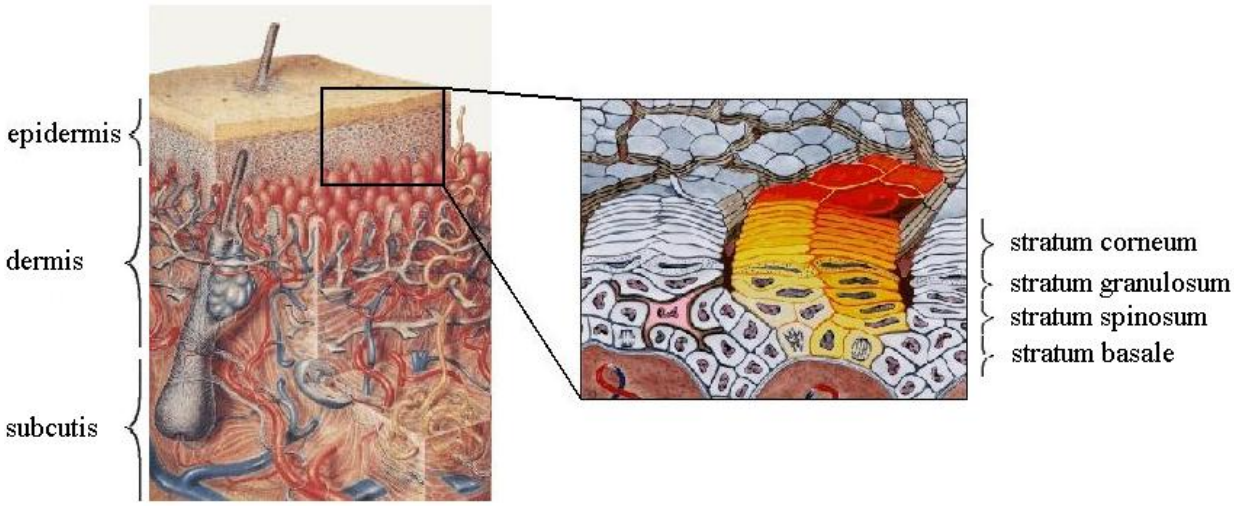

Figure 1: Illustration of the mammalian skin (left) with a magnification of the epidermis (right). (adapted and modified from Cevc et al. (2003b))

The epidermis is a constantly self-renewing tissue. Upon leaving the basal layer where they originate, the keratinocytes in the epidermis start to differentiate in the process of keratinisation. During migration through the stratum spinosum and stratum granulosum, keratinocytes undergo a number of changes in both structure and composition, finally resulting in anucleated corneocytes filled with keratin and surrounded by an envelope of proteins and lipids (Bouwstra et al. 2003). Corneocytes appear like flat "bricks" in the stratum corneum, where they are held together by desmosomes and lipidic "mortar" (Elias et al. 1987). Both components contribute to the protective barrier function of the stratum corneum, which is not a homogeneous wall, however, but rather comprises distinct clusters separated by less well sealed "gorges" (Schätzlein et al. 1998).

Corneocytes protect the skin against external chemical and physical stress whereas intercellular lipidic matrix seals their contacts preventing transdermal water loss and uptake of noxious extracorporeal substances. This biological measure of precaution is a challenge in the development of transdermal drug delivery systems. In other words, epicutaneous pharmaceutical products or application techniques have to focus on all the possible transdermal routes to achieve an effective drug transport through the skin barrier.

The core of the skin barrier is the stratum corneum, which is pretty thin (5 - 8 µm) (Iizuka 1994), but very tight. The layer forming corneocytes are flat and closely packed into stacks of about 30 cells per column. Groups of 3 to 7 of such columns form a cluster separated by a 4 – 6 µm wide and deep cleft, which shortens to a few tens nm at the lipid-filled cleft bottom (Cevc et al. 2003b). Skin lipids in these clefts and in the intercellular lipid matrix are the main pathways for spontaneous drug migration across the skin (Loth 1986; 1987; Bouwstra et al. 2003; Cevc et al. 2003b; Hadgraft 2004); drug transport through skin appendages, such as hair follicles and sweat glands acting as shunts, is usually negligible because such shunts only occupy ~ 0.1 % of the total skin surface (Moser et al. 2001). Transcellular drug transport is also small due to the impermeability of the cornified cell envelope (Bouwstra et al. 2003).

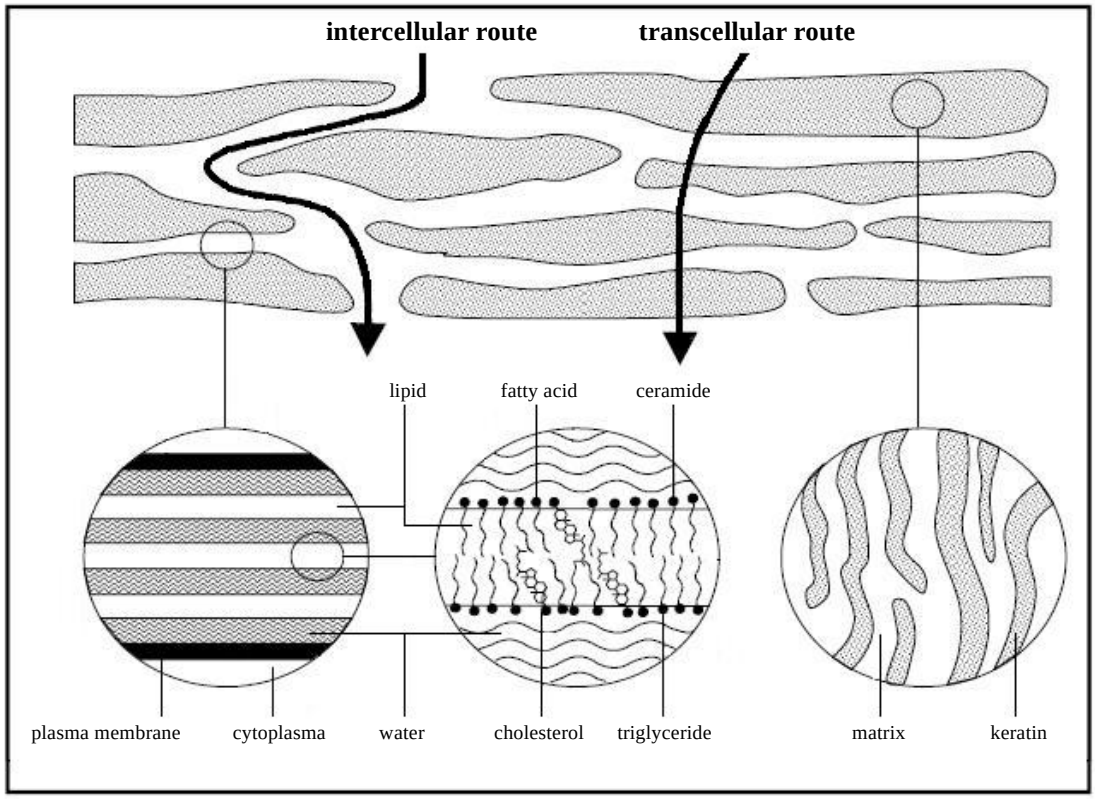

Figure 2: Intercellular and transcellular pathways for drugs and drug transport systems through the stratum corneum. (adapted and modified from Barry et al. (1987))

Figure 2 illustrates schematically the orientation of intercellular lipid matrix, which is composed of 9, mainly saturated, ceramides (~ 50 %), saturated fatty acids (~ 15 %), cholesterol (~ 35 %), and small amounts of triglycerides, cholesterol sulphate, and cholesterol esters (Wartewig et al. 2007). Skin lipids are aligned parallel to the adjacent cell membranes and are in many places in crystalline phase (Bouwstra et al. 1991). Such multilamellar lipid crystals are adjoined by less well structured lipids, however, which are in a fluid phase (Bouwstra et al. 2003). Lipophilic or hydrophilic drug molecules therefore typically diffuse within the lamellar layers through the disordered hydrophobic lipid chains region or via the aqueous pathway, respectively (Trommer et al. 2006). The hydrophilic route is normally unimportant owing to the narrowness of hydrophilic channels between lipids having a pore diameter d_p < 0.7 nm (Ruddy et al. 1992; Yoshida et al. 1993). However, such channels can be widened to ~ 20 nm using external forces, such as vesicular pressure (Cevc 1996) or transdermal electrical potential (Aguilella et al. 1994).

1.2. Amphiphilic molecules forming bilayers membranes and micelles

Amphiphilic or amphiphatic molecules (amphis (Greek) = both) possess both hydrophilic and hydrophobic regions, and therefore dual properties. The hydrophobicity is typically mediated by one or more hydrocarbon segments or chains whereas the hydrophilicity stems from uncharged polar or charged groups.

Amphiphats, such as most drugs, negative, positive, or non-ionic surfactants, long chain alcohols, fatty acids, phospholipids, glycolipids, steroids, etc. can be categorized by their hydrophile-lipophile balance, *HLB*, (Griffin 1949; Davies 1957). This simple ratio is a helpful starting information for gauging utility of different amphiphiles. Excipients with a *HLB* = 3 - 6 can be used as water in oil (W/O) emulsifiers. In contrast, an O/W emulsion is obtained by using emulsifiers with *HLB* = 8 – 18, dependent on total oil and water quantities. Other categories are: wetting agents (*HLB* = 7 – 9), detergents (*HLB* = 13 – 15), and solubilisers (*HLB* = 15 – 18) (Bauer et al. 2006).

Amphiphilic molecules associate into colloidal aggregates above a certain threshold concentration, the so-called critical aggregate concentration, in presence of either polar or non-polar “solvents”. One part of the amphiphat is then in direct contact with the surrounding medium, whereas the other part is sheltered in the aggregate inside. In case of a polar medium, like water, the hydrophobic moieties are embedded inside the aggregate surrounded by the hydrophilic parts, which are in contact with water.

Aggregate shapes are diversified and are affected by amphiphiles molecular geometry (Israelachvili 1985). Figure 3 shows the three basic molecular shapes: a cone, a cylinder and an inverted cone. The different effective molecular geometries are caused by opposing repulsive forces (Tanford 1973) within an interface, and can be explained with the law of the lever. If one assigns the hydrophilic headgroup repulsion to be the load and the hydrophobic chain repulsion to be the effort, the location of the fulcrum in terms of the interfacial attraction then defines the final molecular shape and consequentially the aggregate shape (cf. Figure 3).

A cylindrical molecular shape is thus obtained when repulsion between polar and apolar parts of the molecule are comparable in strength and the fulcrum is located in the middle of the molecule. If one kind of repulsion is excessive, the fulcrum is shifted towards the stronger force, resulting in a cone or inverted cone for more hydrophilic or more lipophilic amphiphats, respectively.

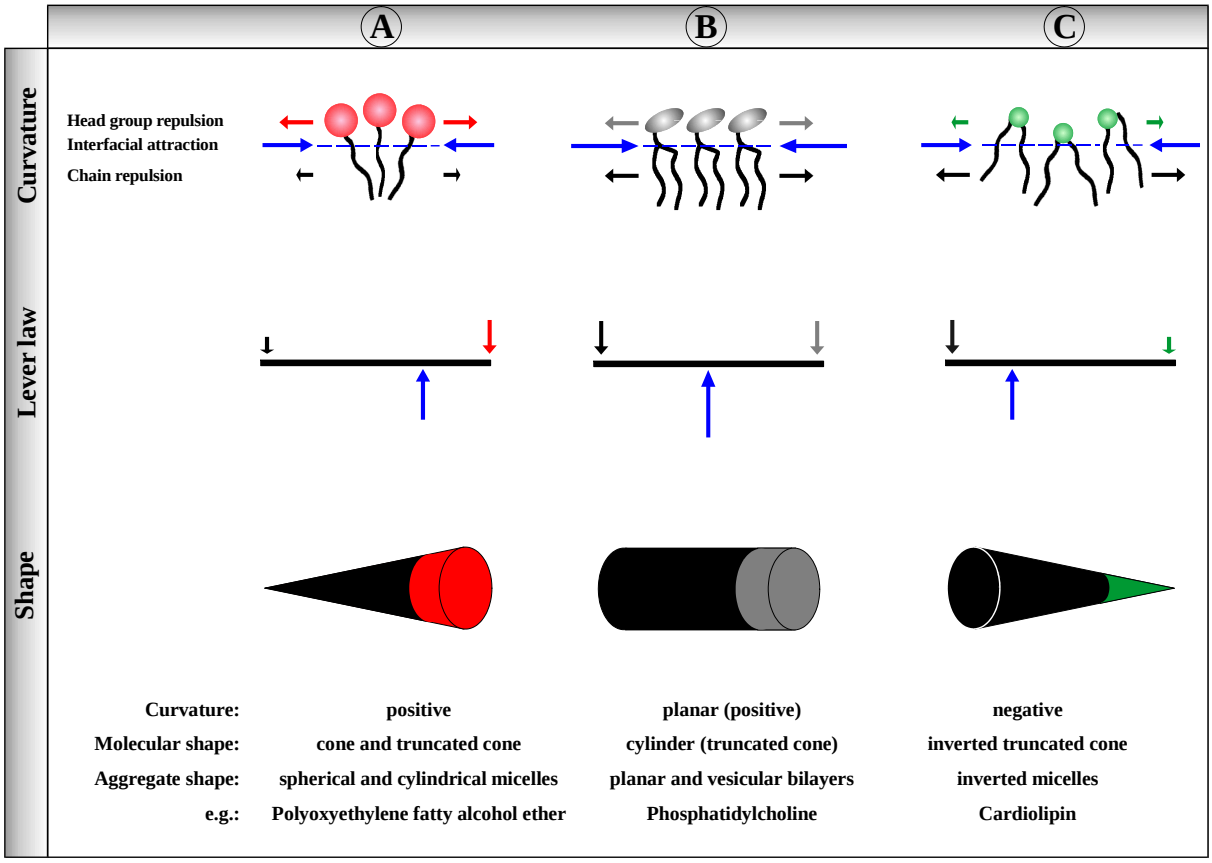

Figure 3: The law of the lever and geometric aspects of different amphiphilic molecules define their molecular and aggregate shape.

Israelachvili and colleagues (1977; 1985) showed that molecular and aggregate structures can be predicted reasonably well in terms of the packing parameter $v/(a_0 \cdot l_c)$, v being the hydrocarbon volume, a_0 the optimum surface area per molecule, and l_c the critical hydrocarbon chain length. An amphiphile with a packing parameter of $v/(a_0 \cdot l_c) < 0.5$ possesses a cone-shaped structure and tends to form spherical or cylindrical micelle aggregates. Cylindrical molecules have $v/(a_0\ l_c) \approx 1$ and spontaneously form planar or vesicular bilayers. Inverted micelle aggregates are the result of inverted cone-shaped amphiphiles with $v/(a_0\ l_c) > 1$. However, one has to keep in mind that the molecular shape of an amphiphile is influenced by hydrocarbon chain unsaturation, temperature, bulk electrolyte concentration, *pH*, etc. (Israelachvili 1985), meaning that one has to reconsider molecular shape after any external changes and modifications.

Phosphatidylcholines are a class of phospholipids with a zwitterionic headgroup composed of a negative phosphate group esterified with glycerol and a positive choline group. The glycerol moiety is further esterified with two saturated and/or unsaturated fatty acid chains which form the lipophilic molecule part. The resulting packing parameter $v/(a_0\ l_c) \approx 1$ suggests that phosphatidylcholines should form bilayer aggregates above the critical aggregate concentration, being ~ 10^{-7} - 10^{-9} M for diacyl-phosphatidylcholines (Marsh et al. 1986).

Combination of such molecules with a packing parameter $v/(a_0\ l_c) \approx 1$ and of amphiphiles with a packing parameter $v/(a_0\ l_c) < 0.5$ changes the mixed aggregate properties and can improve the membrane flexibility (Cevc et al. 2003b; Ly et al. 2004; Zhou et al. 2005). It can also reduce aggregate stability, however (Touitou et al. 2000; Simoes et al. 2005).

Figure 4 illustrates the different vesicular aggregates involving phosphatidylcholine at high water concentrations in dependency on surfactant concentration. A simple and relatively stiff phosphatidylcholine bilayer vesicle can be transformed into a deformable bilayer vesicle by progressive incorporation of a surfactant into the bilayer membrane. The membrane softening surfactant then accumulates at the most deformed sites in the aggregate, which lowers the energetic cost of membrane deformation (Cevc et al. 2003b). Excessive surfactant quantity finally causes lipid solubilisation and disintegration of the bilayer, often into an elongated cylindrical and later spherical mixed micelle (Lichtenberg et al. 1983).

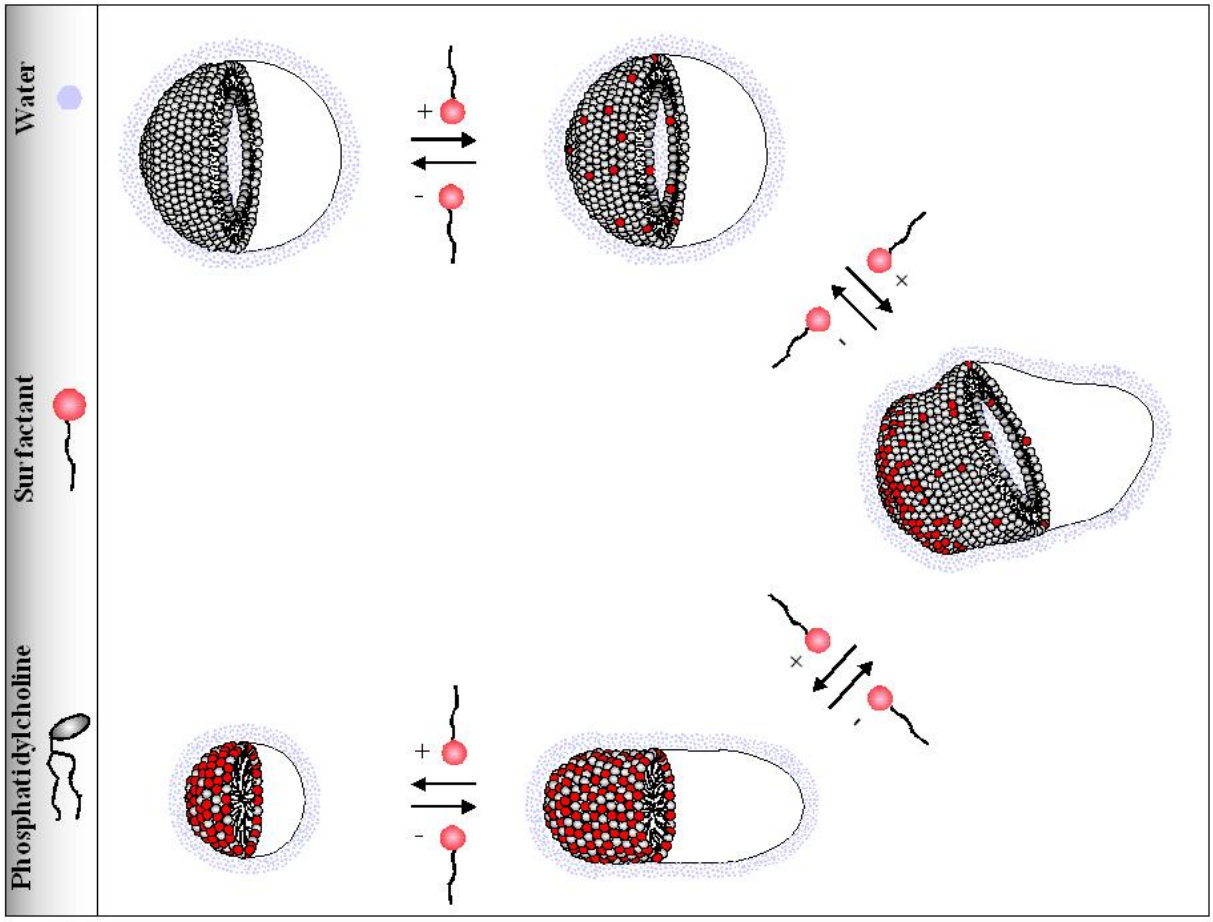

Figure 4: Schematic illustration of different lipid aggregates in dependency on the ratio of bilayer forming phosphatidylcholines and bilayer softening and destabilising surfactants.
With increasing surfactant concentration a stiff lipid bilayer membrane vesicle (top left) transforms into a deformable mixed bilayer vesicle (middle right) and dissolutes into cylindrical and spherical mixed micelles at high surfactant concentrations (down left).

1.3. Transfersome®, ultradeformable lipid bilayer vesicles as drug carriers across the skin

The first attempts to deliver drugs through the skin by vesicular carriers were conducted in 1980, using conventional liposomes (Mezei et al. 1980). It is nowadays generally agreed that such liposomal vesicles, both in the gel and fluid state, (Hofland et al. 1995; Cevc 1996; Kirjavainen et al. 1996) and other vesicular colloids, such as niosomes (non-ionic surfactant based vesicles) (van den Bergh et al. 1999), nano-particles (Jenning et al. 2000), and nano droplets (Rhee et al. 2001), cannot cross the stratum corneum as intact carriers and are therefore not suitable for drug delivery across the skin barrier. This incapability of the latter to penetrate the narrow pores in the stratum corneum is based on their vesicular rigidity and the lack of elasticity.

More recently several other vesicular aggregates, providing elasticity, have been tested as carriers for transdermal drug transport, but only few researchers were successful in the development of ethosomes (Touitou et al. 2000; Godin et al. 2003), elastic surfactant based vesicles (Bouwstra et al. 2002; Loan Honeywell-Nguyen et al. 2006), and ultradeformable mixed lipid vesicles, Transfersome® (Cevc 1995; 1996; Cevc et al. 2003b).

Furthest developed transdermal carrier system is the Transfersome® (a trademark of IDEA AG, Munich, Germany). Transfersome® vesicle consists of a bilayer membrane comprising a minimum of two amphiphiles with different solubilities and consequently with different geometric molecular packing parameters (Cevc 2004). Cylindrical amphiphats, such as phospholipids with a very low critical aggregate concentration (*CAC*) in the nano molar range, form essentially bilayer membranes, which are acceptably weakened by the cone-shaped amphiphats having $CAC > 1$ μM.

The varying molecular amphiphile geometry enables the resulting bilayer membrane to respond to external local stress. Amphiphiles that are uniformly distributed in a spherical bilayer vesicle rearrange during vesicle deformation. The more water soluble, cone-shaped amphiphiles accumulate in the more curved bilayer parts (cf. Figure 4), and thus make the bilayer vesicle more flexible. Simultaneously, such local surfactant-like amphiphile accumulation increases the capability of water exchange across the bilayer, which is also important for a high vesicle shape adaptability (Cevc et al. 2003b). Both these features are combined in a Transfersome® vesicle, which is thus a responsive, self-optimizing, nano-robotic transport device capable of crossing even relative narrow pores, e.g. in the skin.

Deformable, shape-adjusting membranes are also known in nature. Neutrophiles combat diseases by penetrating small apertures in the blood vessels tissue to reach the site of infection or inflammation. They undergo a large deformation, which has been recorded by Tsai et al. (1993) using the micropipette aspiration technique. Figure 5 shows the micrographs of neutrophil deformation and elongation during an aspiration into a narrow pipette. A computer simulation of the skin pore penetration by ultradeformable Transfersome® or a stiff liposome shows a comparable deformation of the former and insufficient deformation of the latter (Cevc 1997). Neutrophils are driven outside a blood vessel by chemotaxis. But what kind of force drives the ultradeformable carriers through the human skin barrier?

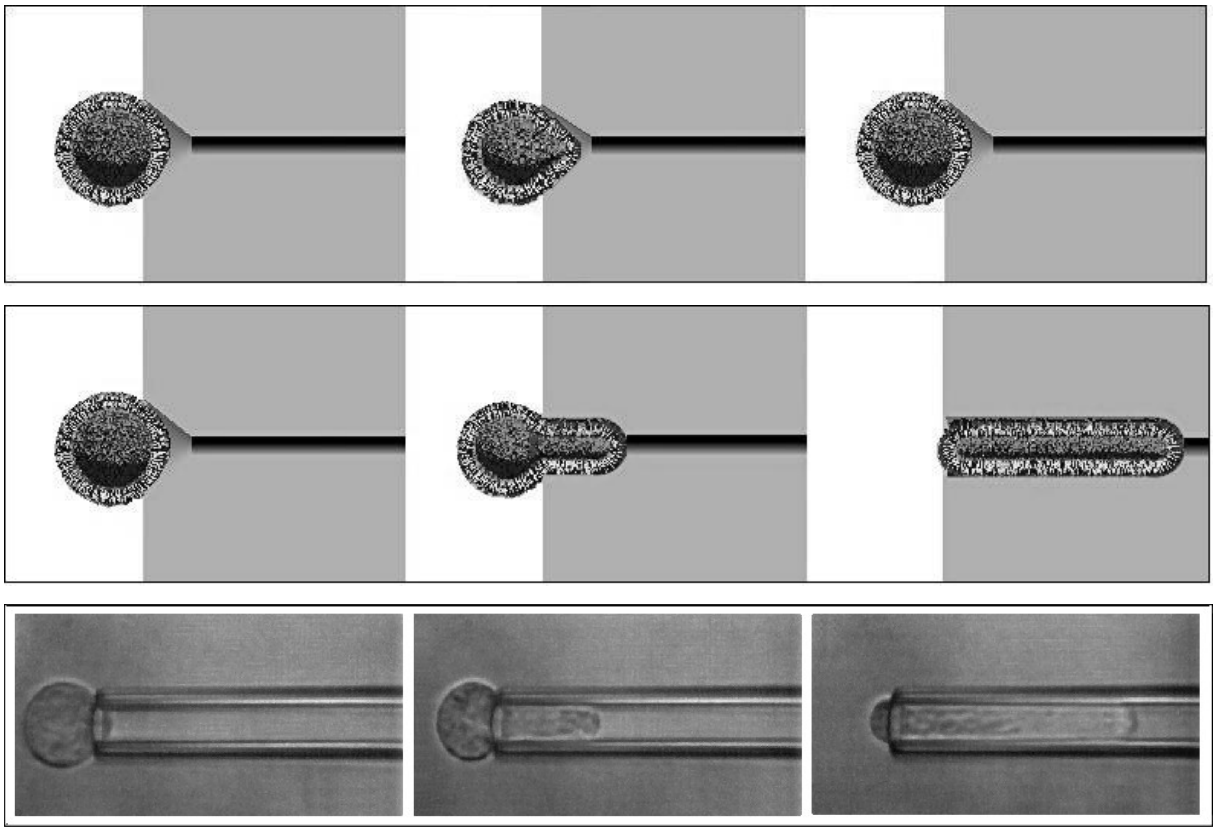

Figure 5: Computer simulation of pore penetration behaviour by a liposome (top) and a Transfersome® vesicle (middle) and micrographs of neutrophil aspiration into pipettes (down). (Both graphs were adapted and modified from Cevc (1997) and Tsai et al. (1993))

The driving force for the skin penetration by a Transfersome® is the transepidermal water gradient within the epidermis, more specifically, within the stratum corneum (Cevc et al. 1992). The water concentration increases from approximately 15 - 30 % at the skin surface to nearly 70 % in the stratum granulosum (Warner et al. 1988; Caspers et al. 2001). After a non-occlusive application of the ultradeformable carriers, the latter try to avoid local dehydration by penetrating, after a lag-time (dehydration time), the hydrophilic intercellular pathways in the horny layer leading to the better hydrated regions with a higher water content (Cevc et al. 2003a). The carrier transfer takes place whenever the energetic gain, in terms of dehydration/hydration energy, is greater than the energetic cost, due to the hydrophilic pore widening and carrier deformation, for barrier crossing (Cevc 1999). Knowledge of the interrelation between the transepidermal water gradient and pore penetrability points out the necessity of non-occlusive application of the drug containing Transfersome® products, due to the required drying and dehydration of a formulation on the skin.

Such vesicular Transfersome® products can then act as transdermal drug carriers for a broad variety of active agents (Cevc et al. 1996), ranging from small molecules, like glucocorticoids

(Lehmann et al. 2003; Cevc et al. 2004a), NSAIDs (Cevc et al. 2001; Rother et al. 2007), local anaesthetics (Planas et al. 1992), to macromolecules and proteins (Paul et al. 1995; Cevc et al. 1998; Paul et al. 1998).

1.4. Objectives and structure of the thesis

The major objective of the present thesis is the development of a new all-purpose ultradeformable Transfersome® formulation suitable for dermal as well as transdermal delivery of different kinds of drugs and thus for the treatment of local diseases in superficial and deeper peripheral tissues.

Polyoxyethylene (20) oleyl ether, a widely used surfactant with different synonyms and trade names ($C_{18:1}EO_{20,}$ macrogol (20) oleyl ether, Brij98, Oleth-20, Volpo N20, etc.) is assumed to be a suitable amphiphilic molecule in softening bilayer membranes without compromising its stability too much, at least within certain membrane concentration range. The low critical micelle concentration of this non-ionic surfactant, $CMC = CAC \approx 25$ µM (Umbreit et al. 1973; Klammt et al. 2005), the high membrane partition coefficient, $\log K \approx 4.3$ M^{-1} (Heerklotz et al. 2000b), and the suitable hydrophile-lipophile balance $HLB = 15.3$ (Ash et al. 1980) makes $C_{18:1}EO_{20}$ worth studying its influence on bilayer membranes based on soybean phosphatidylcholine, SPC.

The main goal is strongly connected with the determination of physico-chemical properties of the simple phosphatidylcholine vesicles, liposomes, of the mixed bilayer vesicles, Transfersome®, but also involves their dissolution products namely the mixed lipid micelles. The underlying questions, which must be answered to develop ultradeformable SPC/$C_{18:1}EO_{20}$ bilayer vesicles suitable for transdermal drug delivery are:

- Saturation of soybean phosphatidylcholine bilayer vesicles with and their solubilisation by polyoxyethylene (20) oleyl ether.
- Effect of polyoxyethylene (20) oleyl ether on bilayer adaptability and bending rigidity of mixed lipid vesicles, Transfersome®.
- Bilayer membrane partitioning and distribution of the drugs bupivacaine and ketoprofen in dependency on the bulk *pH*, membrane electrostatics and polarity.
- Adaptability and elasticity of mixed bilayer vesicles, Transfersome®, in dependency on the tested drug concentration, the bulk *pH*, and ionic strength.

In chapter 1, saturation and solubilisation of phosphatidylcholine bilayer vesicles with $C_{18:1}EO_{20}$ is therefore addressed as measured with two different methods. The diffusion of $C_{18:1}EO_{20}$ and its effects on solubilisation kinetics is moreover tackled with time-resolved dynamic light scattering, highlighting some important aspects of manufacturing such Transfersome® vesicles.

The bending rigidity and adaptability of mixed bilayer membrane vesicles and of mixed micelles is described and analysed in chapter 2 as a function of $C_{18:1}EO_{20}$ in the membrane. This highlights the deformability of mixed bilayer vesicles saturated with $C_{18:1}EO_{20}$, having maximum adaptability. The latter is an important parameter for the carrier mediated drug transport across the stratum corneum, as well as optimum drug vesicle interaction.

The payload of bilayer membrane vesicles with two different drugs is therefore studied in chapter 3. The partition coefficient measurements with the base bupivacaine, a long acting local anaesthetic, and with the acid ketoprofen, a widely used non steroidal anti-inflammatory drug, are quantified in the chapter in dependency on their charge state, the bulk *pH*, bilayer electrostatics, and polarity.

The bilayer bending rigidity and adaptability studies described in chapter 4 conclusively show the synergistic effects of the surfactant polyoxyethylene (20) oleyl ether and of bupivacaine or ketoprofen on bilayer adaptability, which is proportional to the pore penetration ability of the resulting three-component bilayer vesicles.

The structure of this work is organized in independent chapters. Each of them can be read and reviewed individually, but also reveals interrelationship between the chapters with regard to the objectives of this thesis. Each chapter therefore starts with a short introduction, followed by a practical section describing the used material, methods and physico-chemical principles. The results are then presented, illustrated, and discussed in sufficient detail to highlight the importance of the results in relation to the work in general and to the other chapters.

2. SATURATION AND SOLUBILISATION OF SOYBEAN PHOSPHATIDYLCHOLINE BILAYER VESICLES BY POLYOXYETHYLENE (20) OLEYL ETHER, $C_{18:1}EO_{20}$

2.1. Introduction

Fatty alcohol ethoxylates are non-ionic surfactants, used in a wide range of pharmaceutical and healthcare systems. Polyoxyethylene (20) oleyl ether is one in a series of C_xEO_y, having a fatty alcohols of length x and etherified by polymerisation them with y units of ethylene. Its detailed chemical structure is illustrated in Figure 6.

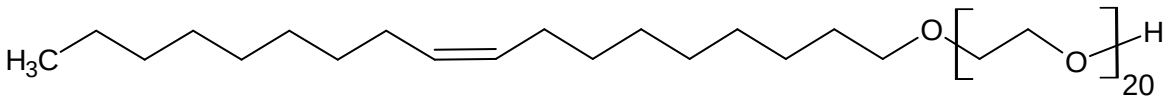

Figure 6: Structure of polyoxyethylene (20) oleyl ether, $C_{18:1}EO_{20}$

Compared to non-ionic esterified surfactants of the fatty acid type (e.g. Tweens and Myrjs) the corresponding ethers (trade names: Brij, Volpo, Oleth …) are not subjects of hydrolysis. This is the reason why fatty alcohol ethoxylates are stable over a wide *pH* range and tolerant to extreme *pH* levels and high electrolyte concentrations. These virtues recommend the C_xEO_y surfactants for usage in pharmaceutical formulations under extreme salt and *pH* conditions. Due to its high degree of ethoxylation, $C_{18:1}EO_{20}$ (Brij98, Volpo N20, Oleth-20) is soluble in water up to the critical micelle concentration of *CMC* = 25 µM (Umbreit et al. 1973; Klammt et al. 2005) and possesses a hydrophile-lipophile balance of *HLB* = 15.3 (Ash et al. 1980).

Polyoxyethylene oleyl ethers (most often y = 10 and 20) are surfactants, that are mainly used as emulsifier/co-emulsifier in microemulsions and oil-in-water (O/W) emulsions (Boonme et al. 2006; Wang et al. 2006; Junyapraserta et al. 2007), as detergent (Ehsan et al. 2006), or as solubiliser (Uniqema 2008). They are also applicable as dispersing (Williams et al. 1999) or gelling agents, in the latter case to modify the rheology of suspensions (Kennedy et al. 2007). In the face of this work, the incorporation of polyoxyethylene (20) oleyl ether into lipid vesicles and combined action of these two components in the resulting mixed bilayer membranes could possibly provide a new class of Transfersome® carriers for non-invasive transdermal drug delivery, a recent and emerging application field (Cevc 1997; Cevc et al.

2003a; Cevc et al. 2003b). Such vesicular carriers are known to be stabilised by the polar lipid and made more adaptable and deformable by the surfactant if they are combined in the right proportion (Cevc et al. 1998; Cevc 2004).

The primary objective of this work was to study the influence of the surfactant polyoxyethylene (20) oleyl ether in soybean phosphatidylcholine bilayer vesicles in terms of bilayer membranes saturation with and solubilisation by the surfactant. Even though a lot of publications deal with C_xEO_y and this topic, a detailed determination, to the best of my knowledge, of the effective surfactant to lipid molar ratio R_e at the membrane saturation limit, R_e^{sat}, and the solubilisation limit, R_e^{sol}, has not been performed for $C_{18:1}EO_{20}$ up to now.

$$R_e = \frac{c_s - c_{s,f}}{c_l} \approx \frac{c_s}{c_l} \qquad \text{for } c_s >> c_{s,f} \tag{1}$$

In equation (1), c_s is the total surfactant concentration, c_l the total lipid concentration, and $c_{s,f}$ the free surfactant monomer concentration. The free surfactant's concentration is comparable to the *CMC* as described and determined for non-ionic surfactants by different authors (Levy et al. 1990; Edwards et al. 1991). If $c_{s,f}$ is negligibly small, compared to the total surfactant concentration, R_e can be calculated directly (Lichtenberg et al. 1983).

The classical three-stage solubilisation model (Helenius et al. 1975; Lichtenberg 1985), which is discussed elsewhere in the text, was determined by the static (SLS) and dynamic (DLS) light scattering due to the fact that turbidity is an indicator of the micro structural changes, which occur during saturation and solubilisation processes in the mixed bilayer membranes. Beyond these two methods electron microscopy (EM), small-angle X-ray (SAXS) and neutrons (SANS) scattering, nuclear magnetic resonance spectroscopy (NMR), spectrofluorimetry and calorimetry are alternative methods to determine the phase boundaries R_e^{sat} and R_e^{sol}; some of the methods were even applied to analyse the kinetics of solubilisation. This secondary, but not less important objective concerning the optimisation and speed-up of pharmaceutical manufacturing processes and the time for system equilibration was measured in this work using DLS, an unusual but auspicious procedure.

The results collected with the performed experiments highlight the potential role of polyoxyethylene (20) oleyl ether in pharmaceutical and healthcare products, e.g. in combination with phosphatidylcholine vesicles forming ultradeformable carriers for non-invasive transdermal drug delivery.

2.2. Material and methods

2.2.1. Materials

Soybean phosphatidylcholine, SPC, (assumed $M_w \approx 800$ g/mol) was purchased from Lipoid (Ludwigshafen, Germany) with a purity grade > 90 % (Lipoid S100). This phospholipid of biological origin is a mixture of phosphatidylcholines with different unsaturated and saturated fatty acid chains. Polyoxyethylene (20) oleyl ether ($M_w \approx 1150$ g/mol) was acquired for the kinetic measurements from Croda/Uniqema (Nettetal, Germany). It met the European Pharmacopoeia specification for macrogol oleyl ether. Determination of R_e^{sat} and R_e^{sol} was performed with polyoxyethylene (20) oleyl ether from Sigma-Aldrich (analytical grade). Phosphate buffer salts from VWR (Darmstadt, Germany) and aqua ad iniectabilia from Deltaselect (Dreieich, Germany) had European Pharmacopoeia quality as well.

2.2.2. Preparation of simple phosphatidylcholine bilayer vesicles and surfactant solutions

Large unilamellar vesicles (LUV) were prepared from SPC as is described in detail elsewhere (Olson et al. 1979; MacDonald et al. 1991). Lipid vesicle stock suspension with c_l = 125 mM in phosphate buffer (c_b = 50 mM) was homogenised by a multi-extrusion step through different track etched polycarbonate membranes (PCTE) of decreasing pore size (d = 400 nm – 50 nm, GE Osmonics). The final vesicle size and polydispersity index (*PDI*) of the LUV were determined by the dynamic light scattering (DLS).

A micellar stock solution of $C_{18:1}EO_{20}$ was prepared by stirring the surfactant in phosphate buffer (c_b = 50 mM) for 1 h above the melting point T_m = 35 °C of $C_{18:1}EO_{20}$, to speed up the dissolution process.

	Lipid vesicle stock suspension			Surfactant stock solution	Dilution phosphate buffer			Diluted mixed lipid vesicles and mixed micelles	
	c_l [mM]	d_{ves} [nm]	*PDI*	c_s [mM]	c_b [mM]	*pH*		c_l [mM]	R_e [mol/mol]
S_{step}	125	110.0	0.075	87	50	7.2	à	10	0 – 3.3
S_{kin}	125	104.3	0.079	100	50	6.5	à	5	3 – 12

Table 1: Composition of mixed lipid vesicles and mixed micelles for SLS and DLS measurements prepared by mixing the lipid vesicle stock suspension with the surfactant stock solution and the dilution buffer resulting in different effective surfactant to lipid molar ratios R_e at constant lipid concentrations.

Stepwise lipid solubilisation (S_{step}) was studied by individually mixing the lipid vesicle stock suspension, the surfactant stock solution, and the dilution phosphate buffer always to a constant SPC content of c_l = 10 mM with an increasing amount of $C_{18:1}EO_{20}$ providing effective R_e = 0.05 – 3.31 mol/mol. The mixtures were stirred at room temperature for one week to equilibrate.

In contrast to the above mentioned vesicle dilution procedure, the determination of the bilayer vesicle solubilisation kinetic (S_{kin}) by $C_{18:1}EO_{20}$ was performed by diluting and vortexing the unilamellar lipid vesicles with the surfactant stock solution and the dilution buffer synchronously at the measurement start. The final SPC content was c_l = 5 mM for each preparation, with an effective surfactant to lipid molar ratio R_e = 2.99 – 12.09 mol/mol.

2.2.3. Bilayer solubilisation: Static light scattering

The solubilisation of lipid bilayer membranes with c_l = 10 mM was measured with the static light scattering using a double-beam UV-VIS spectrophotometer Shimadzu UV-1601, computer controlled by the Shimadzu software UVProbe V.2.0. Optical density was analysed at λ = 550 nm, cell length = 1 cm, T = 25.0 °C as a function of added surfactant concentration.

2.2.4. Bilayer solubilisation: Dynamic light scattering

The stepwise and kinetic solubilisation measurements were done with the photon correlation spectroscopy (PCS) using an ALV (Langen, Germany) device (ALV-NIBS/HPPS High Sensitivity Version, ALV-5000/EPP Multiple Tau Digital Converter, ALV-Correlator Software V.3.0). The dynamic light scattering (DLS) was measured at a scattering angle 173°, λ = 632.8 nm, cell length = 1 cm and T = 25.0 °C. The intensity weighted size distribution of the mixed lipid bilayers and/or the mixed micelles was evaluated by cumulant analysis of the second order (CUM2), based on the assumption of a monomodal distribution. Due to the described (Lichtenberg et al. 2000) and expected multimodal size distribution, a continuous inverse Laplace transformation was also performed using the regularized fit tool comparable to CONTIN (Provencher 1982).

The hydrodynamic radius of the different mixed lipid vesicles and micelles was determined in 6 runs, each lasting 30s, for S_{step} (c_l = 10 mM) and in a single measurement for S_{kin} (c_l = 5 mM). For the kinetic measurements, 30 time points with in an exponentially increasing run time and time interval were recorded during a total reading time of 0.5 h, 9 h and 45 h, depending on the effective ratio R_e.

2.3. Results

2.3.1. Bilayer membrane saturation with and solubilisation by the surfactant

2.3.1.1 Static light scattering SLS

The addition of polyoxyethylene (20) oleyl ether to soybean phosphatidylcholine bilayer vesicles ($d_{ves} \approx 110$ nm) at constant concentration $c_l = 10$ mM results initially in an increase of suspension turbidity. Only if R_e exceeds a surfactant and lipid concentration dependent threshold, light scattering starts to decrease and ends in an optically transparent colloidal system of small mixed micelles ($d_{mic} \approx 10$ nm).

Figure 7 shows the measured turbidity as a function of R_e. The maximum light scattering intensity is reached at a surfactant to lipid ratio $R_e^{sat} \approx 0.25$ mol/mol, when the vesicles membrane seems to be saturated with $C_{18:1}EO_{20}$. Additional amounts of surfactant molecules cause lipid solubilisation and lead to the formation of mixed micelles. Between $R_e = 0.25 - 3.0$ mol/mol the turbidity consequently decreases, reflecting an increasing number of small mixed micelles, which scatter the light less than the much larger mixed lipid vesicles. Optically transparent solutions above $R_e^{sol} \approx 3.0$ mol/mol indicate the state of completed solubilisation and the sole existence of mixed micelles in these colloidal dispersions.

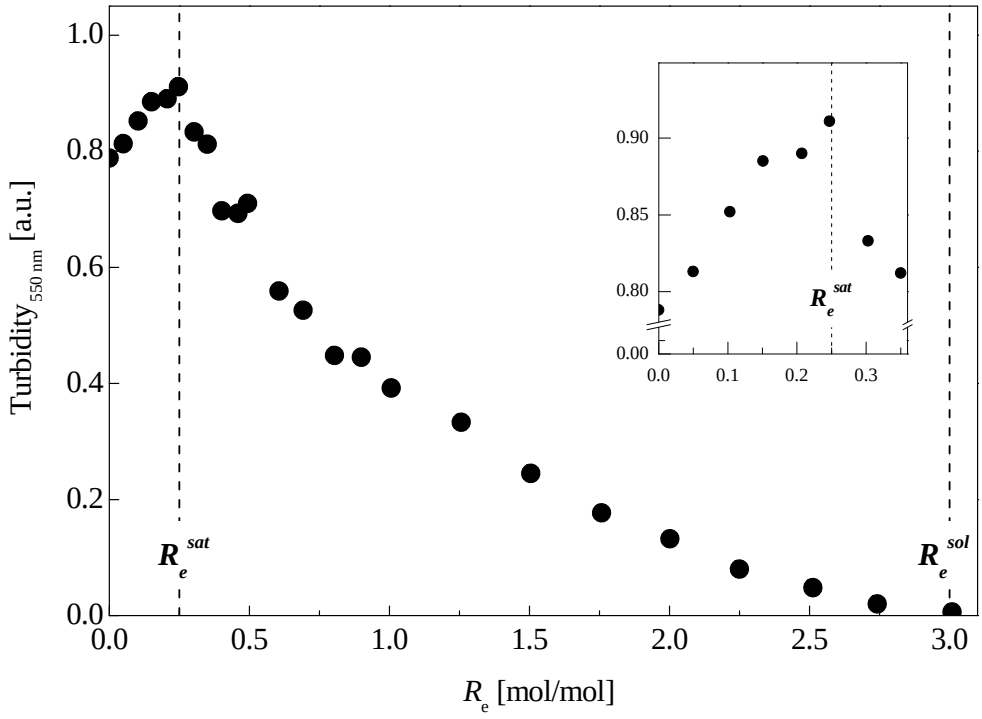

Figure 7: The static light scattering of lipid vesicles (10 mM) with increasing $C_{18:1}EO_{20}$ content. The bilayer membrane is saturated at an effective surfactant to lipid molar ratio $R_e^{sat} \approx 0.25$ mol/mol. Lipid vesicle solubilisation into mixed micelles is completed at at $R_e^{sol} \approx 3.0$ mol/mol.

2.3.1.2 Dynamic light scattering DLS

The dynamic light scattering not only provides information on the average aggregate size, moreover it allows parallel determination and quantification of mixed lipid vesicles and/or mixed micelles. I thus used the DLS measurements to support and confirm the observations, illustrated for bilayer membrane saturation and solubilisation in Figure 7.

The average size of the aggregates, evaluated by CUM2 analysis, increases by adding $C_{18:1}EO_{20}$ up to the saturation limit at $R_e^{sat} \approx 0.25$ mol/mol (black symbols ● in the left panel of Figure 8A). Solubilisation and formation of mixed micelles starts above R_e^{sat}, which can be seen by the initial detection of the latter, having first a diameter d_{mic} = 35 - 38 nm, as evaluated with the continuous inverse Laplace transformation (open triangle ▽ in Figure 8A). Figure 8B, which shows the light scattering intensity, supports the conclusion: Solubilisation begins at $R_e^{sat} \approx 0.25$ mol/mol, where the measured intensity doubles, a consequence of the coexistence of mixed lipid vesicle △ and mixed micelles ▽ as illustrated in Figure 8A.

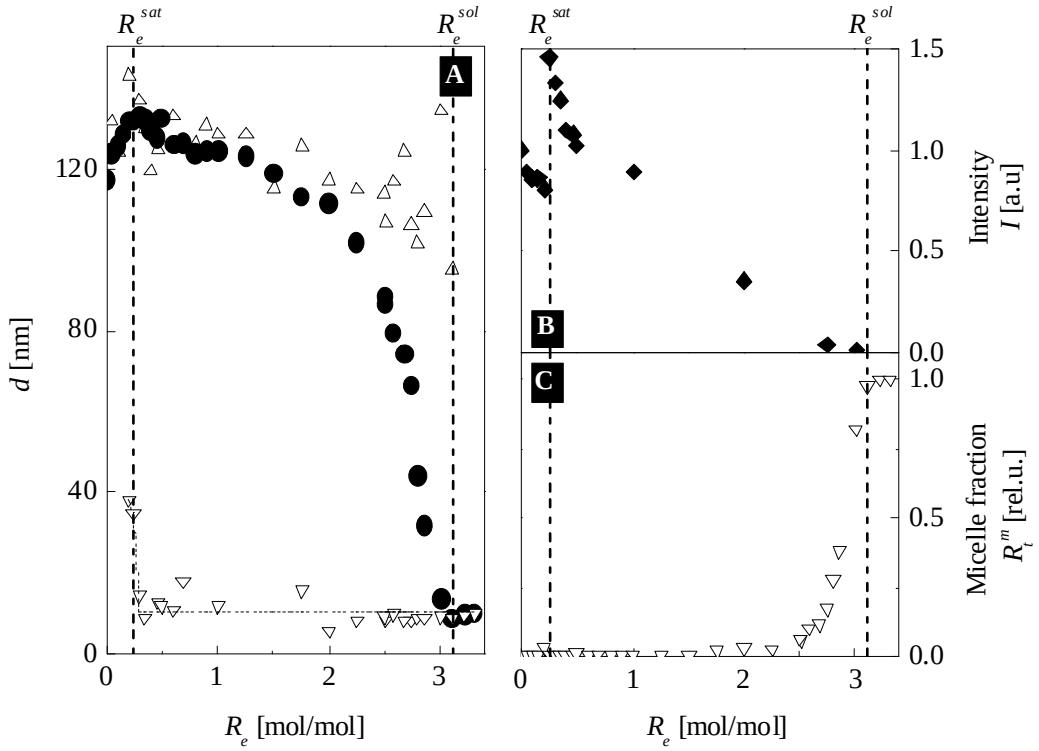

Figure 8: The dynamic light scattering of lipid vesicles (10 mM) with increasing $C_{18:1}EO_{20}$ content. (A) The vesicles and micelles diameter, as determined with CUM2 (●) or regularized fit/CONTIN evaluation (△ vesicles, ▽ micelles), as a function of the effective surfactant to lipid molar ratio R_e . Membrane saturation is reached at $R_e^{sat} \approx 0.25$ mol/mol and solubilisation at $R_e^{sol} \approx 3.11$ mol/mol (vertical dashed lines).
(B) Increase in the light scattering intensity I at the point of membrane saturation, reflecting coexistence of mixed lipid vesicles and micelles, followed by a decrease in the light scattering due to the progressive bilayer solubilisation into mixed micelles.
(C) Gradual formation of mixed micelles with increasing R_e up to the solubilisation point R_e^{sol}.

Solubilisation is reached at $R_e^{sol} \approx 3.11$ mol/mol, where mixed micelles are the only remaining kind of aggregates in the tested colloidal system. This is evident in all panels of Figure 8, in the lower right panel C by the increase of mixed micelles fraction to total aggregates R_t^m with higher surfactant to lipid ratio. The higher number of mixed micelles and the continuous solubilisation of vesicles with increasing R_e cause a decrease in the average aggregate size and in the measured light scattering intensity, due to exponential influence of the aggregate radius on the Rayleigh scattering intensity, $I \propto r^6$ (Boufendi et al. 1994).

2.3.2. Kinetic of aggregate dissolution

Saturation and solubilisation of lipid membranes is a solubiliser concentration driven, time-dependent process as is described for soybean phosphatidylcholine mixed with polyoxyethylene (20) sorbitan monooleate (Simoes et al. 2005). To analyse and quantify kinetics of SPC dissolution by $C_{18:1}EO_{20}$, a set of time resolved DLS measurements with mixtures of them above the membrane solubilisation limit $R_e \geq 3$ mol/mol were performed.

The ratio of mixed micelles to total aggregates R_t^m shows a remarkable dependency of solubilisation time on the surfactant to lipid concentration ratio R_e (Figure 9). The higher the ratio, the faster is solubilisation, ranging from 177 min to 3.2 min for R_e = 4.5 mol/mol and R_e = 12 mol/mol, respectively. The solubilisation process for effective molar ratios R_e = 3 – 4 mol/mol was not finished at the end of the experiments. Figure 7 and Figure 8 show, however, that solubilisation for such low concentrations occurs on a time scale of days and is completed after 7 days.

The measured intensity in dependency on time shows a biphasic progression (data not shown). Both regions were therefore evaluated separately to quantify the kinetics of solubilisation. At short times, the intensity decreases linearly with the square root of time (black symbols in the left panel of Figure 10); the dissolution speed in terms of light scattering intensity decrease per $t^{0.5}$ ranges from -0.091 $min^{-0.5}$ to -0.812 $min^{-0.5}$ for the lowest investigated relative surfactant concentration R_e = 3 mol/mol and the highest ratio R_e = 9 mol/mol, respectively. For R_e = 12 mol/mol, a biphasic curve was not detected, probably a result of the very fast dissolution process in phase one, which was not analysable with our DLS set-up for a total solubilisation time of 3.2 min The dissolution speed at short times and the effective surfactant to lipid ratio R_e are well correlated (r = 0.992) (right panel of Figure 10).

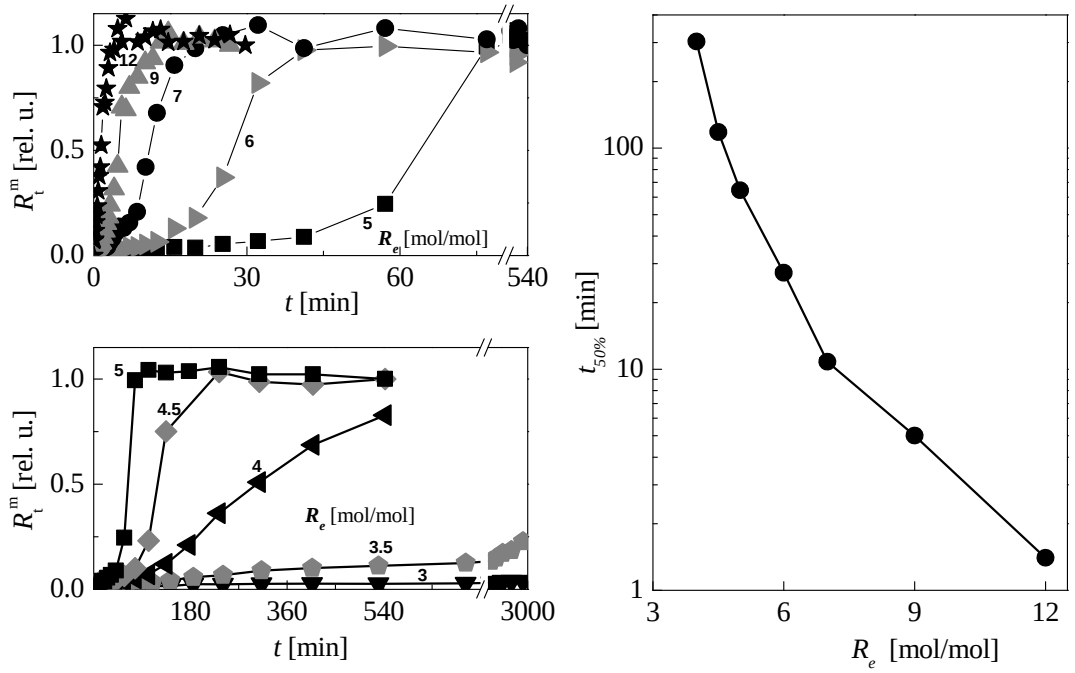

Figure 9: Time-dependent DLS solubilisation measurements of lipid vesicles (5 mM) with different $C_{18:1}EO_{20}$ contents above the solubilisation limit $R_e \geq 3.0$ mol/mol. Left panels: Solubilisation kinetic in terms of the intensity weighted ratio of micelles to the total amount of aggregates R_t^m in dependency on time. Right panel: Half life of vesicle solubilisation respectively micelles formation depending on R_e.

However, the dissolution speed is slowed-down, and becomes non-linear for later time points $t^{0.5}$ (grey symbols in the left panel of Figure 10). Linearity is now found for the reciprocal square root of time however (black symbols in the left panel of Figure 11). Depending on R_e, the dissolution speed, expressed in terms of the light scattering intensity decrease, is now calculated to be 2.66 $min^{0.5}$ and 0.44 $min^{0.5}$ for the lowest and the highest surfactant to lipid ratio of R_e = 3 mol/mol and R_e = 12 mol/mol, respectively. In contrast to the findings made at short times, the long term dissolution speed is found to be proportional to the reciprocal R_e value, with a correlation coefficient of r = 0.984. The linearities are discussed in detail elsewhere.

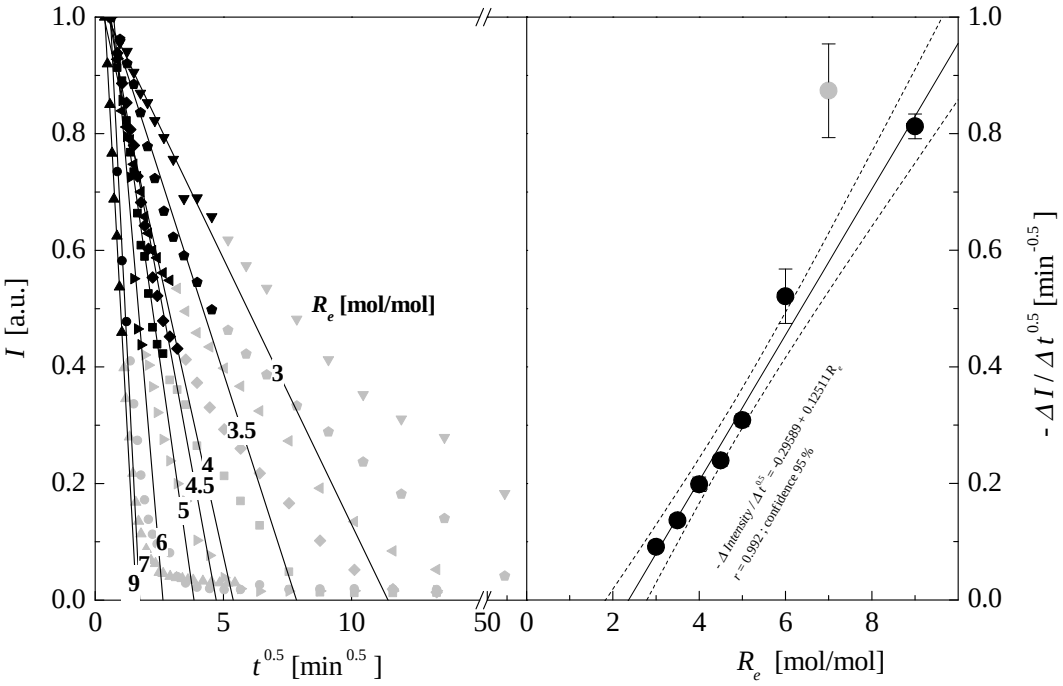

Figure 10: Short term time-dependency of DLS intensity as measure of aggregate solubilisation. The decrease in the light scattering intensity *I* is linear to the square root of time (black symbols) , followed by a slower, non linear vesicle dissolution (grey symbols) (left panel). The slope, i.e. the dissolution speed, in dependency on the effective ratio of surfactant to lipid R_e highlights the surfactant concentration effect on the dissolution speed at short times with a high correlation coefficient *r* = 0.992 (right panel). The outlier ( ) in the right panel was not considered, due to reduced number of fitting points (n=4).

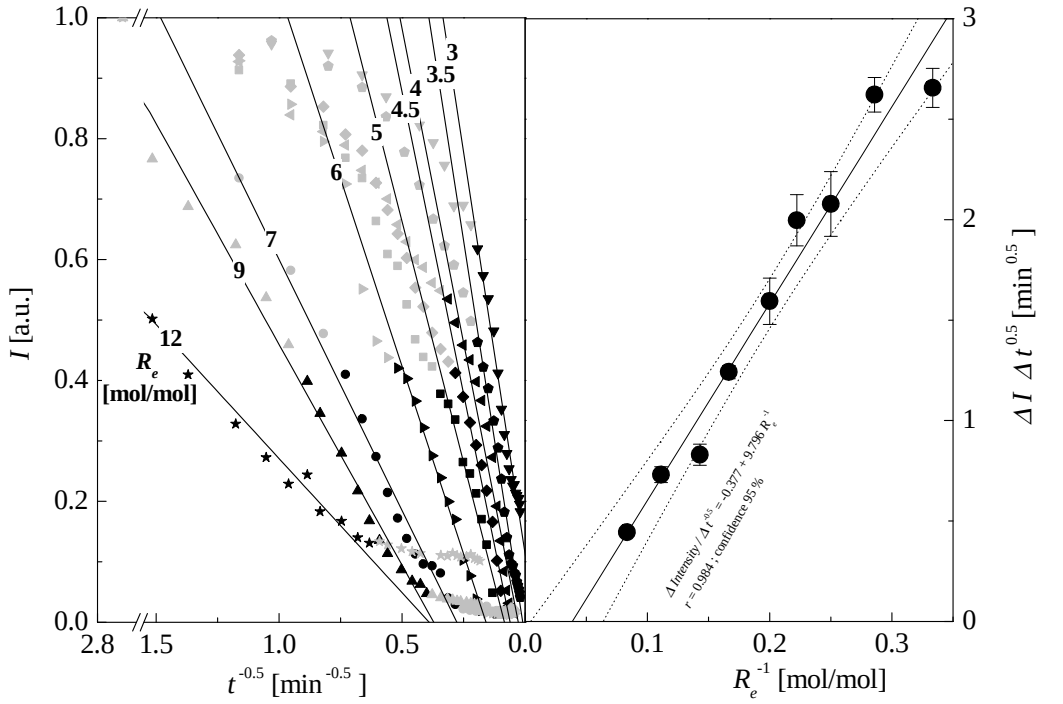

Figure 11: Long term time-dependency of DLS intensity as measure of aggregate solubilisation. The decrease in the light scattering intensity *I* is proportional to the reciprocal square root of time (black symbols in the left panel). A good correlation (*r* = 0.984) was found for the linear fit of the dissolution speed in dependency on R_e^{-1} (right panel).

2.4. Discussion

Polyoxyethylene oleyl ethers are well known surfactants, used in the chemical and pharmaceutical industry due to their broad availability and wide range of application described in 2.1. It is therefore surprising that in spite of extensive research works done with polyoxyethylene alkyl and alkenyl ethers to date, little is known about the detailed function of polyoxyethylene oleyl ethers in pharmaceutical systems. To the best of my knowledge, the detailed solubilisation ability of $C_{18:1}EO_{20}$ and its kinetics have not been published to this day, neither for biomembranes nor for synthetic or natural phospholipids. With my results and their comparison with those measured with different non-ionic surfactants a gap in the huge sector of surfactants and their solubilisation properties will be bridged.

As is described in 2.2.2, the formation of a micellar solution of $C_{18:1}EO_{20}$ in water is accelerated by increased temperature. Above the melting point T_m = 35°C (Shigeta et al. 1997) the originally solid $C_{18:1}EO_{20}$ (S) transforms into a liquid, oily state (O_m). By adding water to such liquid, different two-component phases are formed depending on final water content and temperature. The temperature induced transformation of solid $C_{18:1}EO_{20}$ into a series of mesophases via the primary oily phase and, then secondary, isotropic inverse micelles O_m → hexagonal liquid crystalline phase H_1 → discontinuous cubic phase I_1 → micelles W_m is much faster than the dissolution S → H_1 → I_1-→ W_m at 25°C as described elsewhere (Kunieda et al. 1997; Shigeta et al. 1997), which involves, arguably, at least one isothermal phase transition S → hydrated → H_1.

Solubilisation and different dissolution stages of lipid bilayers by surfactants are the topics, analysed and discussed in many previous publications. The classical three stage model (Helenius et al. 1975; Lichtenberg et al. 1983; Lichtenberg et al. 2000) starts with:

I: Surfactant binding and incorporation into a bilayer membrane, resulting in mixed lipid-surfactant bilayer vesicles with changing composition.

II: Formation of mixed micelles from the bilayers saturated with a surfactant. The bilayer to micelle ratio but neither the mixed bilayer vesicles nor the mixed micelles composition changes during this stage.

III: Complete solubilisation of the mixed bilayer vesicles into mixed micelles and further decrease in average size of the latter with additional surfactant.

Saturation stage I: Mixed lipid-surfactant bilayer vesicles

Interaction of non-ionic surfactants like $C_{12}EO_8$ with a phospholipid bilayer yields a more sophisticated model than that described in previous section (Edwards et al. 1991; Lasch 1995; Almgren 2000). Stage I must be split into a surfactant incorporation phase Ia, with negligible vesicle size increase and bimodal size distribution, and a second phase Ib, with ongoing surfactant incorporation and vesicle growth with monomodal size distribution. The size increase also depends on the preparation procedure of lipid bilayers (Levy et al. 1990; Partearroyo et al. 1992). In their studies a correlation has been found, for example, between the lipid bilayers manufacturing and the vesicle growth induced by adding surfactants. SUV, homogenised by ultrasonification, grow more than LUV, allowing good differentiation between the stages Ia and Ib.

The results in Figure 7 and Figure 8 were achieved with LUV. Despite slight increase in the suspension turbidity of the SLS measurements and a DLS detectable vesicle size increase, the limit of soybean phosphatidylcholine bilayer saturation with $C_{18:1}EO_{20}$ is the same, R_e^{sat} = 0.25 mol/mol for both kind of measurements. Compared to other non-ionic surfactants, the low saturation limit of $C_{18:1}EO_{20}$ is explicable with the widespread headgroup in this cone-shaped surfactant, leading to a packing mismatch in lipid bilayers (Heerklotz et al. 1997). The geometry asymmetry of each surfactant molecule has to be compensated by the lateral headgroup compression and oleyl chain expansion. This is reached by polyoxyethylene headgroup dehydration and oleyl fluidization up to the saturation limit of R_e^{sat} = 0.25 mol/mol. The bilayer saturation for $C_{18:1}EO_{20}$ is comparable to other polyoxyethylene (20) alkyl / alkyl phenyl ethers with the same headgroup length as shown in Table 2.

Hydrocarbon chain		**Polyoxyethylene headgroup**	
C_X		**EO 10**	**EO 20**
Oleyl	$C_{18:1}$	n.a.	0.25
Cetyl	C_{16} [a]	0.88	0.28
Lauryl	C_{12} [b]	0.58 (EO 8)	n.a.
Octyl phenyl	$C_{8\text{-Ph}}$ [c]	0.60	0.20

Table 2: Saturation limit in terms of the molar surfactant to lipid ratio R_e^{sat} for ethoxylated alkylphenols, alkanes and alkenes with different headgroup lengths and hydrocarbon groups. With increasing headgroup length, the packing mismatch also increases, resulting in a lower lipid bilayer saturation limit.
[a] Saturation data obtained from Kim et al. (1991)
[b] Saturation data obtained from Heerklotz et al. (1994)
[c] Saturation data obtained from Ribosa et al (1992)

Whilst the change in turbidity and average vesicle size at R_e^{sat} is small, a transition from phase Ia to Ib is much more obvious in Figure 8B: A minute decrease in the scattered light intensity is followed by a jump in such intensity between R_e = 0.20 and 0.25 mol/mol. The jump is explicable in terms of physical properties of light scattering and the soft vesicle form changes: The Rayleigh scattering intensity is proportional to approximately the sixth power of the scattering particles diameter; the latter is the sole parameter which can change during an experiment with the increasing surfactant concentration. More specifically, with increasing $C_{18:1}EO_{20}$ content, vesicles bilayer adaptability increases during the stage Ib, i.e. with the amount of incorporated surfactant in the bilayer (Gompper et al. 1995; Cevc 1999; Cevc et al. 2003b; Cevc 2004). The resulting changes of fluid membrane conformation is a result of decreasing bending rigidity with accumulation of the cone-shaped surfactants in the region of highest curvature (Kroll et al. 1992), as is illustrated in Figure 12.

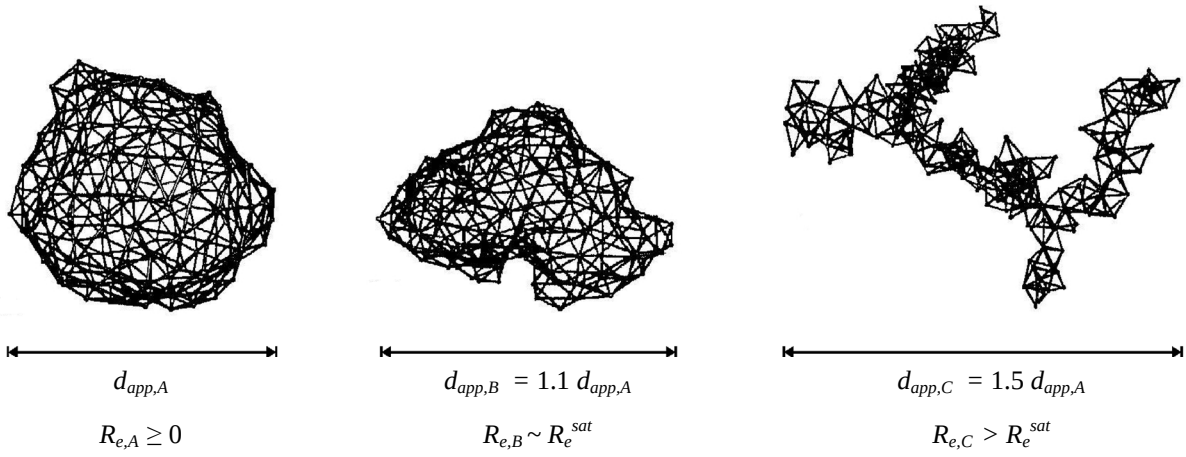

Figure 12: Conformation of mixed lipid vesicles depending on bending rigidity. From left to right a spherical vesicle with 2.5 k_BT, a fluctuating vesicle with 1.25 k_BT, and an ultradeformable crumbled vesicle with 0 k_BT. (Adapted and modified from Kroll et al.(1992))

The vesicles with a low surfactant concentration are spherical. They become more and more flexible, which leads to progressive fluctuations with increasing surfactant concentration and thus decreasing bending rigidity. Above R_e = 0.20 mol/mol, lipid membranes with a high concentration of $C_{18:1}EO_{20}$ form strongly fluctuating, ultradeformable vesicles. This is reflected in larger apparent hydrodynamic diameter $d_{app,}$ and higher scattered light intensity that originates mainly from the surfactant rich bilayer protrusions, driven by entropic reasons. At this point solubilisation starts, resulting in mixed micelles with d = 35 - 38 nm for R_e = 0.25 - 0.30 mol/mol (Figure 8A). Lasch (1995) also described a surfactant-induced transition from surfactant enriched vesicles to cylindrical mixed micelles, but in less detail.

Two component stage II: Mixed bilayer vesicles and mixed micelles

The formation of mixed micelles can be described for the non-ionic surfactants like $C_{18:1}EO_{20}$ by two models. Both have in common that the molar vesicle to micelle ratio but not the composition of neither mixed vesicles nor mixed micelles changes during this stage, as has been demonstrated in the separation experiments described by Levy et al. (1990).

With high-intensity dark field microscopy, Nomura et al. (2001) have determined the time-resolved dissolution behavior of lipids by ionic and non-ionic surfactants. For the latter they described the solubilisation processes of phosphatidylcholine membranes by a continuous shrinkage in several steps. The shrinkage is characterised by an alternating tense and quaking state above the saturation limit R_e^{sat}. During the tense state lipid and surfactant molecules are extracted from the membrane to form surfactant-lipid mixed micelles. The extraction theory is supported by Kragh-Hansen et al. (1998), who describe the extraction procedure for the surfactants with a slow flip-flop rate. Due to their expanded hydrophilic headgroup, ionic surfactants (e.g. SDS) and a non-ionic surfactants (e.g. $C_{18:1}EO_{20}$) show a decelerated flip-flop rate resulting in slow solubilisation kinetics, which is discussed in detail afterwards. Second, following to the tense state, a very quick membrane quaking causes lipid bilayer perforation followed by water discharge from the vesicle interior. A consequence of bilayer components removal and water efflux is the vesicle shrinking seen in Figure 8A. Third, the molecules in the bilayer membrane reorganise themselves by lateral diffusion and repeated tense and quaking states until the solubilisation limit R_e^{sol} is reached.

Alternatively to the continuous-stepwise shrinkage of lipid vesicles, Nomura et al. (2001) have discussed the solubilisation by opening-up of bilayer membranes and accumulation of non-ionic surfactants at the exposed edges, wherefrom micellisation starts. Even though Nomura´s group favours the continuous-stepwise shrinkage for all tested non-ionic surfactants, the opening-up solubilisation is described by Lasch (1995) and Noguchi et al. (2006) as well. In the work of Noguchi a computer-simulation based on consideration of curvature energies, attractive, and repulsive potentials shows membrane opening and dissolution from the edges. Electron microscopic pictures of Lasch show the above mentioned humpbacked vesicles, which dissolve via open vesicles → sheets → cylindrical micelles to spheroidal, mixed micelles.

Solubilisation stage III: Mixed micelles

Complete solubilisation of SPC bilayers is reached by the surfactant $C_{18:1}EO_{20}$ at an effective surfactant to lipid ratio of $R_e^{sol} \approx 3.11$ mol/mol. This value indicates that polyoxyethylene (20) oleyl ether is a potent non-ionic solubiliser of lipid membranes. A correlation between the hydrophile-lipophile balance *HLB* and the solubilisation potency is obvious (Figure 13), and has also been described by others (Helenius et al. 1975; Kim et al. 1991; Ribosa et al. 1992).

The *HLB* value, first introduced by Griffin (1949), is a measure for surfactant partitioning tendency between an oily and an aqueous phase. The most widely used method to calculate the *HLB* is the equation of Davies (1957):

$$HLB = 7 + \sum GN_H + \sum GN_L \qquad (2)$$

GN_H and GN_L are the group numbers for the hydrophilic and lipophilic molecule parts. Nevertheless the Davies´ method is unsuitable for the majority of non-ionic surfactants. A new calculation method for the surfactants with straight alkyl, polyoxyethylene and/or polypropylene chains improves the calculations errors of the Davies´ method by considering the effective chain length (ECL) (Guo et al. 2006). The chain length corrected HLB_c value is defined as:

$$HLB_c = 7 + GN_{CH_2} \times N_{CH_2 eff} + GN_{EO} \times N_{EOeff} + GN_{PO} \times N_{POeff} + \sum GN_h + \sum GN_l \qquad (3)$$

GN_{CH_2}, GN_{EO} and GN_{PO} are the group numbers for methylene, ethylene oxide and propylene oxide, whereas GN_h and GN_l are the group numbers for the other hydrophilic and lipophilic groups. The effective chain length N_{eff} is calculated for CH_2 , EO and PO based on the actual chain length N:

$$N_{CH_2 eff} = 0.965\, N_{CH_2} - 0.178$$

$$N_{EOeff} = 13.45\, ln(N_{EO}) - 0.16\, N_{EO} + 1.26 \qquad \text{for } 1 \le N_{EO} \le 50 \qquad (4)$$

$$N_{POeff} = 2.057\, N_{PO} + 9.06$$

With the listed group numbers (Table 3) the HLB_c values for polyoxyethylene octyl phenyl, cetyl and oleyl ethers could be calculated (Table 4) and plotted versus the solubilisation limit R_e^{sol} (Figure 13).

Group	Group number *GN*
hydrophilic	
$-CH_2CH_2OH$	0.479
-OH	2.255
Lipophilic	
$-CH_2-$	- 0.475
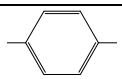	- 1.601

Table 3: Group numbers of the ECL method (Guo et al. 2006)

Surfactant	*HLB*	HLB_c	R_e^{sol} [mol/mol]
Polyoxyethylene (n) octylphenyl ether [a]			
$OP\text{-}EO_{8.5}$	12.9	13.5 [d]	4.10
$OP\text{-}EO_{9.5}$	13.4	14.0 [d]	2.60
$OP\text{-}EO_{12.5}$	14.6	14.9 [d]	1.80
$OP\text{-}EO_{15}$	15.2	15.7 [d]	2.60
$OP\text{-}EO_{20}$	16.1	16.7 [d]	4.20
Polyoxyethylene (n) cetyl ether [b]			
$C_{16}EO_{10}$	12.9	12.1 [d]	5.82
$C_{16}EO_{15}$	14.6	13.7 [d]	2.37
$C_{16}EO_{20}$	15.7	14.7 [d]	3.84
$C_{16}EO_{25}$	16.4	15.4 [d]	4.28
$C_{16}EO_{30}$	16.9	15.9 [d]	7.60
$C_{16}EO_{40}$	17.5	16.7 [d]	13.50
Polyoxyethylene (n) oleyl ether			
$C_{18:1}EO_{10}$	12.4 [c]	11.2 [d]	n.a.
$C_{18:1}EO_{20}$	15.3 [c]	13.8 [d]	3.11

Table 4: Solubilisation limit in terms of the molar surfactant to lipid ratio R_e^{sol} of ethoxylated alkylphenols, alkanes and alkenes with different *HLB* / HLB_c values.
[a] *HLB* and solubilisation data obtained from Ribosa et al.(1992)
[b] *HLB* and solubilisation data obtained from Kim (1991)
[c] *HLB* value obtained from Ash (1980)
[d] HLB_c value calculated with the effective chain length ECL (Guo et al. 2006)

The solubilisation measurements of Kim and Ribosa and the review of Helenius allow the conclusion that surfactants with HLB_c* = 14.1 - 14.8 have the highest solubilisation potency (Figure 13). The commercial available polyoxyethylene (20) oleyl ether with an HLB_c= 13.8 is nearly at this HLB_c* range corresponding to a minimum for the solubilisation limit R_e^{sol}. Assuming that the given range is correct, polyoxyethylene surfactants of the oleyl type $C_{18:1}EO_n$ will have their highest lipid solubilisation potency with n= 23 - 28 EO-units.

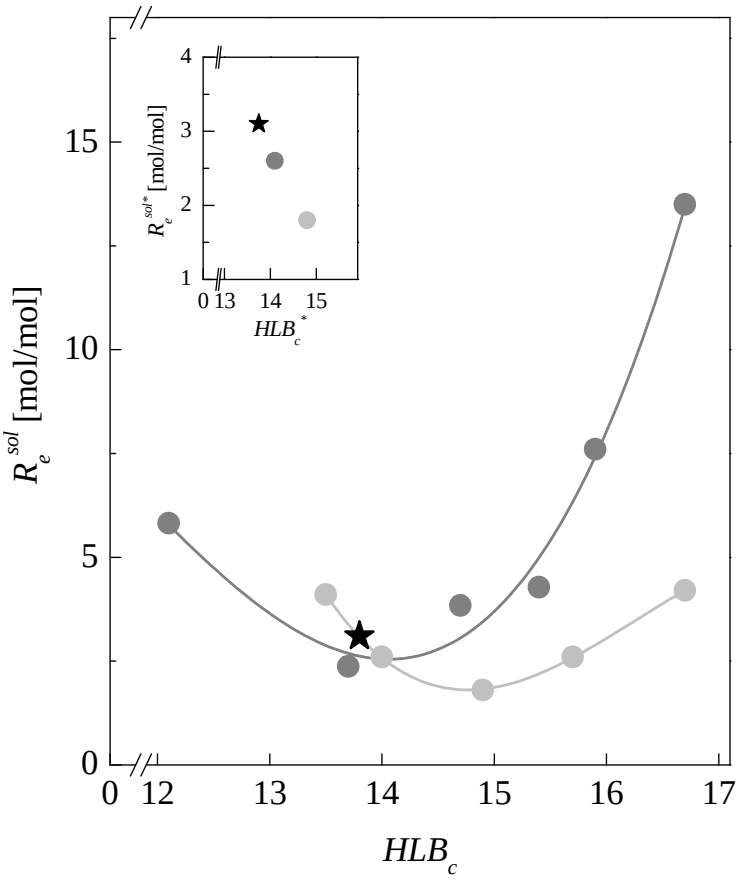

Figure 13: Effective molar surfactant to lipid ratio R_e^{sol} for phosphatidylcholine solubilisation as a function of the calculated HLB_c value for polyoxyethylene octyl phenyl ether (○) and polyoxyethylene cetyl ether (●) in EPC. Te small panel shows the polynomial fitted HLB_c* values of the formers compared to the determined polyoxyethylene (20) oleyl ether (★) value in SPC.

Short and long term dissolution kinetic

The kinetics of lipid bilayer saturation with and dissolution by polyoxyethylene (20) oleyl ether is an interesting topic, also from the applications standpoint, but has not been explored till now. Kragh-Hansen et al. (1998) mentioned that the solubilisation process near R_e^{sol} requires hours up to days, due to a slow flip-flop through the bilayer membrane, reported for surfactants with large hydrophilic headgroups. $C_{18:1}EO_{20}$ with its long polyoxyethylene headgroup showed such a behavior, a prolonging solubilisation time near R_e^{sol} = 3.11 mol/mol. The dissolution half time $t_{50\%}$ for the effective surfactant to lipid ratio R_e = 4 mol/mol was about 5 h, whereas the dissolution half time for R_e = 3.5 and 3 mol/mol is between 45 h (Figure 9), where solubilisation seems to start, and seven days, when complete solubilisation was reached (Figure 8).

A detailed analysis of the light scattering intensity curves in dependency on time – taken as a measure of solubilisation kinetics - reveals biphasic solubilisation. Such biphasic behavior has first been analysed and calculated for the dynamic surface tension measurements by Fainerman for the short times $t \to 0$ and the long times $t \to \infty$, using the Joos approximation (Joos et al. 1982) and the Fainerman approximation for the latter and the former respectively (Fainerman et al. 1994). Based on the theoretical work of Ward and Tordai (1946) for purely diffusion-controlled adsorption to an interface and desorption back into the bulk, both approximations solve the classic Ward and Tordai equation (5) by an asymptotic equation:

$$\Gamma(t) = 2c_{s,f}\left(\frac{Dt}{\pi}\right)^{0.5} - 2\left(\frac{D}{\pi}\right)^{0.5}\int_0^{\sqrt{t}} c_{s,sub}\,\mathrm{d}(t-\tau)^{0.5} \qquad (5)$$

Γ is the surface excess, D the monomer diffusion coefficient and t the solubilisation time. $c_{s,f}$ and $c_{s,sub}$ are the surfactant monomer concentrations in the bulk and the subsurface respectively. By neglecting the back diffusion at short times, $t \to 0$, and applying the Henry isotherm, the Ward and Tordai equation can be simplified (Fainerman et al. 1994):

$$\frac{\gamma(t)_{t\to 0}}{\gamma_0} = 1 - \left(\frac{2RTc_{s,f}}{\gamma_0}\right)\left(\frac{Dt}{\pi}\right)^{0.5} \quad \text{, short times} \qquad (6)$$

A long time approximation for $t \to \infty$ was derived from equation (5) by Joos et al. (1982):

$$\frac{\gamma(t)_{t\to\infty}}{\gamma_{eq}} = 1 + \left(\frac{RT\Gamma^2}{2\gamma_{eq}c_{s,f}}\right)\left(\frac{\pi}{Dt}\right)^{0.5} \quad \text{, long times} \qquad (7)$$

γ_0 , $\gamma_{t\to 0}$ and γ_{eq} are the surface tensions for t = 0 , $t \to 0$ and $t \to \infty$. RT is the thermal energy.

Lipid membranes dissolve when their surface tension approaches or equals that of the supporting bulk solution. In the kinetic solubilisation experiments reported herein, unilamellar lipid vesicles were mixed with colloidal $C_{18:1}EO_{20}$ micelle solutions. A fresh interface lipid bilayer ↔ surfactant solution was thus created. The subsequent diffusion-controlled migration and the surfactant adsorption to the interface lead to an initial dissolution, which is proportional to the square-root of solubilisation time, as suggested by equation (6) and shown in the left panel of Figure 10. In contrast linear relationship was found between the intensity decrease and the reciprocal square-root of solubilisation time at later time points (left panel in Figure 11), in line with the Joos approximation (equation (7)). With the data of this biphasic solubilisation kinetic for $C_{18:1}EO_{20}$, it is consequently possible to determine the slope of solubilisation speed in dependency on R_e to be -0.12511 $min^{-0.5}$ for the short times and to be 9.796 $min^{0.5}$ in dependency on R_e^{-1} for the long times (right panels in Figure 10 and Figure 11). I equated these slopes with the slopes of equations (6) and (7).

$$\left(\frac{2RTc_{s,f}}{\gamma_0}\right)\left(\frac{D}{\pi}\right)^{0.5} = 0.12511\,\mathrm{min}^{-0.5} \quad \text{, short times} \tag{8}$$

$$\left(\frac{RT\Gamma^2}{2\gamma_{eq}c_{s,f}}\right)\left(\frac{\pi}{D}\right)^{0.5} = 9.796\,\mathrm{min}^{0.5} \quad \text{, long times} \tag{9}$$

Using R = 8.314 $Jmol^{-1}K^{-1}$, T = 298.13 K, the surface tension of water γ_0 = 0.072 Nm^{-1}, and the bulk monomer concentration $c_{s,f}$ = CMC = 25 µM (Umbreit et al. 1973; Klammt et al. 2005), I calculated the effective diffusion constant of $C_{18:1}EO_{20}$ to be D_{eff} = 2.77 x 10^{-10} m^2s^{-1}. With this diffusion constant and equilibrium surface tension γ_0 = 0.03 Nm^{-1} (literature data only available for $C_{18:1}EO_{10}$ (Chidambaram et al. 2000; Ko et al. 2003)) I furthermore estimated the surface excess of polyoxyethylene (20) oleyl ether to be Γ ~ 0.1 nm^2 per molecule.

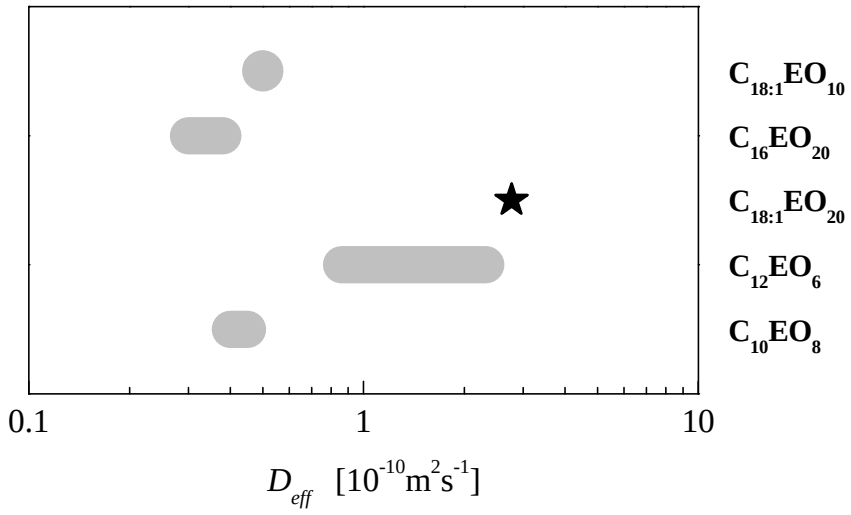

Figure 14: Effective bulk diffusion constants D_{eff} of non-ionic surfactants.
$C_{18:1}EO_{10}$ data obtained from Ko et al. (2003)
$C_{16}EO_{20}$ data obtained from Horozov et al. (1995)
$C_{12}EO_6$ data obtained from Chen et al. (2000)
$C_{10}EO_8$ data obtained from Eastoe et al. (2000)

DLS yields, albeit only indirectly, information about the effective molecular diffusion constant D_{eff} and the surface excess Γ of the tested surfactant $C_{18:1}EO_{20}$, which are in a good agreement with literature (Figure 14). The surface excess of polyoxyethylene (20) oleyl ether in a soybean phosphatidylcholine bilayer membrane with $\Gamma \sim 0.1$ nm^2 per molecule is in reasonable agreement with surface excess values for other polyoxyethylene chain containing surfactants. For example, Rösch (1971) has estimated the values for the surfactants with extended EO chains to be ~ 0.19 nm^2 and 0.28 nm^2. In POPC/surfactant membranes surface excesses of different polyoxyethylene lauryl ethers were measured to be $\Gamma = 0.26 – 0.63$ nm^2 per molecule (Lantzsch et al. 1994). In contrast to the surface excess $\Gamma \sim 0.4$ nm^2 per $C_{18:1}EO_{20}$ molecule at the water ↔ air interface (Inoue et al. 2002), the excess on lipid vesicles is significant lower due to a noticeably higher surface of a lipid molecule ($A_l = 0.63$ nm^2 (Balgavy et al. 2001)) compared to water.

2.5. Conclusion

With the solubilisation of soybean phosphatidylcholine vesicles by the surfactant polyoxyethylene (20) oleyl ether it was demonstrated that, beyond the determination of the saturation and solubilisation limit, the dynamic light scattering is a method, which can be used to analyse the solubilisation kinetics. Indirectly, the results of kinetic solubilisation measurements moreover provide information on molecule properties like the effective diffusion constant or the surface excess.

Polyoxyethylene (20) oleyl ether is a surfactant which can be used as a membrane softening component at an effective surfactant to lipid ratio of $R_e \leq 0.25$ mol/mol. The resulting high fluctuating, ultra-adaptable lipid bilayer vesicles should be able to be potential carriers for non-invasive transdermal drug delivery.

Due to its low solubilisation limit ($R_e^{sol} \approx 3$ mol/mol), its relatively high hydrophile-lipophile balance ($HLB \approx 15$), and low critical micelle concentration ($CMC \approx 10^{-5}$ M), $C_{18:1}EO_{20}$ can be used as a solubiliser, detergent or oil-in-water emulsifier in the pharmaceutical and healthcare industry. However, the concentration dependent equilibration time for saturation and solubilisation processes has to be considered for each application individually. The results collected and analysed in case of this study provide a good starting point for that.

3. BILAYER ADAPTABILITY AND ELASTICITY OF MIXED LIPID VESICLES, TRANSFERSOME®, CONTAINING POLYOXYETHYLENE (20) OLEYL ETHER, $C_{18:1}EO_{20}$

3.1. Introduction

Since their broad popularisation in 1960 – 1963, the lipid bilayer vesicles with an aqueous core, so-called liposomes, have found good usage first as models for biological cell membranes such as red blood cells (Popescu et al. 2006) and then as drug delivery systems (Gregoriadis et al. 1979) or in more modern version as long-circulating liposomes (Needham et al. 1992; Gabizon et al. 1997)).

First described in nineteen-thirties and then re-discovered and named by Bangham et al. (1965), liposomes are most often but not exclusively made from phospholipids (e.g. phosphatidylcholines), with or without additional membrane components.

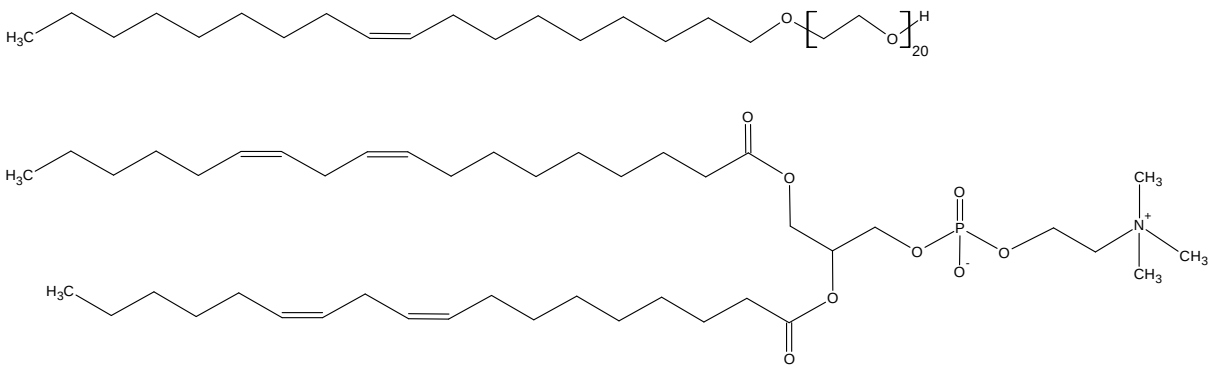

Figure 15: Structure of polyoxyethylene (20) oleyl ether, $C_{18:1}EO_{20}$, (top) and phosphatidylcholine, di-C18:2-PC (bottom).

Herein we use the word *liposome* to describe a *simple lipid bilayer vesicle*, which provides the point of reference for determining influence(s) of membrane additives on the resulting mixed lipid bilayer properties, such as the bilayer bending rigidity, κ_c. The additives, which are typically non-phospholipids (such as cholesterol, surfactants, or drugs), may increase or decrease bilayer elasticity and permeability. For example, the most popular additive cholesterol reduces permeability of phosphatidylcholine membranes for the water soluble molecules and also increases κ_c, both by acting as a bilayer stiffener (Evans et al. 1987; Duwe et al. 1990; Evans et al. 1990; Winterhalter 1995). On the other hand, it is also possible to diminish the bending rigidity of a lipid bilayer from the normally high value in the range κ_c = 5 – 50 k_bT (Winterhalter 1995), and most often around 20 k_bT (Petrov 1999), to the thermal stability limit $\kappa_c \approx k_BT$ by using suitable bilayer destabilisers. The resulting controllably

destabilised bilayer is much more flexible than a simple phosphatidylcholine membrane and more prone to fluctuate. Such membranes are referred to as *mixed lipid bilayer vesicles* in the following. The best explored vesicles with increased deformability consist of a bilayer forming lipid, like phosphatidylcholine, and a membrane softening component, like the surfactant polysorbate 80 (Cevc et al. 2004a), a bile salt (Evans et al. 1994; Cevc et al. 1998), lyso-phosphatidylcholine (Zhelev 1998), alcohols (Ly et al. 2004) etc..

Sufficiently high membrane flexibility paired with increased membrane permeability enable the resulting deformable vesicle to penetrate narrow pores, even if the constriction is far too narrow for the undeformed vesicle to fit in. The *adaptability* of such a suitably optimised ultradeformable vesicle, Transfersome®, had already been used successfully for non-invasive transdermal delivery of small (M_w < 500 Da) or big (M_w > 100 kDa) drug molecules (Cevc et al. 1996). To reach the goal, the ultradeformable vesicles loaded with a drug must penetrate the fine pores in the stratum corneum to reach even deeper target sites below application site. As introduced in chapter 1.3, the underlying transport is driven by transcutaneous water activity gradient, and thus involves carrier mediated active transport of drugs (Cevc et al. 2003a), unlike the drug transport of conventional transdermal drug delivery system (TDDS) that relies on passive drug diffusion (i.e. permeation) across the skin.

The primary objective of this study was to develop an all-purpose, ultradeformable drug carrier based on the surfactant polyoxyethylene (20) oleyl ether and the phospholipid soybean phosphatidylcholine. More specifically, I studied the surfactant induced diminution of lipid bilayer rigidity in sub-solubilisation range (cf. chapter 2.3) with different effective surfactant to lipid molar ratios $R_e = c_s/c_l$**.** This property, common to all the above mentioned membrane softeners, is the basis for making $C_{18:1}EO_{20}$ containing deformable vesicles useful for transdermal applications.

Due to the strong effect of membrane thickness d_{mem} on the bilayer's bending rigidity ($\kappa_c \propto d_{mem}^2$) (Evans 1974; Bermudez et al. 2004), the experiments were performed with unilamellar lipid vesicles. In contrast to the well established but rather difficult to use micropipette aspiration technique (Evans et al. 1987) and different optical methods (Schneider et al. 1984; Duwe et al. 1990), I measured the bending rigidity and adaptability of simple and mixed lipid bilayer vesicles with a relatively new membrane adaptability assay (CMA) (Cevc et al. 2003b). The test is based on a pressure-dependent aggregate transport across nanoporous, semi-permeable barriers with fixed size openings and in its basic form (Cevc et al. 1998; Cevc et al. 2003a) requires no fancy equipment to conduct.

3.2. Material and Methods

3.2.1. Materials

The natural, bilayer forming lipid soybean phosphatidylcholine, SPC, was purchased from Lipoid (Ludwigshafen, Germany) with the grade Lipoid S100 (purity > 90 %). As a product of biological origin, its composition of esterified unsaturated and saturated fatty acids varies. The average fatty acid content is presented in Table 5:

Fatty acids	palmitic acid C16:0	stearic acid C18:0	oleic acid C18:1	linoleic acid C18:2	linolenic acid C18:3	others
Content [%]	15.8	4.6	13.3	60.9	5.3	0.1

Table 5: Fatty acid content of natural soybean phosphatidylcholine, SPC (Avanti Polar Lipids 2006)

The non-ionic surfactant polyoxyethylene (20) oleyl ether, Brij98®, was of analytical grade and supplied from Sigma-Aldrich. Phosphate buffer salts were from VWR (Darmstadt, Germany) and aqua ad iniectabilia was from Deltaselect (Dreieich, Germany); both had European Pharmacopoeia quality.

3.2.2. Preparation of simple and mixed lipid bilayer vesicles, and of mixed micelles

Mixed micelles with an effective surfactant to lipid ratio R_e = 3.0 mol/mol and large unilamellar vesicles (LUV) with R_e = 0 - 1 mol/mol were prepared by individually mixing a clear micellar surfactant solution (10 w-% $C_{18:1}EO_{20}$ in phosphate buffer, *pH* = 7.2, 50 mM) and an opaque vesicle suspension (10 w-% SPC in phosphate buffer, *pH* = 7.2, 50 mM). The resulting blend was stirred for 2 h before extrusion through a set of different track etched polycarbonate membranes (PCTE, GE Osmonics) with decreasing pore diameter (d = 400 nm – 100 nm (Olson et al. 1979; Mayer et al. 1986; MacDonald et al. 1993)). Subsequent freeze-thaw cycles (180 min at -70°C, 30 min at 40°C) and final multi-extrusion through the PCTE membranes (d = 400 nm – 80 nm) were used to accelerate the surfactant exchange across the bilayers and to improve uniformity of final $C_{18:1}EO_{20}$ distribution between the outer and inner monolayers (Biondi et al. 1992) as well as a narrow final vesicle size distribution. The average vesicle size (d_{ves}) and polydispersity index (*PDI*) were checked by the dynamic light scattering (DLS), as is described in chapter 2.2.4.

R_e [mol/mol]	SPC suspension [mg/g]	$C_{18:1}EO_{20}$ suspension [mg/g]	d_{ves} [nm]	*PDI*	*pH*
0.00	1000	0	118.6	0.072	7.10
0.10	874	126	103.3	0.069	7.15
0.17	807	193	109.1	0.081	7.20
0.20	777	223	106.6	0.072	7.20
0.25	736	264	103.7	0.051	7.15
0.32	685	315	100.9	0.063	7.20
1.00	410	590	104.9	0.111	7.20
3.00	188	812	13.9	0.383	7.20

Table 6: Vesicle size, polydispersity index and bulk *pH* of simple and mixed lipid bilayers, and of the mixed micelles comprising soybean phosphatidylcholine (assumed $M_w \approx$ 800 g/mol) and polyoxy-ethylene (20) oleyl ether (assumed $M_w \approx$ 1150 g/mol) .

3.2.3. Membrane adaptability measurements

Experimental set-up

Continuous membrane adaptability measurement (CMA) relies on pressure driven filtration of the tested vesicle suspension through a nanoporous filter, which acts as transport obstacle for the stiff and inflexible simple bilayer vesicles with diameter d_{ves}, significantly larger than the pore size d_p (d_{ves} = 100 - 120 nm >> d_p = 20 nm). In contrast, the adaptable mixed bilayer vesicles can penetrate the barrier, which is used in the test as the "skin surrogate". Analysis of the suspension flow as a function of pressure dependency provides information on the average vesicle bilayer adaptability. The experimental set-up of a CMA device is schematically shown in Figure 16.

In a typical CMA measurement, about 3 - 10 ml of the test suspension are placed in a tempered filtering device containing a highly porous inorganic filter. The measurement is started by applying a continuously changing pressure difference Δp over the filter typically starting with Δp_s = 0.5 - 2.0 MPa and ending with Δp_f = 0.05 - 0.1 MPa. During the vesicle penetration test the time-course of pressure difference $\Delta p(t)$ and the actual filtrated mass $m(t)$ are constantly recorded using a personal computer to finally obtain experimental penetrability function:

$$P_{exp}(\Delta p) = \frac{1}{\Delta p \cdot A_f} \cdot \frac{dm}{dt} \qquad (10)$$

The value of P_{exp} is defined as a mass flow *dm* per time *dt* through the filter area A_f for each applied pressure difference Δp across the barrier. (Due to slightly noisy data points, nearest neighbour averaging is performed on the actually measured data)

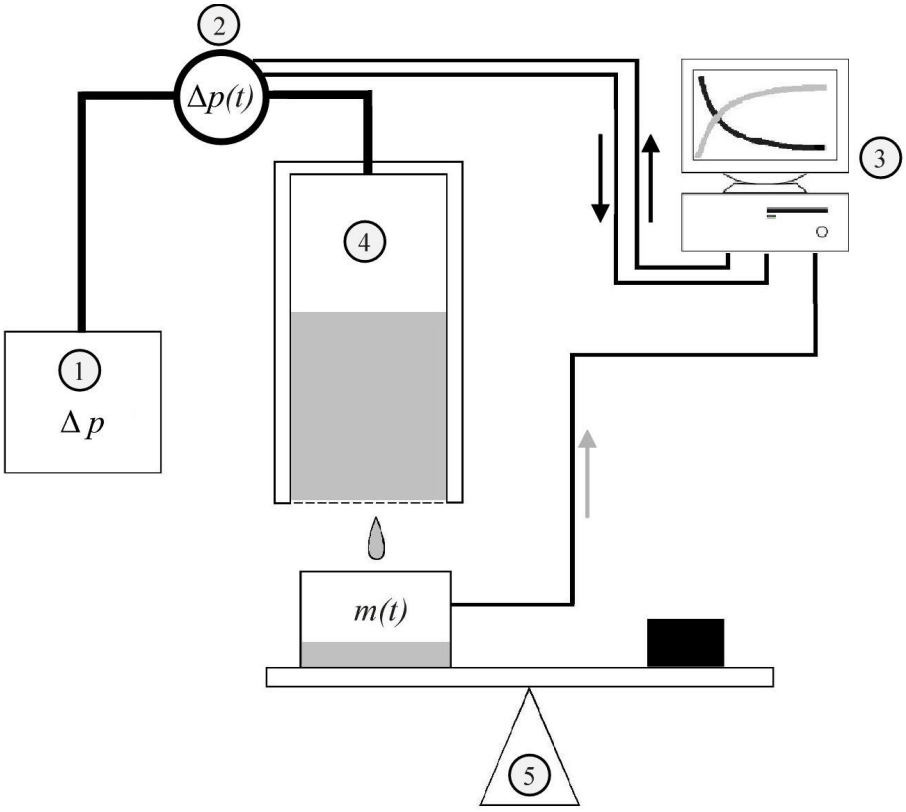

Figure 16: Schematic illustration of the set-up used for membrane adaptability measurements (CMA): (1) pressure supply; (2) pressure controller; (3) controlling and recording of pressure and filtrate weight by a computer; (4) tempered filtering device with a narrow inorganic pore filter, d_p = 20 nm; (5) analytical balance, measuring the transported suspension quantities.

Theoretical description and evaluation

The filter penetration by a vesicle suspension can be described within the framework of a thermodynamic model assuming an activated transport process (Cevc et al. 2003b). To penetrate pores smaller than the average vesicle diameter, each vesicle must deform, consuming activation energy E_A. The energy of the pore penetrating vesicle E_{ves}, consists of bilayer deformation energy W_d and, to a negligible extent, of thermal energy k_BT.

$$E_{ves} = k_BT + W_d = k_BT + \frac{1}{2} A_p l_p n_p \cdot \Delta p \qquad (11)$$

The deformation work depends on the transport-driving pressure Δp and on the dimensions of the pore with a cross section A_p and length l_p, of which there are n_p per unit area.

In thermodynamic equilibrium a distribution of energetic states with certain population density rather than just a well-defined energy level exists. The equilibrium vesicle population density n of different energetic levels can be described by the Maxwell-Boltzmann distribution (Skrdla et al. 2005):

$$n(E_A, E_{ves}) = \frac{2}{\sqrt{\pi}} \cdot E_{ves}^{-\frac{3}{2}} \cdot \sqrt{E_A} \cdot \exp\left[-\frac{E_A}{E_{ves}}\right] \tag{12}$$

Integration of equation (12) yields the ratio of the vesicles with ability for barrier penetration, i.e. the penetrability P (erf is the error function):

$$P(E_A, E_{ves}) = 1 - \mathrm{erf}\left(\sqrt{\frac{E_A}{E_{ves}}}\right) + \sqrt{\frac{4E_A}{\pi E_{ves}}} \cdot \exp\left[-\frac{E_A}{E_{ves}}\right] \tag{13}$$

Alternatively, the penetrability P can be expressed in terms of applied pressure Δp with only two fitting parameters: P_{max}, corresponding to the maximum penetrability at $\Delta p \rightarrow \infty$, and p^*, corresponding to the characteristic pressure at which the average vesicle energy equals the activation energy ($E_A / E_{ves} = 1$) when $P(\Delta p = p^*) = 0.57\, P_{max}$.

$$P(\Delta p) = P_{max} \cdot \left\{1 - \mathrm{erf}\left(\sqrt{\frac{p^*}{\Delta p}}\right) + \sqrt{\frac{4p^*}{\pi \Delta p}} \cdot \exp\left[-\frac{p^*}{\Delta p}\right]\right\} \tag{14}$$

Gompper et al. (1995) described the proportionality between E_A and p^* with a model similar to that given in equation (13), but used the more general driving field f^* instead or the threshold p^*.

The p^* value thus gauges the average vesicle's bending rigidity and the barrier's penetrability in units of inverse pressure, $a^* = 1/p^*$; this is the only vesicle-characterising parameter and independent of the other suspension parameters, such as the average vesicle size (Cevc et al. 2003b; Cevc 2004). In contrast, the P_{max} value depends on the filter and sample parameters (such as filter porosity, filter area, sample viscosity, temperature, etc.) and can be referenced to the vesicle free suspension medium.

By adjusting the curve described in equation (14) to the measured experimental penetrability curve P_{exp}, the system-specific parameters p^* and P_{max} can be derived using Levenberg-Marquard standard least square fitting procedure (Levenberg 1944; Marquardt 1963).

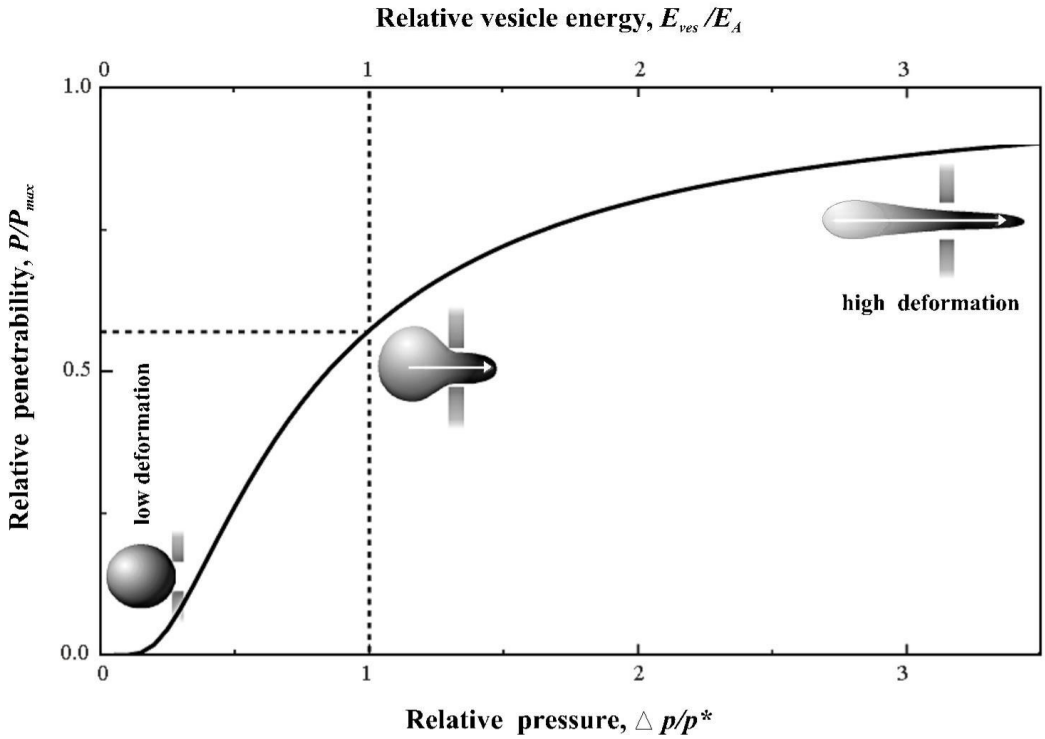

Figure 17: Illustration of relative pore penetrability P/P_{max} by a vesicle as a function of the penetration-driving pressure difference across the pore Δp and of the vesicle energy E_{ves}, based on the Maxwell-Boltzmann distribution.

3.3. Results

3.3.1. Penetrability of simple and mixed lipid bilayer vesicles, or of mixed micelles

The penetrability curves given in Figure 18 for different bilayers mixtures, made from polyoxyethylene (20) oleyl ether and phosphatidylcholine membranes, reveal an increasing ability of the vesicles with increasing R_e to penetrate narrow pores; the penetration is clearly different for the simple lipid vesicles, the mixed lipid bilayer vesicles, or the mixed micelles, however all aggregates.

The pore penetration P function for the mixed lipid vesicles with 100 - 110 nm diameter (Table 6), pressed through pores with $d_{ves}/d_p \geq 5$, increases until the effective surfactant to lipid ratio reaches R_e = 0.25 mol/mol. The flow behavior of much smaller mixed lipid micelles ($d_{mic} \approx 14$ nm) contrasts the flux of simple or mixed vesicle suspensions. Even at low trans-pore pressure differences, the colloidal suspension of mixed micelles flows nearly freely, similar to the pressure-independent flow of simple buffer solution through the filters (cf. Figure 19 and Cevc et al. (2003b; 2004)).

The mixed micelles with a relative size of d_{mic}/d_p = 0.7 can thus demonstrably pass the obstacle without any difficulty or transformation.

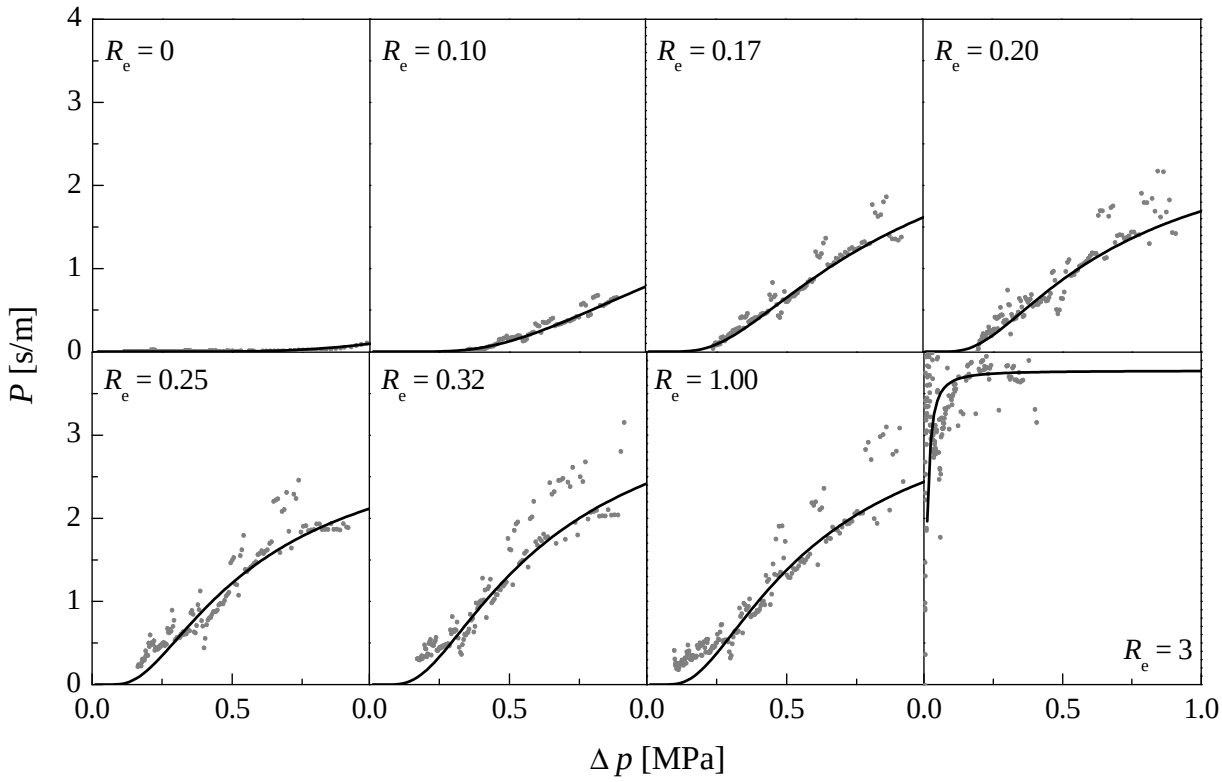

Figure 18: Pore penetrability in dependency of the driving pressure (*P* values — P_{exp} data ●) for a suspension of simple lipid vesicles (top left; R_e = 0 mol/mol, $d_{ves}/d_p \geq 5$) or for the mixed bilayer vesicles (from top left to bottom right) with different molar surfactant to lipid ratios R_e; the corresponding mixed micelles are shown for reference (bottom right; R_e = 3 mol/mol, $d_{mic}/d_p \leq 0.7$). With increasing relative $C_{18:1}EO_{20}$ content the pore penetration ability of mixed lipid vesicles increases. For the mixed micelles, no significant pressure dependency is observed.

Simple lipid bilayers, liposomes, with an average size ($d_{ves} \approx 120$ nm) comparable to that of the tested mixed lipid bilayer vesicles are nearly unable to penetrate a nanoporous filter when driven with a pressure difference of up to $\Delta p \leq 1$ MPa; a driving pressure at which the mixed lipid bilayer vesicles show a high and increasing penetrability depending on R_e. The small amount of liposomes, which have passed the filter at the high driving pressure, have arguably been ruptured rather than deformed during the narrow pore penetration. This is evidenced by approximately -50 % reduction in the average vesicle size after penetration compared to the starting value. The mixed lipid vesicles, in contrast, retain their original size within -10 – -20 % size reduction. (The higher is the suspension flux the greater degree of fragmentation, probably owing to the corresponding increase in shearing force (1 MPa), especially at the measurement's start (data not shown)).

A more detailed and quantitative comparison of the data measured with the tested mixed lipid bilayer vesicles in Figure 19 requires penetrability curves fitting. This then reveals an increase in penetrability values with increasing $C_{18:1}EO_{20}$ contents in phosphatidylcholine bilayers, up to the limiting surfactant to lipid ratio of $R_e \geq 0.25$ mol/mol = R_e^{sat}, where the membrane is saturated with the surfactant and vesicle solubilisation begins (cf. chapter 2.3.1).

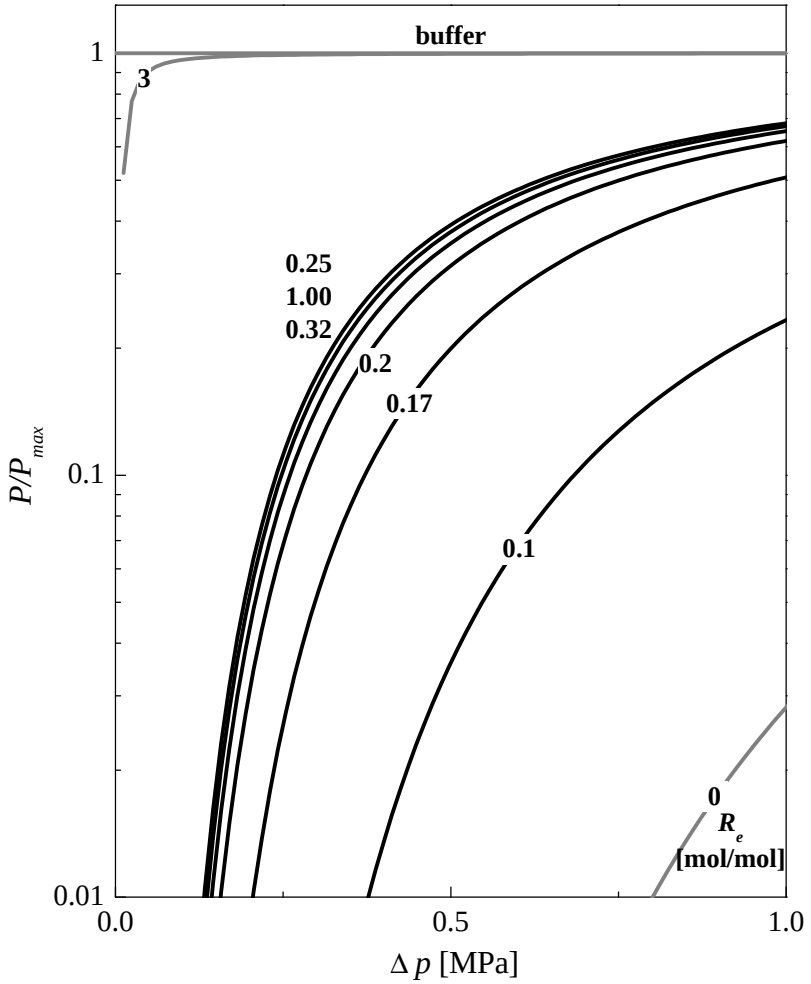

Figure 19: Relative penetrability P/P_{max} curves for the mixed lipid vesicles with different $C_{18:1}EO_{20}$ to SPC molar ratios, R_e. Pure buffer and mixed micelle suspension (R_e = 3 mol/mol) data, as well as results of measurements with simple lipid vesicles (R_e = 0 mol/mol) are shown for comparison.

As soon as lipid solubilisation is complete, leaving the mixed lipid micelles as the only residual aggregate form, the penetrability curve becomes nearly pressure independent and is comparable to that of a pure buffer solution. The reason is that $p^* \rightarrow 0$ makes the model underlying equation (14) no longer applicable due to the fact that for the mixed micelles with an aggregate size smaller than the pores deformation is no longer necessary.

3.3.2. Adaptability of simple and mixed lipid bilayer vesicles, or of mixed micelles

The characteristic pressure p^* at which the average vesicle energy equals the pore penetration activation energy decreases with increasing R_e up to the membrane saturation limit R_e^{sat}. This is highlighted logarithmically in Figure 20. In other words: at R_e^{sat} = 0.25 mol/mol the maximum possible vesicle shape adaptability is therefore reached (in inverse pressure terms: $a^* = 1/p^* \approx 1.5$ MPa^{-1}). This emphasises polyoxyethylene (20) oleyl ether ability to lower the activation energy for pore penetration by the vesicles containing such surfactant, and thus for membrane deformation. Compared to simple (R_e = 0 mol/mol) or mixed bilayer vesicles with relatively low surfactant content (R_e = 0.1 mol/mol), the adaptability of mixed lipid bilayer vesicles saturated with $C_{18:1}EO_{20}$ is improved by a factor of 8 for the former and by 3 for the latter composition.

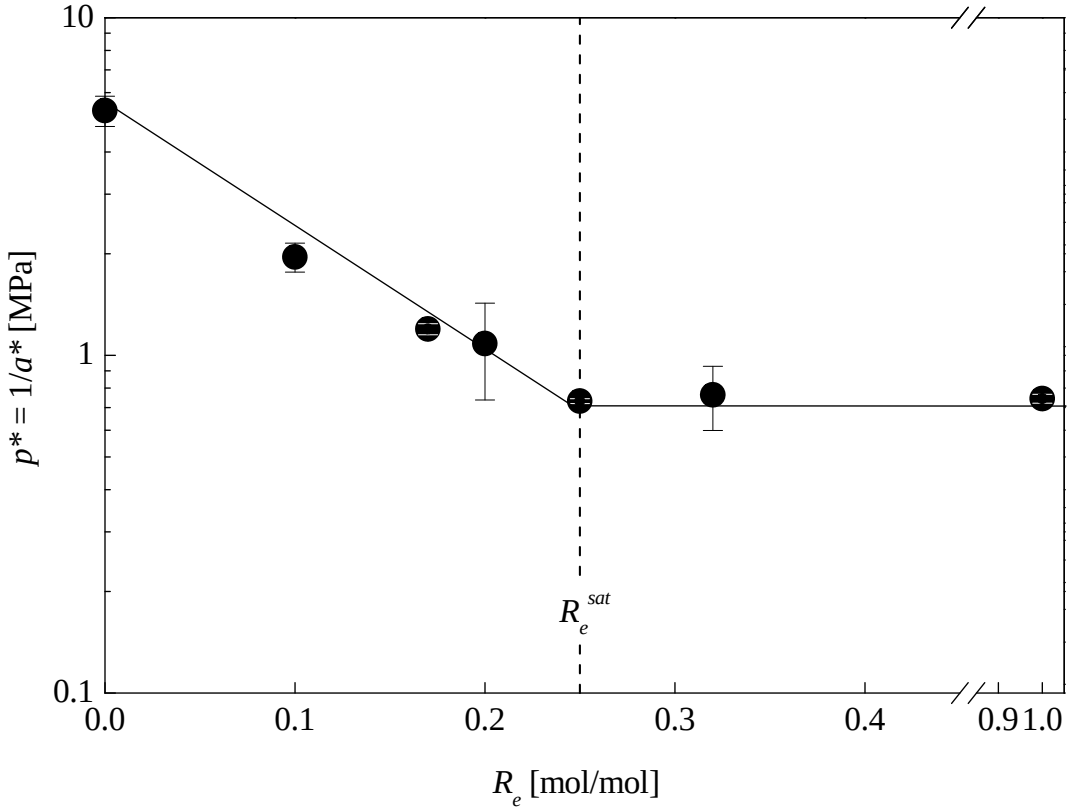

Figure 20: Characteristic pressure p^* in dependence of different molar surfactant to lipid ratio R_e. With increasing R_e the p^* value, at which the average vesicle energy equals the activation energy, decreases up to the saturation limit R_e^{sat} = 0.25 mol/mol, highlighted logarithmically through the triple measured data points (●).

3.4. Discussion

The use of phosphatidylcholine bilayer vesicles in research and pharmaceutical products is sensitive to their physico-chemical properties, such as the average vesicle size, lipid bilayer phase (gel or fluid), membrane permeability, bilayer elasticity, etc. The latter property is a topic that has been intensively studied and discussed for both simple and mixed lipid bilayers vesicles, with or without a second membrane component. Mixtures of phosphatidylcholine with various surfactants, monoacyl-phosphatidylcholines, alcohols, cholesterol, etc. provide ample examples for that.

Polyoxyethylene fatty alcohol ethers are edge-active compounds that can influence phosphatidylcholine bilayers rather strongly ((Heerklotz et al. 2000a). Within the framework of this work, I studied relative surfactant concentration effect on the pore penetration ability of the mixed lipid vesicles comprising SPC and $C_{18:1}EO_{20}$, which yielded information not only on vesicle adaptability a^* or the corresponding lipid bilayer bending rigidity κ_c but also on lipid bilayer solubilisation, which I had studied independently to even greater level of detail with the static and dynamic light scattering in chapter 2.

Membrane saturation limit

Polyoxyethylene (20) oleyl ether is a rather "strong" surfactant that can disintegrate lipid bilayers at surfactant/lipid ratio $R_e^{sat} < 1$ mol/mol (Heerklotz et al. 2000a); the substance also possesses a relative high partition coefficient in phosphatidylcholine bilayers: $\log K \approx 4$ M^{-1} (Heerklotz et al. 2000b), due to its relatively low *CMC* = 25 µM (Umbreit et al. 1973; Klammt et al. 2005). As a result, the saturation limit of SPC membranes with $C_{18:1}EO_{20}$ is quite low as is illustrated in Figure 20 and as has also been confirmed in chapter 2.3.1. Both, membrane adaptability and the light scattering measurements thus reveal similar membrane saturation limit of $R_e^{sat} = 0.25$ mol/mol.

Penetrability curves for the mixed lipid bilayers with $R_e^{sat} \geq 0.25$ mol/mol do not differ from each other. This is indicative of progressive lipid solubilisation, leading to progressive formation of mixed micelles co-existing with a diminishing number of surfactant-saturated mixed lipid vesicles above this ratio. The composition of the mixed lipid vesicles in the solubilisation range ($R_e \approx 0.25 - 3.0$ mol/mol) is arguably constant and independent of R_e (Levy et al. 1990) causing all vesicles above R_e^{sat} to have approximately similar energy E_{ves}.

Thus, the same membrane deformation energy E_A is necessary for pushing the vesicles through narrow pores, according to equation (13), explaining congruent penetrability curves at low penetration driving pressures.

Membrane adaptability and bending rigidity

The deformation energy E_A involved in pore penetration is proportional to the membrane bending rigidity κ_c, as described by the Helfrich Hamiltonian (Helfrich 1986). This is to say that the shape and fluctuations of lipid bilayer vesicles are controlled by κ_c, as the total energy for membrane deformation is independent of vesicle size (Helfrich 1973). The independency is explicable for the pore penetration by the spherical vesicles of different sizes ($d_{ves} > d_p$), when the work of vesicle deformation stems nearly exclusively from the highly curved ends of the resulting spherocylinder (Cevc et al. 2003b; 2004).

Bending rigidity of various phosphatidylcholine bilayers has been measured to be between 5 k_bT and 50 k_bT, depending on the hydrocarbon chains composition (Winterhalter 1995). The actual value is particularly sensitive to the fatty acid chains length and the degree of unsaturation: in contrast to the di-saturated and mono-unsaturated phosphatidylcholine bilayers, poly-cis-unsaturated membranes are more elastic (Beblik et al. 1985; Rawicz et al. 2000).

To compare elasticity of soybean phosphatidylcholine membranes containing polyoxyethylene (20) oleyl ether in terms of κ_c, a bridging between the measured characteristic pressure p^* and bilayer bending rigidity must be done. Due to proportionality $E_A \propto \kappa_c \propto f^* \propto p^*$ (Gompper et al. 1995), the bending rigidities and inverse adaptabilities of different SPC/$C_{18:1}EO_{20}$ mixed bilayer membranes can be scaled, in the first approximation, as follows:

$$\kappa_c = \frac{p^* \cdot \kappa_{c,l}}{p_l^*} \tag{15}$$

p_l^* is the characteristic inverse adaptability of simple SPC bilayer vesicles, and $\kappa_{c,l}$ the corresponding bilayer bending rigidity. Unfortunately, to the best of my knowledge, no $\kappa_{c,l}$ value for simple soybean phosphatidylcholine bilayer membranes has been published to date. I therefore estimated $\kappa_{c,l}$ by considering the fatty acids chains composition of SPC and calculating $\kappa_{c,l}$ additive with the proportionate bilayer bending rigidities of the different diacyl-phosphatidylcholines in SPC.

Fatty acids	$C_{16:0}$	$C1_{8:0}$	$C_{18:1}$	$C_{18:2}$	$C_{18:3}$	$C_{20:4}$	others
κ_c [k_BT]	48.6 [a]	43.7 [a]	20.7 [b]	10.7 [b]	9.2 [b]	10.7 [b]	-------
EPC [%] [c]	34.0	11.0	32.0	18.0	-------	3.3	1.7
SPC [%] [c]	15.8	4.6	13.3	60.9	5.3	-------	0.1

	$\kappa_c^{measured}$	$\kappa_c^{calculated}$
EPC	26.7 – 27.9 k_BT [d,e]	30.7 k_BT
SPC	n.a.	19.5 k_BT

Table 7: Estimation of κ_c for the simple soybean phosphatidylcholine bilayers based on proportionate bending rigidities of different diacyl phosphatidylcholines in SPC.
The same estimate for egg-yolk phosphatidylcholine (EPC) yields a result consistent with published data.
[a,b] Bending rigidity for diacyl-PCs obtained from Beblik et al. (1985)[a] and Rawicz et al. (2000)[b]
[c] Fatty acid composition of EPC and SPC obtained from Avanti Polar Lipids (2006)
[d,e] Bending rigidity for EPC obtained from Duwe et al. (1990)[d] and Schneider et al. (1984)[e]

As a control for the estimate, literature data of κ_c for egg-yolk phosphatidylcholine (EPC) were used and are listed together with the calculated results in Table 7. For EPC a bending rigidity of κ_c = 30.7 k_BT was calculated, which is in a good agreement with published measured results κ_c = 26.7 – 27.9 k_BT (Schneider et al. 1984; Duwe et al. 1990). SPC bilayer membranes should then have a slightly lower value $\kappa_{c,l}$ = 19.5 k_BT, and thus a higher elasticity. Therefore, SPC seems to be better suited as educt for manufacturing ultradeformable, mixed carrier vesicles in combination with $C_{18:1}$EO20 than EPC.

Nevertheless, the bending rigidity of simple SPC vesicles is much higher than the required low bending rigidity of ultradeformable carriers, which is and should be in the range of $\kappa_c \approx k_BT$ (Safinya et al. 1989; Gompper et al. 1995; Cevc et al. 1998).

Edge-active substances with a high affinity for the strongly curved membranes lower the vesicle deformation energy by way of curvature-induced lateral demixing of membrane components; this leads to accumulation of the membrane softening ingredients in the most curved parts of the deformed bilayer vesicle (Gompper et al. 1995; Cevc et al. 1996; Cevc et al. 2003b). A significantly higher artificial and mammalian skin penetrability for the mixed, surfactant containing bilayer membranes compared to simple lipid bilayer vesicles has indeed been reported (Bouwstra et al. 2003; Cevc et al. 2003a; Cevc et al. 2003b; Cevc et al. 2004a).

The non-ionic, edge-active, surfactant polyoxyethylene (20) oleyl ether was shown in this study to reduce κ_c in concentration dependent manner by nearly a factor of 8; from $\kappa_c \approx$ 19.5 k_BT for simple SPC vesicles the mixed bilayer elasticity energy decreases to $\kappa_c \approx$ 2.5 k_BT for

the membranes with 20 mol-% $C_{18:1}EO_{20}$ in the SPC matrix. Figure 21 illustrates the phenomenon for $C_{18:1}EO_{20}$ up to 20 mol-%, which corresponds to the membrane saturation limit R_e^{sat} = 0.25 mol/mol. Beyond this threshold, the surfactant starts to dissolve some bilayer vesicles resulting in coexistence of mixed bilayer vesicles, with essentially constant properties, and the corresponding mixed micelles, with no aqueous core and practically zero penetration resistance in case of 20 nm pores.

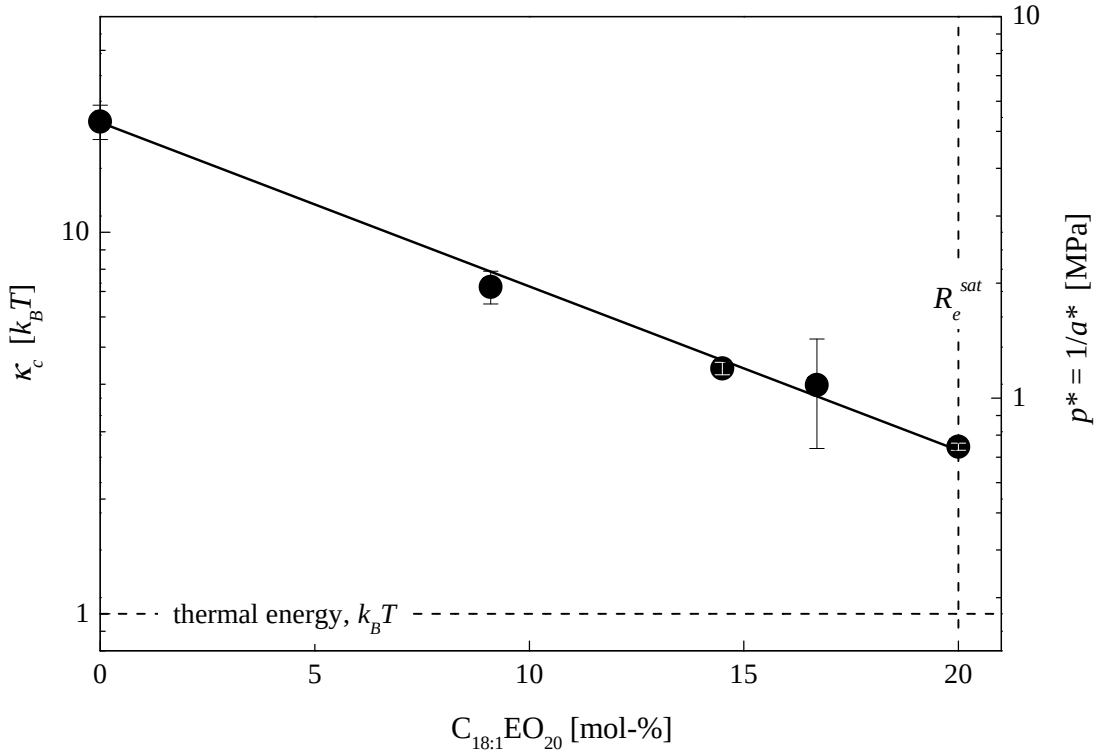

Figure 21: Bending rigidity, κ_c, and characteristic pressure, p^*, in dependency on the molar ratio of $C_{18:1}EO_{20}$ in the lipid bilayer membrane.
The bending rigidity of simple soybean phosphatidylcholine vesicles with $\kappa_c \approx 20\ k_BT$ softens to a low value of $\kappa_c \approx 2.5\ k_BT$ at the saturation limit with 20 mol-% $C_{18:1}EO_{20}$ in ultradeformable carrier vesicles, Transfersome®.

The bending rigidity $\kappa_c \approx 2.5\ k_BT$ of the $C_{18:1}EO_{20}$ saturated bilayer membranes approaches optimum elasticity of ultradeformable bilayer vesicles near the thermal energy k_BT. This is illustrated in the computer simulation of pore penetration by a vesicle with a bending energy of 2 k_BT in Figure 22 (Gompper et al. 1995). By inference, such mixed bilayer vesicles are flexible enough to penetrate also even narrow hydrophilic pathways in the stratum corneum of mammalian skin.

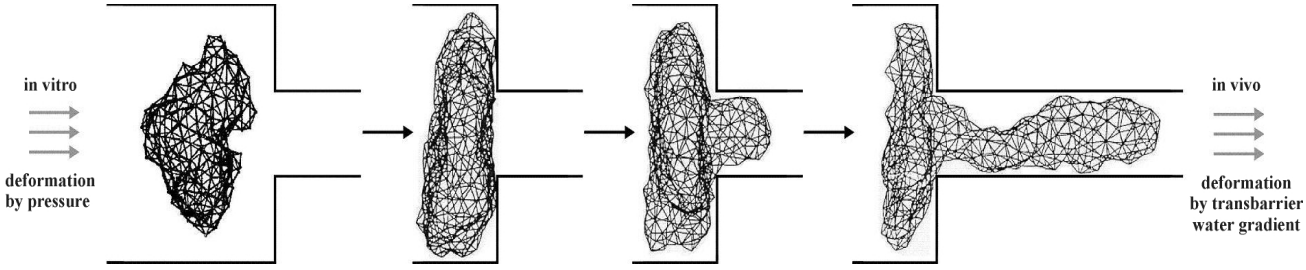

Figure 22: Computer simulation of vesicle penetration through pores with $d_p << d_{ves}$.
The ultradeformable vesicle with a bending rigidity of 2 k_BT can penetrate through artificial or human skin pores driven by an applied pressure (in vitro) or a transbarrier water gradient (in vivo) (Adapted and modified from Gompper et al. (1995)).

Highly flexible, and fluid vesicles transport through the stratum corneum is detectable by electron microscopy as well, e.g. in the freeze fractures micrographs of the skin-strip tapes shown in Figure 23. Related data have been published for other kinds of elastic vesicles, composed of a bilayer-forming non-ionic surfactant plus a micelle-forming ionic surfactant (Honeywell-Nguyen et al. 2002).

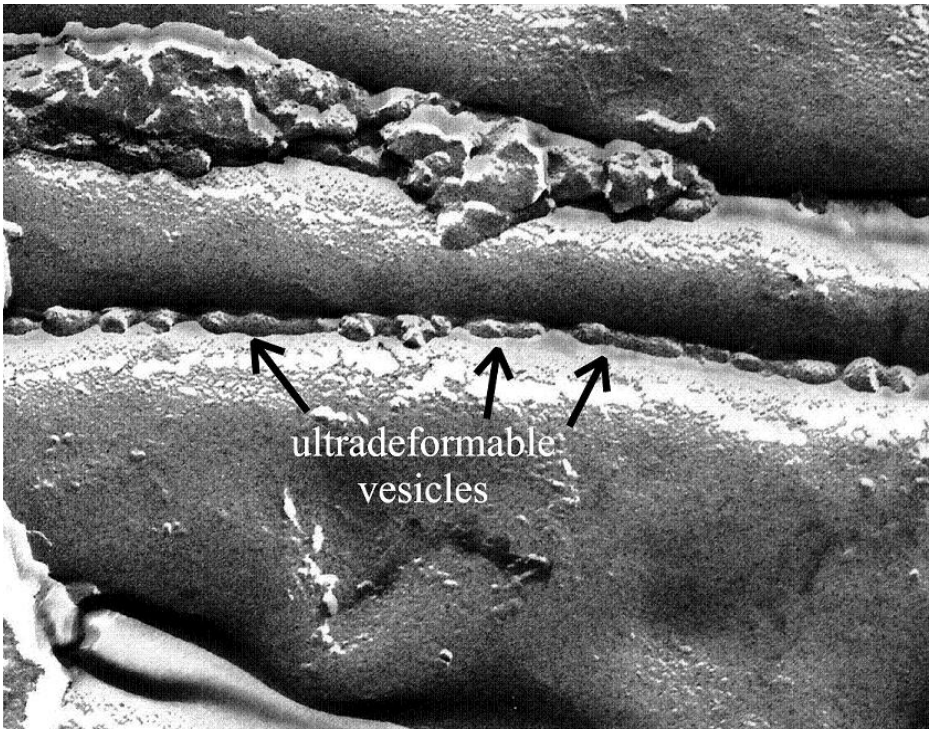

Figure 23: The skin: freeze fracture electron micrograph of ultradeformable vesicles in hydrophilic skin pores of the stratum corneum.
(by courtesy of Prof. Dr. J. Bouwstra)

Mixed micelles

Penetrability curves of mixed micelles and mixed lipid bilayer vesicles are shown in Figure 19. Coexistence of both such aggregate types between R_e^{sat} = 0.25 mol/mol and R_e^{sol} = 3 mol/mol should also be reflected in detailed penetrability data derived from the corresponding suspensions. However, the penetrability fits given in Figure 19 reveal no significant difference between the surfactant saturated vesicle suspension and the suspension containing a mixture of such vesicles and mixed micelles. This is not surprising given that equation (14) only allows for one kind of penetrating aggregates. One therefore has to revert to the raw data, and focus on the low pressures regime to see anomalies (cf. Figure 18): at $\Delta p \rightarrow 0$ the measured penetrability is slightly increased compared to the penetrability fit derived using equation (14). This is an indication of the relatively higher rate of micellar suspension penetration at low pressures compared to vesicles suspension. Co-consideration of vesicles and micelles with the following formula

$$P_{tot}(\Delta p) = \alpha_{mic} \cdot P_{mic}(\Delta p) + (1-\alpha) \cdot P_{ves}(\Delta p) \tag{16}$$

thus permits calculation of the micellar fraction α_{mic} in the tested suspension.

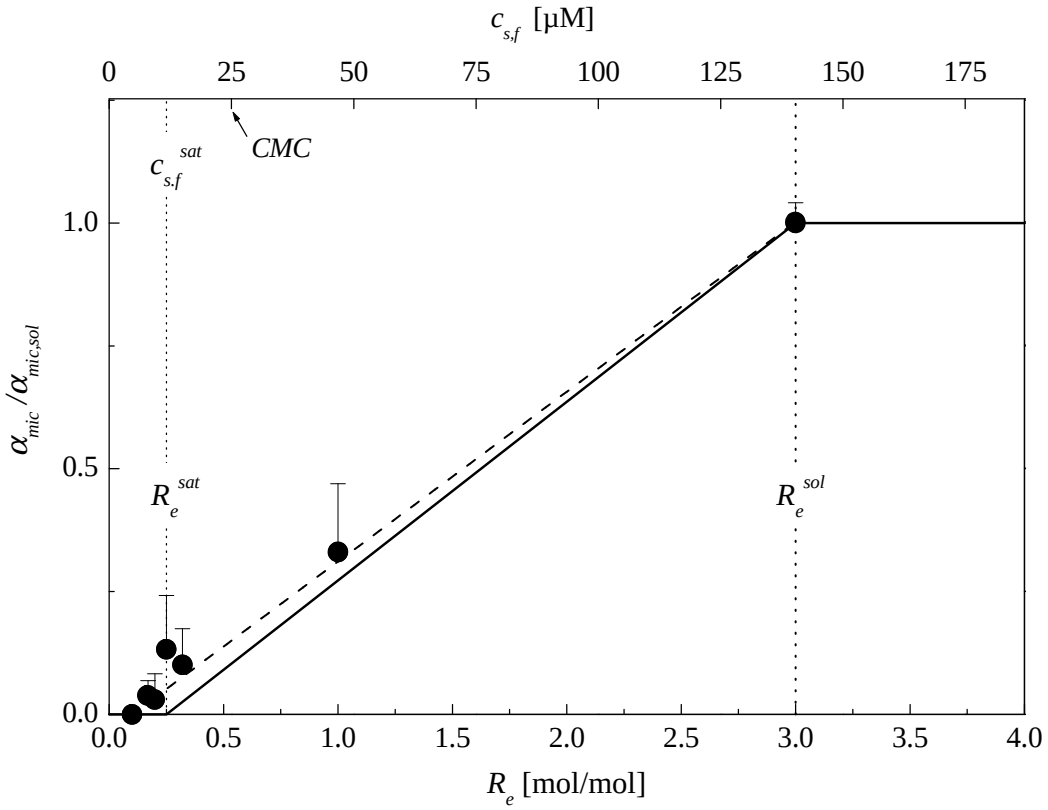

Figure 24: Relative micellar concentration $\alpha_{mic}/\alpha_{sol}$ in dependence of the surfactant to lipid ratio, R_e or the free surfactant concentration $c_{s,f}$, respectively. The micellar fraction increases between R_e^{sat} and R_e^{sol} linear as is described by Levy et al. (1990) (solid line), however with a slight micelle detection below R_e^{sat} (dashed line, r = 0.999).

Figure 24 suggests a linear increase of micellar fraction with increasing surfactant to lipid ratio R_e till complete solubilisation is reached at R_e^{sol} = 3 mol/mol. The linear and continuous formation of micelles is consistent with the results of Levy et al. (1990) and Heerklotz et al. (1994). The former determined phospholipid and surfactant concentrations in the supernatant and pellet of ultracentrifuged suspensions and reported a linear increase for the former and a linear decrease for the latter component between R_e^{sat} and R_e^{sol}. Given the micellar size constancy in this range (cf. Figure 8 in chapter 2.3), the number of mixed micelles should therefore increase linearly between R_e^{sat} and R_e^{sol}, in agreement with our finding.

Existence and detection of mixed micelles is not limited to the range of progressive vesicles solubilisation between R_e = 0.25 – 3 mol/mol, however. I also detected some micelles below that range, for R_e = 0.17 - 0.25 mol/mol. An explanation could be the high used total surfactant concentration, which had been c_s = 10 – 23 mM in the latter range of R_e values. With the molar partition coefficient value of log $K \approx 4.3$ M^{-1} (Heerklotz et al. 2000a; 2000b) the corresponding free, i.e. monomeric non-aggregated, surfactant concentration is calculated from equation (17) to be $c_{s,f}$ = 9 – 12 µM, which is close to *CMC* = 25 µM (Umbreit et al. 1973; Klammt et al. 2005).

$$c_{s,f} = c_s - \frac{K \cdot c_l}{1 + K \cdot c_l} \cdot c_s \qquad (17)$$

Lichtenberg et al. (1993; 2000) reported for most surfactants a free monomer concentration at the saturation limit $c_{s,f}^{sat} < CMC$. Depending on total lipid and surfactant concentrations he considered the formation of mixed micelles below R_e^{sat} and $c_{s,f}^{sat}$, respectively, a possibility especially for highly concentrated vesicle suspensions used in this work.

3.5. Conclusion

With this study it was shown that it is possible to correlate results of membrane adaptability measurements with several key properties of simple and mixed lipid bilayer vesicle membranes. Most importantly, I have shown that the adaptability a^* of such vesicles can be assessed and translated into bilayer bending rigidity κ_c, using a suitable phenomenological theoretical model. We furthermore provided an experimental alternative for measuring the saturation limit R_e^{sat} of surfactants in lipid bilayers compared to the more conventional, mostly spectroscopic, methods. Such physical option had been, indeed, demanded by Lichtenberg et al.(1983) long ago, and seems to be suitable for this purpose, whilst being also indicative of the tested vesicles ability to cross narrow pores. Better resolved CMA curves, in

the future, could also be used to detect the presence of micelles in a suspension of lipid vesicles, and to quantify the concentration of the former. A good estimate of the latter was achieved already with the current set-up.

Polyoxyethylene (20) oleyl ether is a “strong” surfactant with concentration dependent, but on the whole excellent, membrane softening activity. Using this surfactant and soybean phosphatidylcholine, ultra-adaptable bilayer vesicles can be produced, provided that the surfactant/lipid concentrations ratio is kept below $R_e \leq 0.25$ mol/mol.

The results collected and analysed in this study provide a good starting point for future practical developments based on such all-purpose ultradeformable vesicles, Transfersome®, with the intended use as carriers for either low or high molecular weight drugs for non-invasive transdermal drug delivery.

4. WATER-MEMBRANE PARTITIONING AND DISTRIBUTION OF BUPIVACAINE AND KETOPROFEN IN BILAYERS IN DEPENDENCY ON *pH* AND ELECTROSTATICS

4.1. Introduction

The pharmacokinetic and pharmacodynamic characteristics of a new drug molecule, or a well-established drug with a new indication or application form, are important and interesting in therapeutic product development. The hydrophilicity ↔ lipophilicity ratio often relates to the drug's biological properties, as observed during **A**bsorption, **D**istribution; **M**etabolism, and **E**xcretion. Beyond ADME, the drug's interaction with specific and unspecific targets (receptors, enzymes, proteins etc.) may also depend on relative hydrophilicity or lipophilicity of the active agent.

The widely used determination of 1-octanol/water partition coefficient, $P_{o/w}$, can yield useful information on the drug's relative lipophilicity. However, 1-octanol is not a biological molecule. It is therefore much better and more relevant to study the drug's partition coefficient between phospholipids and water, P_{mem}, which can be measured using lipid bilayer membrane vesicles. The membrane model simulates physiological drug surrounding more precisely than an isotropic solvent, such as 1-octanol. In vitro pharmacokinetic and pharmacodynamic properties are thus correlated better with an in vivo situation in which numerous membrane ↔ drug interactions are expected during ADME, e.g the transcellular passage of an orally applied drug through lipid bilayers in the intestinal epithelium.

Beyond pharmacological aspects, galenic problems can also be tackled by studying bilayer membrane partition and distribution coefficient. Optimum loading of a drug on/into lipid vesicles is among others a major key in the development of good pharmaceutical products based on lipid bilayer vesicles (Langner et al. 1999; Cevc et al. 2001; 2004a; Allison 2007; Rother et al. 2007). Knowledge of P_{mem} will thus provide a good basis in galenic research works.

In contrast to the common shake-flask method (Bouchard et al. 2002), which is used for $P_{o/w}$ but inapplicable to P_{mem} determination, the drug membrane partition coefficient can be measured using different methods such as ultrafiltration (Austin et al. 1995), titration (Avdeef et al. 1998), dialysis (Kramer et al. 1998), immobilized artificial membrane (IAM)-HPLC (Ottiger et al. 1999), and the predictable quantitative structure activity relationship

simulations (QSAR) (Patel et al. 2001). Each of these methods has its merits, but *pH*-metric titration is the only one that allows determination of partition and distribution coefficients as a function of the drug dissociation.

The current commercial drug substances can be divided into three groups (Balon et al. 1999): bases (75 %), acids (20 %) and neutral molecules (5 %). The basic or acidic drugs often coexist in a charged and neutral form, dependent on the formulation or ambient *pH*. Detailed *pH*-metric titrations by Avdeef (2003) showed that for the neutral molecules the partition coefficient in bilayer membranes is comparable with that in 1-octanol, $P^N_{mem} \approx P^N_{o/w}$, while for the ionized drug form the partition coefficient is significantly higher in a membrane than in 1-octanol, $P^I_{mem} >> P^I_{o/w}$. Therefore, the resulting *pH* dependent drug distribution coefficient, D_{mem}, is higher in the membrane at *pH* values where the ionized species predominates.

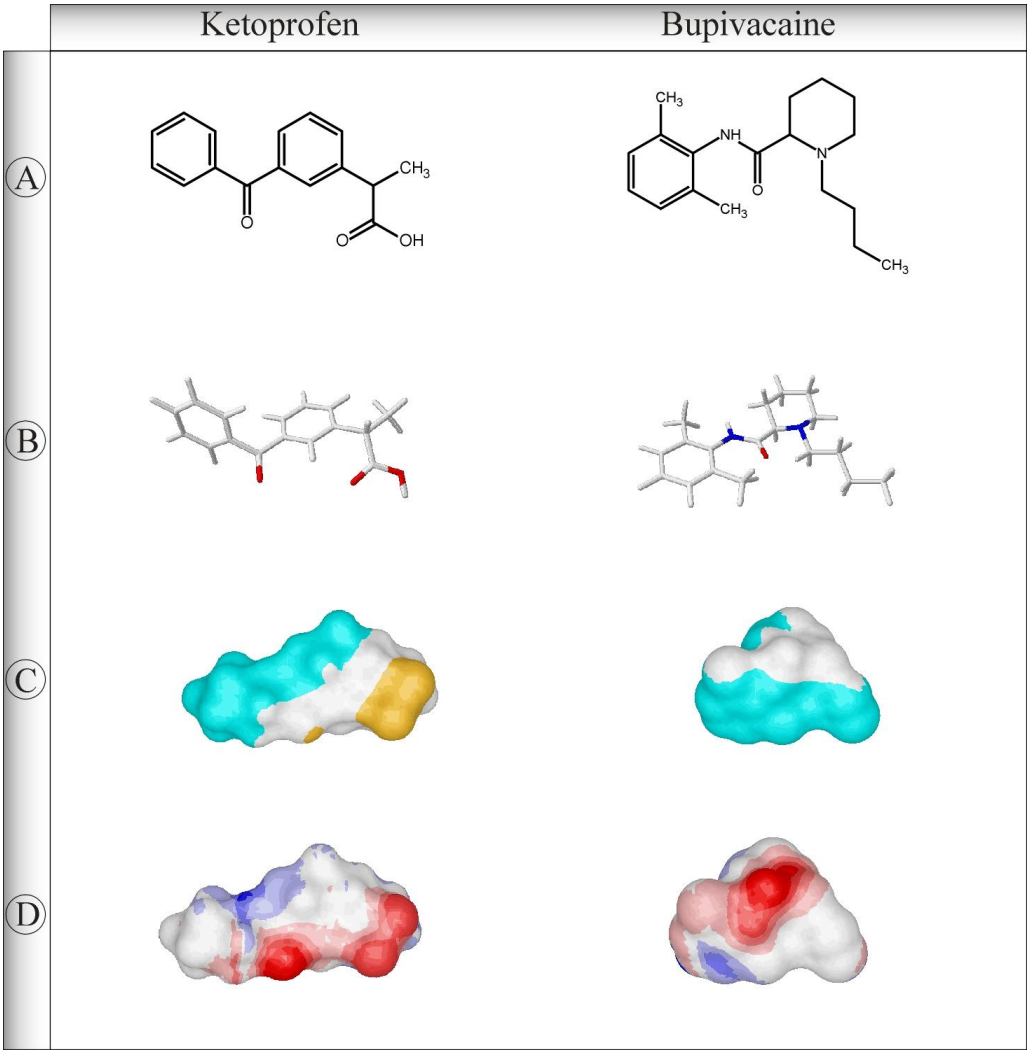

Figure 25: Structures of the acid ketoprofen (left) and the base bupivacaine (right). (A) chemical structure; (B) 3-D structure; (C) surface lipophilicity; (D) surface charge (Generated with HyperChem.)

Drug partitioning into membranes is also sensitive to electrostatic and polarity effects, and to interactions between the drug molecules and phospholipid bilayers (Cevc et al. 1987). This explains why different salt concentrations (Bauerle et al. 1991; Alcorn et al. 1993; Thomas et al. 1993; Austin et al. 1998) or different choice of phospholipids, such as phosphatidylcholine, phosphatidylethanolamine, and phosphatidylserine (Langner et al. 1995; Pedros et al. 1997; Takegami et al. 2005), influence P^{I}_{mem} and D_{mem}.

I therefore studied partitioning and distribution of the basic local anaesthetic bupivacaine and of the acidic non-steroidal anti-inflammatory drug (NSAID) ketoprofen (Figure 25) into bilayers of soybean phosphatidylcholine. I measured the drug partitioning in this work in dependency on the bulk *pH* but also explored the influence of salt concentration on equilibria. To the best of my knowledge, no bilayer membrane partitioning data have been published for these molecules to date, at least not considering electrostatic interactions between the drugs and the membrane in parallel. Such interactions are important, however, in designing drug containing ultradeformable bilayer membranes, with the intended use as vesicular carriers for transdermal drug delivery (Cevc et al. 2003b; Cevc 2004).

The outcome of the present study will confirm observations of different authors which also measured and considered electrostatic effect on drug membrane distribution. Unfortunately, numerousness partition and distribution coefficient data published for various drugs and excipients to date neglect such electrostatic interactions. With the results of the following partition coefficient measurements, I tried to study drug partitioning as a function of bilayer's charge density, surface potential, and polarity, finding out that these interactions are substantial when measuring and presenting P^{N}_{mem}, P^{I}_{mem}, and D_{mem}.

4.2. Theoretical background

The dissociation constant, pK_a, of an ionizable acid or base in water is defined as the negative common logarithm of the dissociation equilibrium, K_a,

$$pK_a = -\log K_a \quad = -\log \frac{[H_3O^+][A^-]}{[AH]} \quad \text{for acids}$$
$$= -\log \frac{[H_3O^+][B]}{[BH^+]} \quad \text{for bases} \qquad (18)$$

with a *pH* dependent dissociation degree, α, defined as:

$$\alpha = \frac{10^{pH-pK_a}}{10^{pH-pK_a}+1} \qquad (19)$$

Any drug's dissociation is influenced by polar and electrostatic effects involving the surrounding solvent as well as ions. Dissociation constant is therefore different in a lipid bilayer membrane, pK_{mem}, and in water, pK_a. *pH*-metric titration of an acid or base in lipid bilayer vesicles suspension therefore yields an effective dissociation constant for the molecules in contact with water and with lipid aggregates. The relationship is not a straight one however, but rather a result of four coupled equations of equilibrium, as is illustrated in Figure 26.

The resulting apparent dissociation constant, pK_{app}, depends on partition coefficients of the charged and the neutral drug forms, P^I_{mem} and P^N_{mem}, respectively, as well as on the pK_a and pK_{mem} values, with the apparent value being between the two.

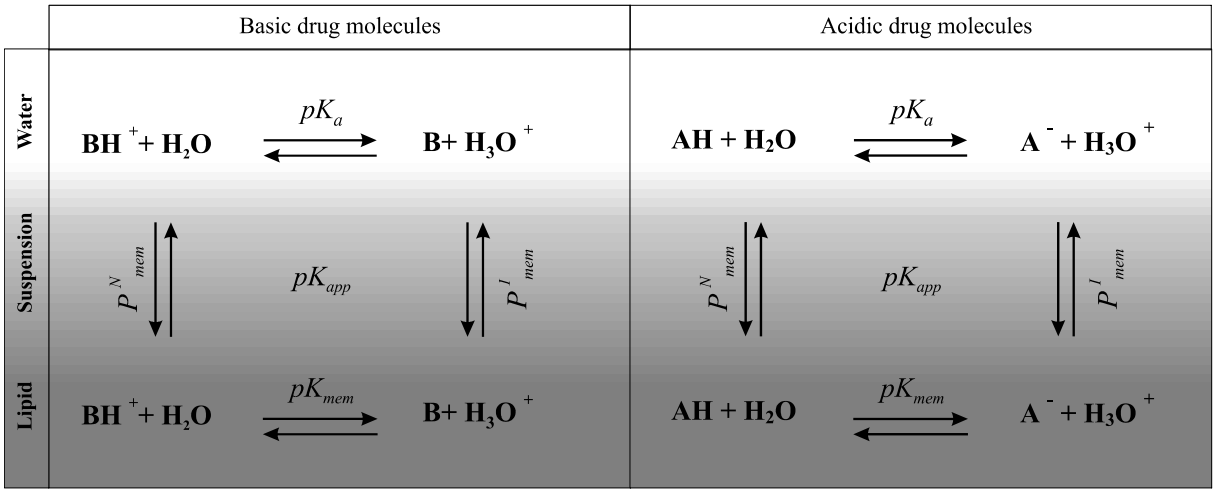

Figure 26: Schematic illustration of dissociation and partitioning of bases (i.e. cationic acids) and acids in a system consisting of an aqueous bulk phase and lipid bilayer membranes.

The charge-specific partition coefficients for the neutral and for the ionized molecules can be calculated from the respective, directly measured, drug concentrations in the bilayer membrane, c_{mem}, and in water, c_w (Miyazaki et al. 1992):

$$P^N_{mem} = \frac{c^N_{mem}}{c^N_w} \qquad\qquad P^I_{mem} = \frac{c^I_{mem}}{c^I_w} \tag{20}$$

The associated *pH* dependent, phenomenological drug distribution coefficient, D_{mem}, considers both the neutral and ionized molecules (Miyazaki et al. 1992):

$$D_{mem} = \frac{c^N_{mem} + c^I_{mem}}{c^N_w + c^I_w} \tag{21}$$

Alternatively, by measuring the apparent dissociation constants, $pK_{app}(j)$, for at least two different lipid volume ratios $v_j = V_{lipid} / V_{total}$ (j = 1 and 2), the neutral and ionized drug's partition coefficients in lipid bilayers can be calculated from the known dissociation constant in water, pK_a (Avdeef 1992; Avdeef et al. 1998):

$$P^N_{mem} = \frac{v_2 \cdot 10^{\left|\left(pK_{app}(2) - pK_a\right)\right|} - v_1 \cdot 10^{\left|\left(pK_{app}(1) - pK_a\right)\right|} - \left(v_2 - v_1\right) \cdot 10^{\left|\left(pK_{app}(1) + pK_{app}(2) - 2\,pK_a\right)\right|}}{v_1 v_2 \cdot \left[10^{\left|\left(pK_{app}(1) - pK_a\right)\right|} - 10^{\left|\left(pK_{app}(2) - pK_a\right)\right|}\right]} \tag{22}$$

$$P^I_{mem} = \frac{v_1 \cdot 10^{\left|\left(pK_{app}(2) - pK_a\right)\right|} - v_2 \cdot 10^{\left|\left(pK_{app}(1) - pK_a\right)\right|} + v_2 - v_1}{v_1 v_2 \cdot \left[10^{\left|\left(pK_{app}(1) - pK_a\right)\right|} - 10^{\left|\left(pK_{app}(2) - pK_a\right)\right|}\right]} \tag{23}$$

Knowledge of both partition coefficients enables *pH*-dependent evaluation of the drug's distribution including both charged and neutral molecular forms:

$$log\, D_{mem} = log\left(P^I_{mem} + P^N_{mem} \cdot 10^{s(pK_a - pH)}\right) - log\left(1 + 10^{s(pK_a - pH)}\right) \tag{24}$$

with the drug specific sign s = +1 for acidic and s = –1 for basic drug substances.

Equations (20) - (24) are valid so long as membrane properties are not affected significantly by the membrane bound drug. Practically speaking, this is true for high lipid/drug ratios or small partition coefficient P^I_{mem}. Otherwise, when an appreciable drug quantity is bound to the membrane, corrections must be made for the drug-induced changes in the membrane properties, especially for the membrane's electrostatic potential. The influence of electrostatics on the drug partitioning must then be considered. This is typically done as a function of the membrane surface charge density, σ, the bulk ions concentration, $c_{w,i}$, and the polarity of the membrane/water interface, ε_{mem}.

The surface charge density can be estimated from the known dissociation degree, α, of an acid or a base at the bilayer membrane surface (Austin et al. 1998):

$$\sigma = \frac{\alpha \cdot r_{drug} \cdot z \cdot e}{A_{drug} \cdot r_{drug} + A_l \cdot r_l} \tag{25}$$

z is the drug's charge number and e the elementary electronic charge. A_{drug} and A_l are the surface area of the drug and the bilayer forming lipid in the membrane, respectively ($A_l >> A_{drug}$ within this work). r_{drug} and r_l are the mole ratios of the former and of the latter.

The Debye screening length, λ_D, which gives the "thickness" λ_D of the diffuse electric double layer near a charge, influences the surface potential as well, in dependency on ions, i, with bulk concentrations $c_{w,i}$ and the charge number z_i (Cevc 1990):

$$\lambda_D = \sqrt{\frac{\varepsilon \cdot \varepsilon_0 \cdot k_B T}{N_A \cdot e^2 \cdot \sum_i z_i^2 \cdot c_{w,i}}} \tag{26}$$

ε and ε_0 are the dielectric constant of the solution and the permittivity of free space, respectively. The remaining parameters are the thermal energy, $k_B T$, and the Avogadro number, N_A.

At 25 °C equation (26) simplifies for monovalent salts with total bulk salt concentration $c_{w,t}$ (Israelachvili 1992):

$$\lambda_D = 0.304 \cdot c_{w,t}^{\ -0.5} \tag{27}$$

The surface potential, $\psi_{0,GC}$, is usually calculated within the framework of the Gouy-Chapman model (Gouy 1910; Chapman 1913):

$$\begin{aligned} \psi_{0,GC} &= \frac{2 \cdot k_B T}{z \cdot e} \cdot \sinh^{-1}\left[\frac{z \cdot e \cdot \sigma \cdot \lambda_D}{2 \cdot \varepsilon \cdot \varepsilon_0 \cdot k_B T}\right] \\ &= \frac{\sigma \cdot \lambda_D}{\varepsilon \cdot \varepsilon_0} \quad \text{for } \psi_0 < 25 \text{ mV} \end{aligned} \tag{28}$$

Within a membrane interface, e.g. near a phospholipid bilayer membrane, the polarity changes. In terms of the dielectric constant, the difference is from $\varepsilon_{mem} \approx 35$ at the headgroup to $\varepsilon_{mem} \approx 2$ within the fatty acid chains or to $\varepsilon \approx 78$ in the "bulk" (Marsh 2001).

Therefore, the membrane surface potential ψ_0 has to calculated based on equation (28)

$$\begin{aligned}\psi_0 &= \frac{2 \cdot k_B T}{z \cdot e} \cdot \sinh^{-1}\left[\frac{z \cdot e \cdot \sigma \cdot \lambda_D}{2 \cdot \varepsilon_{mem} \cdot \varepsilon_0 \cdot k_B T}\right] \\ &= \frac{\sigma \cdot \lambda_D}{\varepsilon_{mem} \cdot \varepsilon_0} \quad \text{for } \psi_0 < 25 \text{ mV}\end{aligned} \tag{29}$$

which only differs from the latter in the dielectric constant value.

In this work, I assumed the location of the charged bupivacaine and ketoprofen, i.e. the position of the surface charge, near the headgroup and fixed the polarity to $\varepsilon_{mem} = 30$.

Knowledge of electrostatic surface potential then allows calculation of the drug's concentration at the membrane surface, based on equation (20), simply by:

$$c^I_{mem} = c^I_w \cdot P^I_{mem} \cdot \exp\left[\frac{-z \cdot e \cdot \psi_0}{k_B T}\right] \tag{30}$$

Coming back to the experimental determination and evaluation of partition coefficients via *pH*-metric titrations, it is clear that, under electrostatic consideration and influence, the apparent dissociation constant is a function of lipid volume ratio, v_j. pK_{app} values determined for at least two different lipid volume ratios thus allow derivation of the partition coefficients P^N_{mem} and P^I_{mem} for the neutral and ionized drug forms, respectively:

$$pK_{app}(v_i) = pK_a + s \cdot \log\left[\frac{P^N_{mem} \cdot v_j + 1}{P^I_{mem} \cdot \exp\left[\frac{-z \cdot e \cdot \psi_0}{k_B T}\right] \cdot v_j + 1}\right] \tag{31}$$

Equation (31) must be solved together, and consistent, with equations (25),(29), and (30), using least squares fitting procedure.

The *pH* dependent distribution of ionizable molecules in a lipid bilayer membrane is then given, based on equation (24), by:

$$log\, D_{mem} = log\left[P^I_{mem} \cdot exp\left[\frac{-z \cdot e \cdot \psi_0}{k_B T}\right] + P^N_{mem} \cdot 10^{s(pK_a - pH)}\right] - log\left[1 + 10^{s(pK_a - pH)}\right] \tag{32}$$

4.3. Material and Methods

4.3.1. Materials

Soybean phosphatidylcholine (SPC) was chosen as the bilayer forming lipid and was purchased from Lipoid with the purity grade Lipoid S100 (Ludwigshafen, Germany). Bupivacaine (hydrochloride monohydrate) and ketoprofen were supplied by Heumann PCS (Feucht, Germany) and Bidachem (Fornovo S. Giovanni, Italy), respectively; both met the quality specifications of the European Pharmacopoeia (EP). Potassium chloride, sodium hydroxide, hydrochloric acid (all VWR, Darmstadt, Germany), and water for injection (Deltaselect, Dreieich, Germany) had EP quality as well.

4.3.2. Preparation of drug containing large unilamellar lipid bilayer vesicles and blank solutions

Large unilamellar vesicle suspensions with two different lipid concentrations (160 mg/g and 50 mg/g, assuming ρ = 1 g/ml) were used in the study. The corresponding SPC quantity was interspersed into an aqueous solution of either bupivacaine or ketoprofen, always keeping the final drug concentration constant (c_d = 20 mM). To determine the influence of electrostatics on the drugs partitioning, different amounts of potassium chloride were added to each suspension.

For better homogeneity, the suspensions were stirred for 2 h, and then extruded through a set of different track-etched poly-carbonate membranes (PCTE, GE Osmonics) with decreasing pore size (400 nm – 100 nm); a freeze-thaw cycle (180 min at -70 °C, 30 min at 40 °C) and multi-extrusion through PCTE membranes with decreasing pore sizes (400 nm – 80 nm) finished the vesicle preparation (Olson et al. 1979; Mayer et al. 1986; MacDonald et al. 1993). The resulting vesicle size and polydispersity were determined by the dynamic light scattering (DLS), as is described in chapter 2.2.4. This yielded an average vesicle diameter of d_{ves} = 100 ± 15 nm and polydispersity index of PDI < 0.15.

The drug free blank solutions without any lipid vesicle were prepared by dissolving the required potassium chloride quantities in water.

Directly before a *pH*-metric titration, the *pH* value of the vesicle suspension and its allocated blank solution were adjusted to the starting pH < 3 and pH > 11 for bupivacaine and ketoprofen titrations, respectively. This was done using adequate volumes of sodium hydroxide (10 M) or hydrochloric acid (4 M). The resulting final ionic strength, comprising

all ions (potassium chloride, sodium hydroxide, hydrochloric acid, and drug counter ions) was calculated to be in the range of I_c = 35 mM to 265 mM.

4.3.3. *pH*-metric determination of the apparent dissociation constants, membrane partition coefficients, and distribution coefficients

Determination of drug partition coefficients for the uncharged (neutral) molecule and for the charged (ionized) entity, as well as analysis of the *pH*-dependent distribution coefficient, are based on the pioneer work of Avdeef (1992; 1998).

According to the fundamental equations (22) and (23), the pK_{app} of lipid vesicle suspensions with two different total lipid volume ratios, v_j, is needed to derive P^N_{mem} and P^I_{mem}. As pointed out by Balon et al. (1999), the partition coefficients for the neutral and ionized drug forms are independent on the tested lipid ratios; in contrast, the membrane partitioning of a drug is typically temperature sensitive. Thus, all the measurements were done at 25 ± 0.3 °C. Blank solutions provided controls, and supported the calculation of the mol equivalent of the titrated drug substance.

The *pH* glass electrode DG111-SC was calibrated using the titrator DL67 and the LabX Pro titration software (all from Mettler-Toledo, Giessen, Germany). This was done daily before the measurements, which were done in triplicate for the drug vesicle suspension and its reference blank solution. For the ketoprofen containing suspensions, a “down”-titration (from high to low *pH*) was employed. For the oppositely charged bupivacaine, an “up”-titration in opposite direction was chosen (lower panels in Figure 27). The analytes were determined with two different titrants: sodium hydroxide (0.5 M) and hydrochloric acid (1 M) for bupivacaine and ketoprofen samples, respectively.

In all experiments, the *pH* change per titrant addition was limited to $\Delta\, pH \leq 0.1$. This was done dynamically by the software. The *pH* equilibration between the lipid vesicle exterior and interior was adjusted to be 1 - 2 min between each addition, as had been suggested in the literature (Pauletti et al. 1994).

To evaluate the pK_{app} values, the ratio of the ionized drug molecules

$$r_{ionized} = \frac{c_t \cdot s(V_{tb} - V_{ts})}{c_d \cdot V_{total}} \tag{33}$$

was first calculated. c_t is the titrant concentration and V_{tb} and V_{ts} are the titrant volumes used for titrating blank solution and vesicle suspension in dependency on *pH*, respectively. c_d and V_{total} are the total drug concentration and the measured volume, respectively.

The ratio of the ionized drug molecules as a function of *pH* yields an apparent dissociation constant, pK_{app}, read-off at the inflexion point of the sigmoidal curve given in Figure 27. At $pH = pK_{app}$, the ratio of the charged and neutral molecules is 1:1.

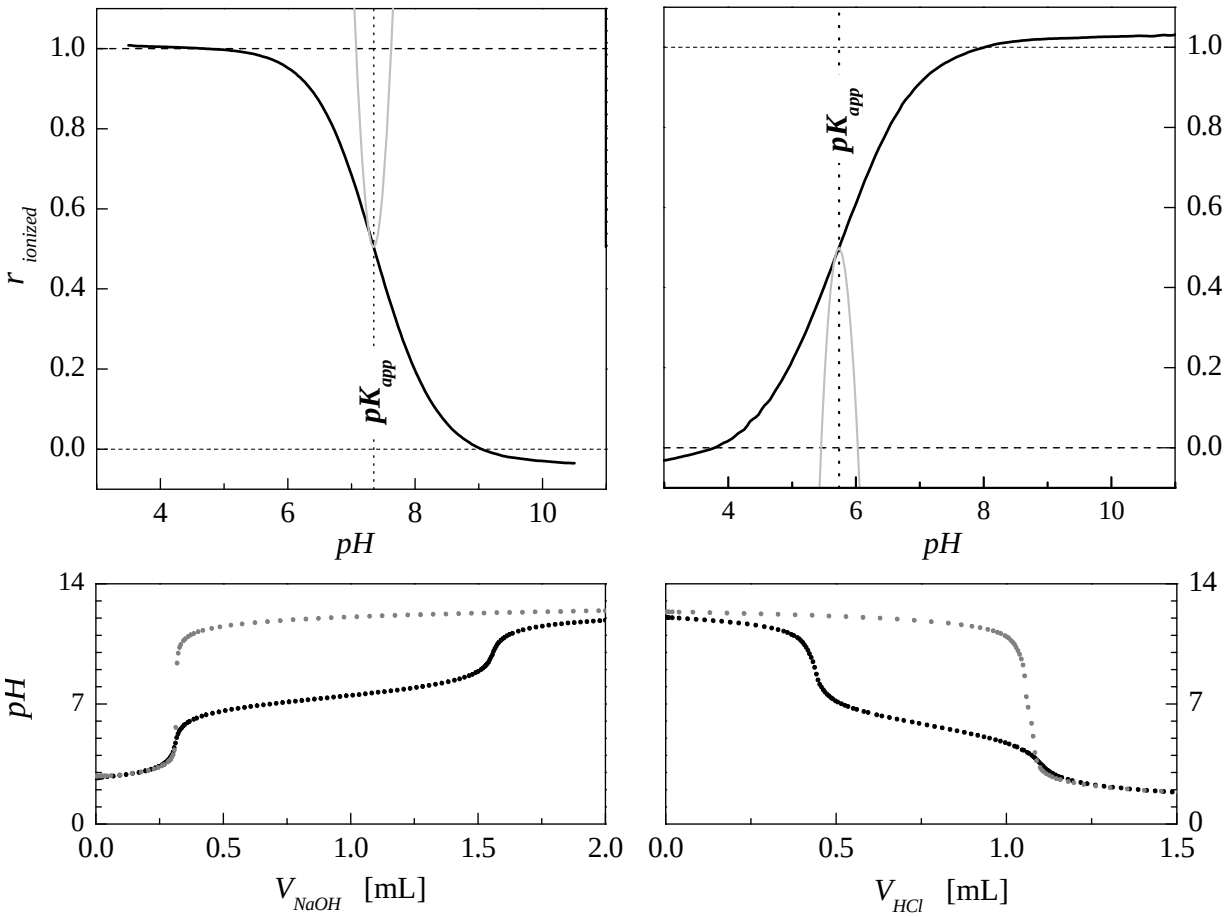

Figure 27: Illustration of *pH*-metric titrations for the determination of the apparent dissociation constant, pK_{app}, of bupivacaine (left panels) and ketoprofen (right panels) in bilayer vesicle suspensions. The lower panels show the measurements of the drug containing lipid vesicle suspensions (black dotted line) and the blank solutions (grey dotted line). The upper panels illustrate the ratio of ionized drug (black line) and its derivation (grey line) in dependency on *pH*.

With the pK_{app} derived from the experimental data measured with two different lipid ratios, v_j, and further considering the known aqueous dissociation constants of bupivacaine, pK_a = 8.09 (Friberger et al. 1971)) or of ketoprofen, pK_a = 4.36 (Rafols et al. 1997), the various partition and distribution coefficients were derived in dependency on electrostatics with a least square fitting procedure involving equations (31) and (32). The results are given in the following section.

4.4. Results and discussion

4.4.1. Apparent dissociation equilibrium of bupivacaine and ketoprofen

pH-metric titrations of bupivacaine or ketoprofen containing bilayer membranes yielded different apparent dissociation equilibria in dependency on lipid/drug ratio and total ionic strength, I_c (symbols in Figure 28).

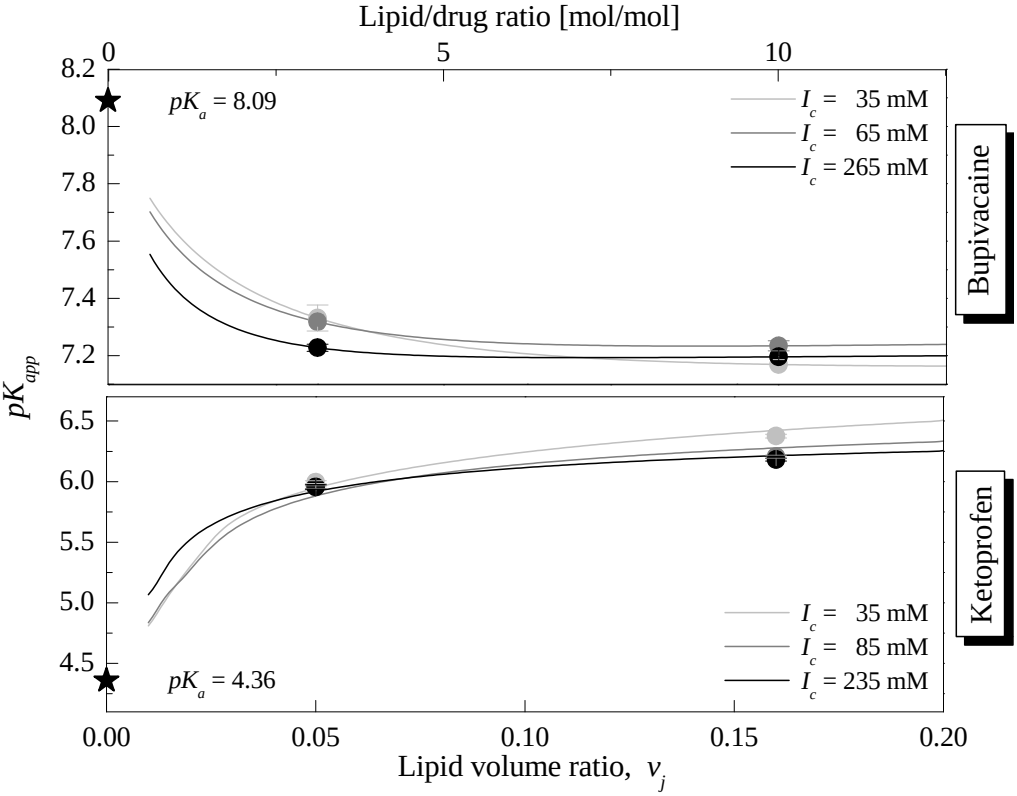

Figure 28: The apparent dissociation constant, pK_{app}, of bupivacaine and ketoprofen in bilayer membrane with different lipid/drug ratios.
With decreasing lipid/drug ratio, the pK_{app} shift is reduced due to lower lipid volume ratio, v_j, and due to electrostatic repulsion between the charged bilayer membrane and the drug molecules at the membrane/water interface.
(●●● measured data ; ▬▬ fitted data ; ★ reference data)

The pK_a shift between the bilayer membrane and water is empirically in the range of –1 to –1.5 units for bases (Miyazaki et al. 1992) and +2 to +3 units for acids (Austin et al. 1998). For the base bupivacaine, which has an intrinsic dissociation constant of pK_a = 8.09 in water, the apparent dissociation constant is shifted downwards to pK_{app} = 7.15 – 7.33. For ketoprofen the shift is upwards, from pK_a = 4.36 to pK_{app} = 5.96 – 6.38. Figure 28 suggests, that the magnitude of this effect depends, among others, on lipid/drug ratio, as is illustrated in Figure 26 for the four coupled equations of equilibrium. In addition, the data fitting curve based on equation (31) shows an electrostatic influence on pK_{app} shift, which will get attention in the following section.

4.4.2. Bilayer surface charge in dependency on *pH*

The fitted pK_{app} curves given in Figure 28 highlight electrostatic effects on drug partitioning. They show, for example, that at low lipid/drug ratio the pK_{app} shift increases with salt concentration. This is not surprising given that ions from the surrounding bulk solution not only affect the Debye screening length, λ_D; they moreover affect the surface charge density, σ, and the resulting surface potential, ψ_0 (cf. equations (25),(26), and (29)).

Figure 29 for bupivacaine and Figure 30 for ketoprofen furthermore illustrate that for constant drug concentration the drug dependent bilayer surface charge density decreases with increasing lipid concentration. This is due to enlarged lipid area in case of high total lipid concentration. High ionic strength, and the corresponding short screening length, reduce repulsion of the equally charged drug molecules from the membrane/water interface, where more such molecules reside, and increase pK_{app} shift, as is shown in Figure 28.

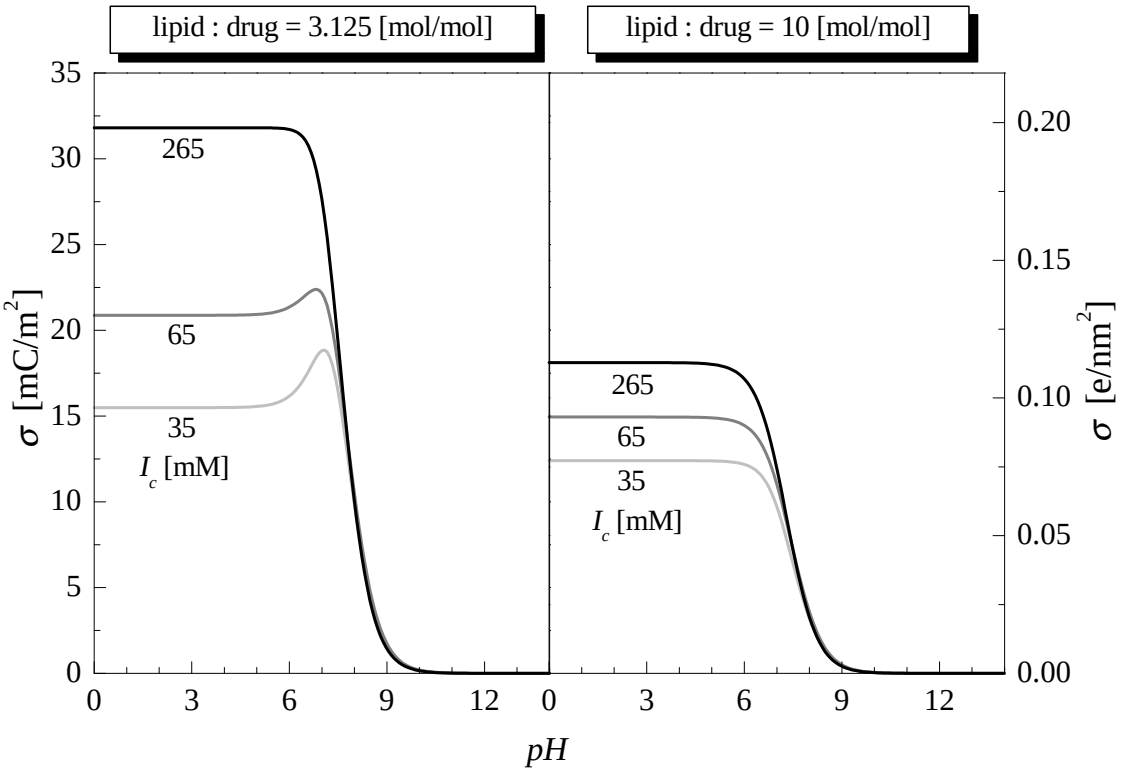

Figure 29: Surface charge density, σ, of bupivacaine containing bilayer membranes in dependency on the bulk *pH*, ionic strength, I_c, or the drug/lipid ratio.
Bupivacaine, a tertiary amine base, is positively charged at low *pH* and neutral at high *pH*. With increasing *pH*, the drug dependent surface charge density therefore changes. Decreasing lipid/drug ratio and increasing I_c both results in higher surface charge densities, due to weakened electrostatic repulsions.

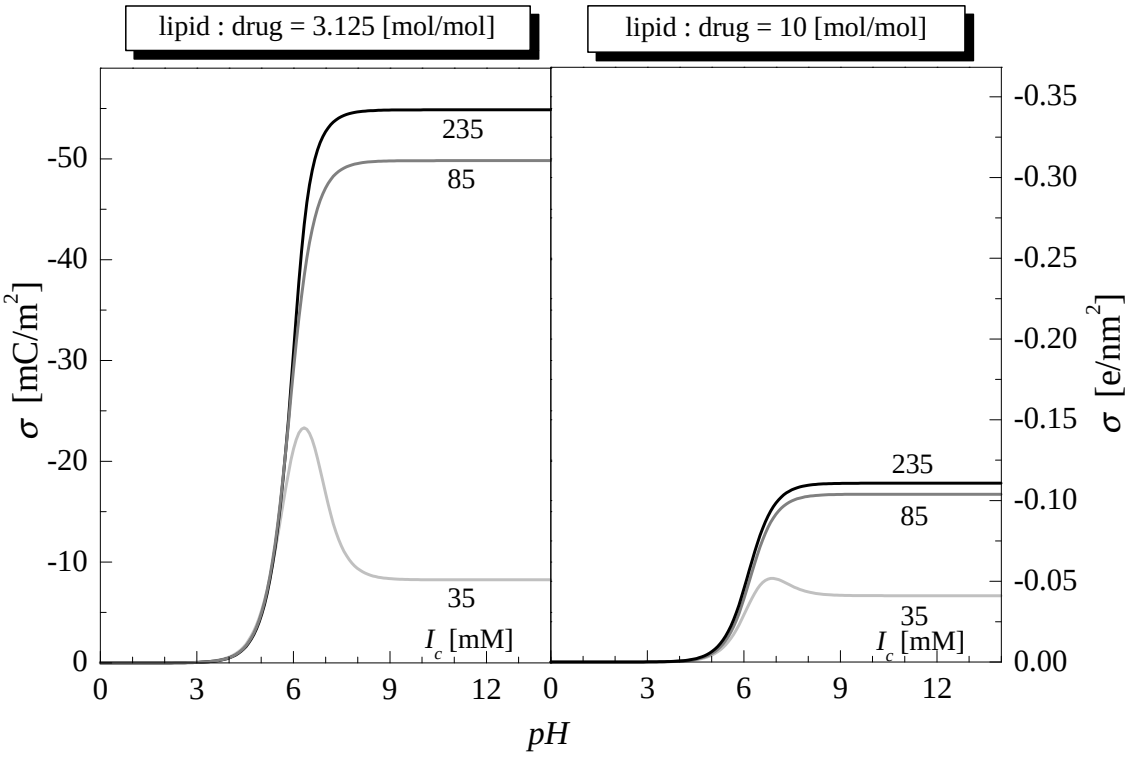

Figure 30: Surface charge density, *σ*, of ketoprofen containing bilayer membranes in dependency on the bulk *pH*, ionic strength, I_c, or the drug/lipid ratio.
Ketoprofen, a propionic acid derivative, is negatively charged at high *pH* and neutral at low *pH*. With increasing *pH*, the drug dependent surface charge density therefore changes. Decreasing lipid/drug ratio and increasing I_c both result in higher surface charge densities, due to weakened electrostatic repulsions.

The deviation from sigmoidal curve progression, which is seen in Figure 29 and Figure 30 at low ionic strengths, highlights a phenomenon. Theoretically, in absence of any repulsion, the membrane bound drug molecules should change from neutral form into the charged one according to dissociation equation, i.e. sigmoidally with decreasing or increasing *pH* for bupivacaine or ketoprofen suspensions, respectively. In reality, the *pH*-induced changes of bilayer surface charge density can actually force some of the charged drug molecules out of the bilayer, thus reducing the final surface charge density. The propensity for this is higher at low salt concentration, when electrostatic interactions are less screened.

Electrostatic surface potential is therefore one reason why charged and neutral drugs show different membrane partitioning in dependency on the surrounding salt concentration, an observation, which will be presented and discussed in the following section.

4.4.3. Bilayer membrane partition and distribution in dependency on charge state and electrostatics

The widely used 1-octanol/water partition coefficient ($P^N_{o/w}$) of neutral molecules is similar to the value measured with phospholipid bilayer membranes in water (P^N_{mem}) (Avdeef et al. 1998). For the charged molecules, however, the partition coefficients $P^I_{o/w}$ and P^I_{mem} are totally different for the most part (Miyazaki et al. 1992; Austin et al. 1995; Avdeef et al. 1998). The reason is that partitioning of amphiphilic acidic or basic drugs from water into a membrane depends, among others, on electrostatic effects, on the drug's charge state, and on polarity. For example:

The propionic acid derivative ketoprofen in neutral form possesses an 1-octanol/water partition coefficient log $P^N_{o/w}$ = 3.12 (La Rotonda et al. 1983). This is in good accord with log P^N_{mem} = 3.27 found in this study. For the ionized ketoprofen the partition values in octanol and membrane differ significantly: log $P^I_{o/w}$ = -0.95 (Avdeef 2003) and log P^I_{mem} = 0.15 - 1.18, in dependency on ionic strength.

Bupivacaine, a tertiary amine base, has a similar log $P^N_{o/w}$ = 3.38 (Razak et al. 2001) but ten times lower partition coefficient in the neutral form in a bilayer: log P^N_{mem} = 2.43. However, the partitioning of the positively charged bupivacaine is significantly higher compared to ionized ketoprofen, particularly at low salt concentrations: log P^I_{mem} = 1.23 - 1.58. Unfortunately, to the best of my knowledge, there are no other comparable literature data for the partitioning of charged bupivacaine in 1-octanol/water.

	I_c [mM]	log $P^N_{o/w}$	log P^N_{mem}	log $P^I_{o/w}$	log P^I_{mem}
Ketoprofen	35	3.12 [a]	3.00	- 0.95 [b]	0.15
	85		3.19		0.92
	235		3.27		1.18
Bupivacaine	35	3.38 [c]	2.08	n/a	1.23
	65		2.17		1.41
	265		2.43		1.58

Table 8: Partition coefficients of neutral (*N*) and ionized (*I*) ketoprofen and bupivacaine in a 1-octanol/water, $P_{o/w}$, or bilayer membrane/water, P_{mem}, system in dependency on the ionic strength, I_c.
[a] (La Rotonda et al. 1983), [b] (Avdeef 2003), [c] (Razak et al. 2001)

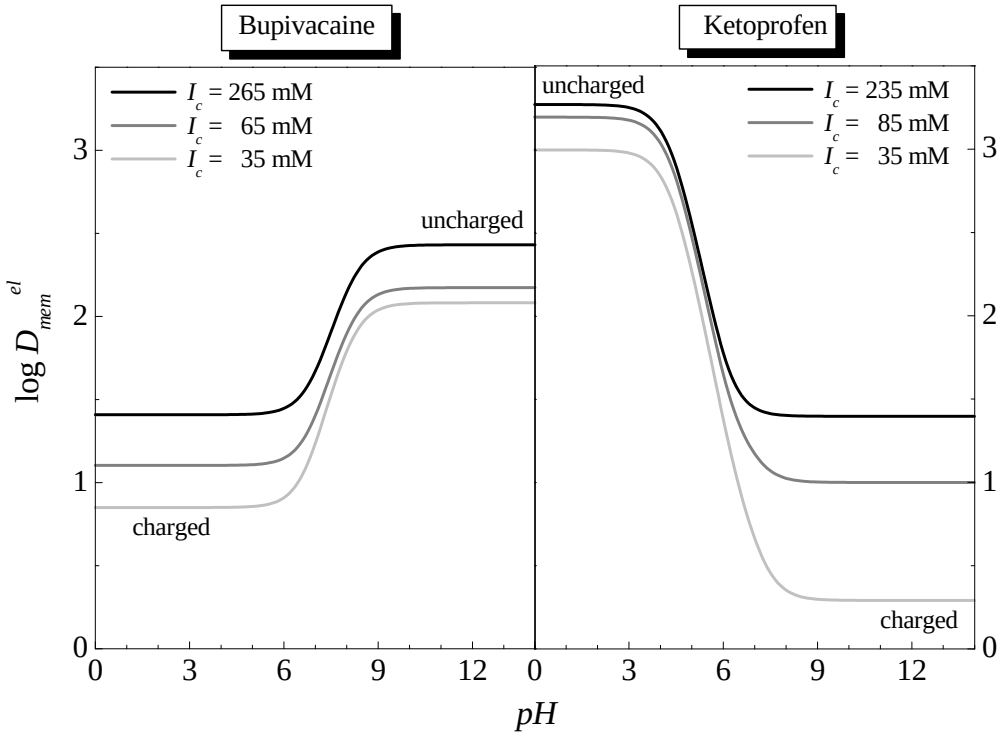

Figure 31: Bilayer membrane distribution of bupivacaine (left panel) and ketoprofen (right panel) in dependency on *pH* and ionic strength.
With increasing *pH* bupivacaine shows an increasing membrane distribution whereas the ketoprofen distribution decreases. Both drug molecules reveal a higher logD^{el}_{mem} value with increasing ionic strength. Data representing lipid/drug ratio 10 mol/mol.

Since both ketoprofen and bupivacaine have a similar log $P^{N}_{o/w}$ value but different partition coefficients for the neutral as well as the ionized molecular form (cf. Figure 31), these observations are interesting and form the basis for a deeper theoretical discussion at molecular level.

Uncharged ketoprofen partitions into a bilayer membrane more than uncharged bupivacaine. In contrast, positively charged bupivacaine is more bilayer-affine than negatively charged ketoprofen, at least at low ionic strengths (Figure 31). These observations are consistent with the results of Avdeef et al. (1998) for other NSAIDs or local anaesthetics, and can be explained with different location of the charged and neutral molecular forms in the membrane-water interface (cf. Figure 32).

Ionized amphiphiles, like the positively charged bupivacaine and the negatively charged ketoprofen, are located closer to the bulk. Both drugs displace water of lipid hydration, as was shown for other charged amphiphiles by Hogberg et al. (2007). The drugs may moreover interact with the negatively charged phosphate group (bupivacaine) or the positively charged trimethylammonium group (ketoprofen). However, the drugs orientation is likely to be different for the two tested drugs, owing to more central position of the bupivacaine's charge

in comparison with ketoprofen. This makes the ionized ketoprofen more sensitive to electrostatic effects, as is shown in Figure 31.

The neutral drug molecules are inserted deeper in the water-membrane interface, near the fatty acid ester group. Ketoprofen can then bind via hydrogen bonds to the fatty acid carbonyl group, finally resulting in an increased P^{N}_{mem} (Avdeef et al. 1998; Hogberg et al. 2007). The following section supports this conclusion and provides deeper insight into the electrostatic and polarity induced contributions to the drug's partitioning into lipid membranes.

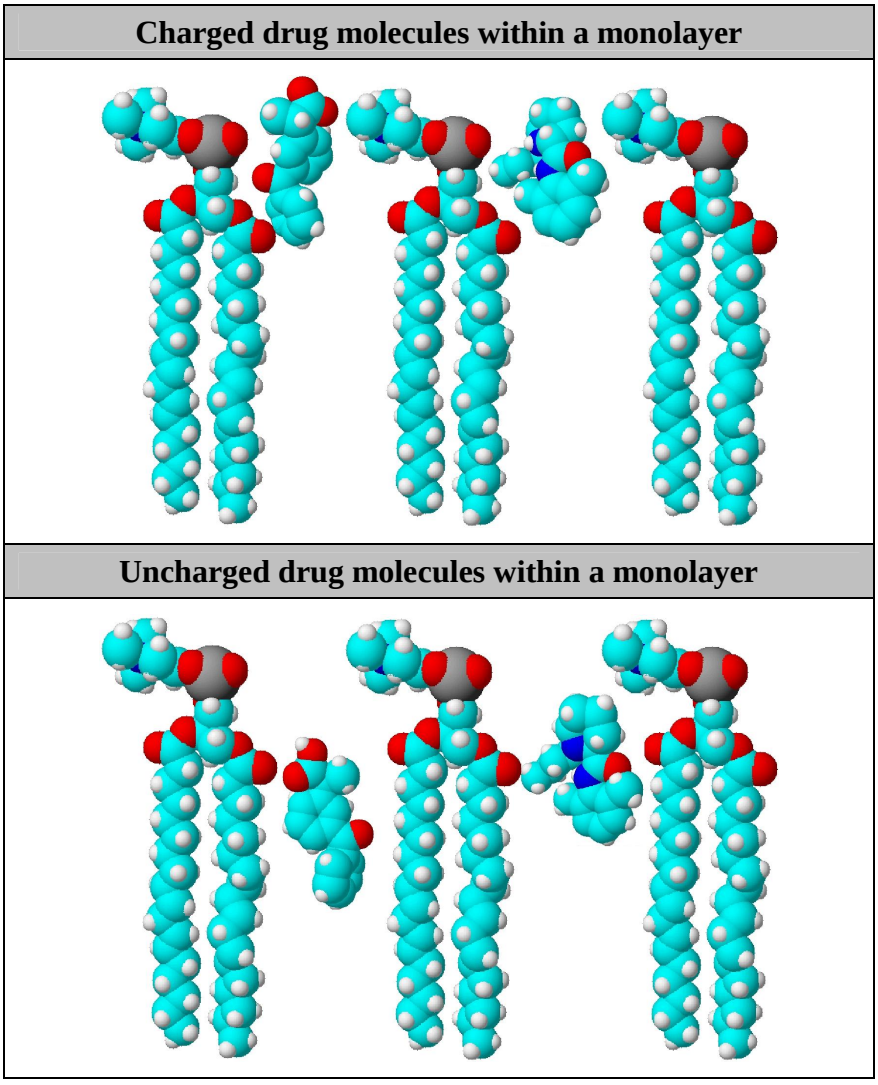

Figure 32: Schematic illustration of ketoprofen and bupivacaine location within a phosphatidylcholine membrane in dependency on their ionization. (only a monolayer is presented). The upper graph shows charged ketoprofen (left molecule) and charged bupivacaine (right molecule) incorporated in the upper part of lipid headgroup region. The lower graph illustrates the position of the neutral drugs in the deeper lipid monolayer regions. (Generated with ACD/3D-viewer.)

4.4.4. Influence of electrostatics and polarity on membrane dissociation

The dissociation equilibrium of acids and bases in bilayer vesicle suspensions is shifted by polar and electrostatic effects compared to the bulk pK_a (Cevc et al. 1987):

$$pK_{app} = pK_a + \Delta\, pK_a^{el} \pm \Delta\, pK_a^{pol} \tag{34}$$

$\Delta\, pK_a^{el}$ is the electrostatic contribution and $\Delta\, pK_a^{pol}$ is the polarity dependent contribution to the shift.

The electrostatic shift is given by:

$$\Delta\, pK_a^{el} = \frac{z \cdot e \cdot \psi_0}{2.3 \cdot k_B T} \tag{35}$$

The value of $\Delta\, pK_a^{pol}$ depends on interfacial dielectric constant, ε_{mem}, at the drug binding site. Its sign depends on the change in total number of charges on dissociation (Fernandez et al. 1977; Cevc et al. 1981). In other words, interaction of zwitterionic phosphatidylcholine membranes with the molecular acid ketoprofen AH should cause a positive polarity induced shift, due to increase of total charge from (+ -) to (+ - -). For dissociation of the cationic acid bupivacaine BH^+ the reverse should be true, owing to total charge decrease from (+ - +) to (+ -).

The values for $\Delta\, pK_a^{el}$ and $\Delta\, pK_a^{pol}$ for different salt concentrations at lipid/drug ratio of 10 mol/mol were calculated from the measured pK_{app} values and the determined surface potential ψ_0 (cf. equations (29)) using equations (34) and (35).

	I_c [mM]	ψ_0 [mV]	$\Delta\, pK_a^{el}$	$\Delta\, pK_a^{pol}$
Bupivacaine	35	61	1.03	- 1.95
	65	55	0.93	- 1.79
	265	37	0.63	- 1.52
Ketoprofen	35	- 36	0.61	1.41
	85	- 54	0.91	0.93
	235	- 38	0.64	1.18

Table 9: Surface potential ψ_0 and the derived values of the electrostatic and polarity induced contribution to the pK_a shift for bupivacaine and ketoprofen in phosphatidylcholine bilayer membranes at different ionic stengths with a lipid/drug ratio of 10 mol/mol.

Table 9 reveals that the polarity induced shift, which is an indicator of charged molecules location in the membrane-water interface (Fernandez et al. 1977), is different for bupivacaine

and ketoprofen. For ketoprofen $\Delta\ pK_a^{pol}$ is in the range of 0.9 to 1.4, which is in good accord with the values reported for other amphiphiles: ± 1.1 (Fernandez et al. 1977). The polarity induced shift for bupivacaine is negative and somewhat larger, $\Delta\ pK_a^{pol}$ = -1.5 – -2.0, consistent with general expectations and the assumedly deeper insertion of this drug into the interface.

Fernandez and Fromherz (1977) published polarity induced shifts as a function of different dioxin-water mixtures representing various dielectric constants. Knowledge of the latter information on dielectric profile near a phosphatidylcholine bilayer membrane (Marsh 2001) enables semi-quantitative estimation of the drug's location in the membrane-water interface. The location of ketoprofen is then concluded to be between the trimethylammonium and phosphate groups, having polarity of $\varepsilon_{mem} \approx 28 – 35$. Bupivacaine is located somewhat deeper in the membrane, more precisely, between the phosphate and the fatty acid carbonyl groups ($\varepsilon_{mem} \approx 20 – 28$). This observation is consistent with the discussion in section 4.4.3, where the higher P^I_{mem} value for bupivacaine prompted me to assume its location more inside the membrane compared to ketoprofen.

4.5. Conclusion and outlook

Knowledge of the dissociation equilibria of basic and acidic drug molecules, such as bupivacaine and ketoprofen, and defined information on their partition and distribution behaviour in bio-mimetic phosphatidylcholine membranes are important and useful for solving pharmacological or galenic questions related to these drugs.

Primarily with regard to the development of modern pharmaceutical forms based on bilayer membrane vesicles, the partition and distribution behaviour in dependency on *pH*, electrostatics, and polarity will provide a good starting point for optimising drug loading, improving formulation stability, and simulating in vivo behaviour. The *pH* and salt concentration dependent effects studied herein are being used in the development of new medicinal products based on Transfersome® technology (Cevc et al. 2003b; Cevc 2004). Especially the combination of bupivacaine or ketoprofen with such ultra adaptable, highly fluctuating lipid vesicles, e.g. based on polyoxyethylene (20) oleyl ether saturated phosphatidylcholine bilayer membranes, could generate new products for the local and carrier mediated treatment of neuropathic pain or inflammation in near future.

Furthermore, membranes comprising phosphatidylcholine, which is the most common lipid in living cells (Yorek 1993), are suitable models to study biologically relevant partitioning of

new drugs or novel drug applications. Knowledge of the charged and uncharged drug distribution into such bio-mimetic membrane can thus provide a good starting point for optimisation of drug action, e.g. for potentiating local anaesthetics action or reducing adverse side effects of NSAIDs.

Local anaesthetics of the bupivacaine type, both in neutral and ionized form, bind to the 6th transmembrane segment of the α-IV subunit in the voltage-gated sodium ion channel (Ragsdale et al. 1994). The resulting channel blocking hinders action potential building and nerve pulse transmission (Chernoff et al. 1990). However, before interacting with the sodium channel, a local anaesthetic must first diffuse, predominantly in its neutral form, through the nerve cell membrane (Hogberg et al. 2007). This allows the drug to reach its binding site, which is only accessible from the cell interior. An uncharged local anaesthetic unbinds much faster from the channel, resulting in accelerated recovery from the nerve block (Schwarz et al. 1977). This relationship could be a prospective challenge in development of new or optimised anaesthetics comprising both: a high membrane partitioning to reach the site of action and a prolonged binding to the latter.

Partition coefficient measurements should therefore be used as a starting point for solving such pharmacological questions. To be more reliable, such future studies should be performed with a negatively charged membrane similar to that in nerve cell, e.g. composed of the zwitterionic phosphatidylcholines and the negatively charged phospholipids (Inouye et al. 1988).

Ketoprofen belongs to the group of non-selective cyclooxygenase COX-I and -II inhibitors, which are broadly used to treat any kind of mild to moderate pain and inflammation. Like the other plentifully administered non-selective NSAIDs, ketoprofen can induce gastrointestinal injuries due to COX-1 inhibition and to hindrance of the cytoprotective prostaglandin expression in the gastrointestinal tract. The scientific evidence of this theory is inconsistent, however, e.g. different drug potencies in COX-1 inhibition at comparable “COX-1 induced” adverse side effects were reported (Lichtenberger 2001). The non-selective NSAID-caused gastrointestinal injuries can therefore also be explained by chemical reaction with and destabilisation of the protective phospholipid lining of the mucus gel layer (Lichtenberger et al. 1995; Giraud et al. 1999). Therefore, knowledge of ketoprofen’s and any other NSAIDs partitioning and distribution into lipid bilayers could support further development of “safe” NSAIDs.

5. ADAPTABILITY AND ELASTICITY OF TRANSFERSOME®, MIXED BILAYER VESICLES, IN DEPENDENCY ON DRUG CONCENTRATION, *pH*, AND IONIC STRENGTH

5.1. Introduction

Transfersome® vesicles are mixed lipid aggregates with an ultra-adaptable bilayer membrane and are suitable for transdermal drug delivery. The carriers are composed of at least one bilayer-forming lipid and one or more bilayer softening amphiphiles, e.g. a phospholipid and a surfactant (Cevc et al. 2003b). The mixed lipid vesicle is able to penetrate fine skin pores smaller than its average size, driven by hydration gradient in the mammalian skin barrier, i.e. the epidermis, and more specifically spoken the stratum corneum (Cevc et al. 1992; Cevc et al. 2003a; Kiselev et al. 2005). In contrast to diffusion based, more conventional, transdermal drug delivery systems, TDDS, such as gels, crèmes, ointments and patches, the carrier based delivery systems can transport drug substances more or less independent of their molecular weight and lipophilicity/hydrophilicity through the natural skin barrier, and into deeper, peripheral tissues (Cevc 1997).

Simple, stiff soybean phosphatidylcholine (SPC) vesicles, i.e. the conventional liposomes, can be transformed into flexible Transfersome® by addition of membrane softening surfactants, such as polyoxyethylene (20) oleyl ether ($C_{18:1}EO_{20}$), as is described prior in this work. In this study, the amphiphilic molecules ethanol, bupivacaine, and ketoprofen (Table 10) were combined with $C_{18:1}EO_{20}$ saturated SPC mixed lipid bilayer vesicles having an effective surfactant to lipid molar ratio of R_e = 0.25 mol/mol. The combination served the major objective of this study: development of different polyoxyethylene (20) oleyl ether based Transfersome® formulations for optimum transdermal drug delivery.

Bupivacaine is a cationic, long acting local anaesthetic of the anilide type, which to date is mainly applied by infiltration, peripheral, epidural, and spinal injection (Ruetsch et al. 2001). The two former methods are predestined for drug delivery from a topically applied formulation to the site of local anaesthesia and analgesia. Unfortunately, the current, medicinal products comprising mainly lidocaine have only have a short and weak analgetic effect, let alone an anaesthetic one. The development of locally acting, bupivacaine containing, ultra-adaptable lipid carrier formulations could lead to stronger and longer acting anaesthesia, due to the four times higher potency of bupivacaine compared to lidocaine (Ruetsch et al. 2001). The expectation is also supported by the published data of Grant et al.

(2001; 2004) who reported prolonged bupivacaine action after subcutaneously injection of the drug in combination with liposomes.

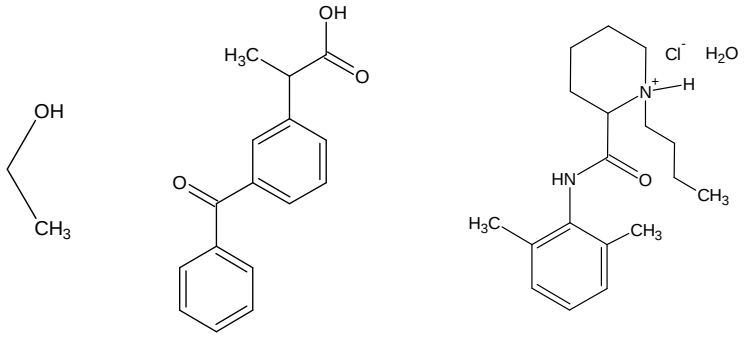

	Ethanol	**Ketoprofen**	**Bupivacaine** x HCl x H_2O
pK_a	15.9 [a]	4.36 [b]	8.09 [c]
Charge	0*	$0 \xrightarrow{pH \uparrow} -1$	$0 \xrightarrow{pH \downarrow} +1$

Table 10: The structure of ethanol, ketoprofen, and bupivacaine and their electrostatic charge in dependency on *pH* and pK_a value. (Vollhardt et al. 1998) [a], (Rafols et al. 1997) [b], (Friberger et al. 1971) [c]. *Ethanol is a very weak acid in aqueous media and thus uncharged.

In contrast to the base bupivacaine, i.e. a cationic acid, the non-steroidal anti-inflammatory drug ketoprofen is a propionic acid derivative, normally negatively charged under physiological conditions. This NSAID is commercially applied orally or topically against rheumatoid arthritis and osteoarthritis. As a nonselective COX1-/COX2-inhibitor its local application is favoured due to several gastrointestinal adverse effects after orally application, but at the expense of relatively poor efficacy for the diffusion based TDDS. The carrier mediated transport of ketoprofen through the skin has been reported to be as effective as an orally administered selective COX2-inhibitor, celecoxib, provided that the former drug was used in suitable carriers, Transfersome® (Rother et al. 2007). I therefore chose ketoprofen in this study to determine primarily its influence on the mechanics of $C_{18:1}EO_{20}$ saturated, mixed lipid vesicle membranes.

The second study objective was the determination of the influence of the amphiphilic drugs bupivacaine, ketoprofen, and the manufacturing excipient ethanol on the carrier's adaptability and bending rigidity, respectively. Numerous publications report alterations of membrane mechanics and stability by alcohols (Lobbecke et al. 1995; Chanturiya et al. 1999; Ly et al. 2004), which increase lipid bilayer elasticity and even cause membrane solubilisation. A

reduction of bilayer bending rigidity has also been reported for many other amphiphilic drug molecules such as salicylate (Zhou et al. 2005), azithromycin (Fa et al. 2007), lidocaine (Hogberg et al. 2007), and others (Ondrias et al. 1991). The investigations in this work were performed with different amphiphile concentrations and at different *pH* and ionic strengths, due to the well known effect of amphiphile geometry, membrane charge, and salts on the membrane mechanics and electrostatics (Israelachvili 1985; Winterhalter et al. 1988; Cevc 1990).

5.2. Material and Methods

5.2.1. Materials

The active drug substances bupivacaine hydrochloride monohydrate and ketoprofen were supplied in European Pharmacopoeia quality by Heumann PCS (Feucht, Germany) and Bidachem (Fornovo S. Giovanni, Italy), respectively. Soybean phosphatidylcholine (assumed $M_w \approx 800$ g/mol) with a purity grade > 90% (Lipoid S100) was purchased from Lipoid (Ludwigshafen, Germany). Polyoxyethylene (20) oleyl ether (assumed $M_w \approx 1150$ g/mol) was acquired from Croda / Uniqema (Nettetal, Germany) and met the European Pharmacopoeia specification for macrogol oleyl ether as well the following used ingredients: phosphate or acetate buffer components, sodium chloride, sodium hydroxide, hydrochloric acid (all VWR, Darmstadt, Germany), ethanol (BfB, Munich, Germany) and water for injection (Deltaselect, Dreieich, Germany).

5.2.2. Preparation of simple and mixed lipid bilayer vesicles with/without active drug substances

Lipid vesicle suspensions used in this study had typically a total lipid dry mass between TL = 7.7 - 10 w-% (SPC + $C_{18:1}EO_{20}$) with experimental dependent different effective surfactant to lipid molar ratios, $R_e = c_s/c_l$, and varying drug concentrations, c_d (Table 11). The *pH* of the investigated suspensions was adjusted with a suitable buffer, e.g. a phosphate or an acetate buffer, resulting in various but comparable ionic strengths, I_c, to which the drug counter ions contributed as well. Ionic strength is defined as:

$$I_c = 0.5 \cdot \sum_{i=1}^{n} z_i^{\,2} \cdot c_i \qquad (36)$$

c_i being the bulk molar concentration of the ion i with the charge number z_i .

The simple and mixed lipid suspensions were manufactured with two different, widely-used methods, depending on their ethanol content. For the ethanol containing suspensions, the injection method was used (Batzri et al. 1973; Lasic 1993) whereas for the ethanol free formulations freeze-thaw cycles combined the lipophilic and hydrophilic components (MacDonald et al. 1993). Both manufacturing processes were finished with a homogenisation step (Olson et al. 1979; Mayer et al. 1986). The measurement of the vesicle sizes and the polydispersity indices using the dynamic light scattering (DLS) are described in chapter 2.2.4. In detail:

Ethanol containing mixed lipid vesicle suspensions

All lipophilic components, i.e. the SPC and the amphiphilic surfactant $C_{18:1}EO_{20}$, were dissolved in ethanol, whereas water acted as solvent for the hydrophilic substances such as the active agent. The lipophilic phase was then slowly injected by a syringe through thin-walled needle into the stirring water phase, resulting in an inhomogeneous lipid vesicle suspension. Homogenisation of the original, polydispersed suspension to large unilamellar vesicles (LUV) with a diameter d_{ves} = 110 ± 15 nm and polydispersity index PDI < 0.15 was achieved by multi-extrusion through different track etched polycarbonate membranes (PCTE, GE Osmonics) of decreasing pore diameters (d_p = 400 nm – 80 nm).

Ethanol free mixed lipid vesicle suspensions

Most of the studied lipid vesicle suspensions were free of ethanol and thus produced by mixing all lipophilic, amphiphilic and hydrophilic compounds and stirring them for > 12 h. Afterwards, the oligo- (OLV) and multilamellar (MLV) vesicle suspension was extruded through different PCTE membranes of decreasing pore diameters (d = 400 nm – 100 nm), followed by subsequent freeze-thaw cycles (180 min at -70°C, 30 min at 40°C), and finished with a multi-extrusion step through PCTE membranes (d = 400 nm – 80 nm) as is described above. The resulting large unilamellar vesicles (LUV) had a diameter d_{ves} = 110 ± 15 nm and a polydispersity index PDI < 0.15.

Test series	R_e [mol/mol]	c_d [mM] , *[M]	I_c [mM]	*pH*
SERIES "S"	0.00	---------	~ 100	7.2
	0.10	---------	~ 100	7.2
	0.17	---------	~ 100	7.2
	0.20	---------	~ 100	7.2
	0.25	---------	~ 100	7.2
SERIES "SB"	0.00	67	~ 60	4.7
	0.10	67	~ 60	4.7
	0.175	67	~ 60	4.7
	0.25	67	~ 60	4.7
SERIES "E"	0.25	0.50 *	~ 100	7.2
	0.25	0.76 *	~ 100	7.2
	0.25	1.30 *	~ 100	7.2
	0.25	1.74 *	~ 100	7.2
	0.25	2.17 *	~ 100	7.2
SERIES "K"	0.25	14	~ 125	7.2
	0.25	27	~ 125	7.2
	0.25	39	~ 125	7.2
	0.25	50	~ 125	7.2
SERIES "I_c"	0.25	53	206	4.7
	0.25	53	356	4.7
	0.25	53	556	4.7
SERIES "pH"	0.25	40	~ 100	7.25
	0.25	40	~ 100	6.65
	0.25	40	~ 100	6.45
	0.25	40	~ 100	6.20
	0.25	40	~ 100	5.75
	0.25	53	~ 60	4.70

Table 11: Composition of the tested suspensions comprising simple and mixed lipid vesicles used for membrane adaptability measurements in dependency on effective $C_{18:1}EO_{20}$ to SPC molar ratio, R_e, active drug concentration, c_d, ionic strength, I_c, and *pH*.

- **Series "S": Mixed lipid bilayer vesicles with different Surfactant to lipid ratio, R_e**
- **Series "SB": Mixed lipid bilayer vesicles with different Surfactant to lipid ratio, R_e, and constant Bupivacaine x HCl x H_20 concentration**
- **Series "E": Ethanol in mixed lipid bilayer vesicles with R_e = 0.25 mol/mol**
- **Series "K": Ketoprofen in mixed lipid bilayer vesicles with R_e = 0.25 mol/mol**
- **Series "I_c": Different ionic strength in bupivacaine containing mixed lipid bilayer vesicles having R_e = 0.25 mol/mol**
- **Series "pH": Different *pH* values in bupivacaine containing mixed lipid bilayer vesicles at R_e = 0.25 mol/mol**

5.2.3. Membrane adaptability measurements and bending rigidity

Membrane bending rigidity and the overall vesicle adaptability were determined with the recently introduced continuous membrane adaptability assay (CMA), which is described in more detail in chapter 3.2.3.

In short: the CMA relies on a tempered, pressure driven filtration of the tested vesicle suspension through a nanoporous filter with area A_f, which acts as an obstacle to the transport of stiff and inflexible bilayer vesicles, when the pore diameter d_p is at least 50 % smaller than the average vesicles diameter d_{ves} (Hunter et al. 1998; Cevc et al. 2003b). Adaptable vesicles with a flexible bilayer in contrast are able to penetrate the pores. This ability is analysed quantitatively in terms of mass flow $\dot{m}(t)$ in dependency on driving pressure $\Delta p(t)$ and finally yields an experimental penetrability function

$$P_{exp}(\Delta p) = \frac{1}{\Delta p \cdot A_f} \cdot \frac{dm}{dt} \tag{37}$$

in which the trans-filter flow-driving pressure is the independent variable.

The penetrability described by equation (37) is an activated process that can be modelled theoretically (Cevc et al. 2003b). To penetrate relatively narrow pores, the pore crossing vesicles with energy E_{ves} must be deformed using activation energy, E_A. Based on the Maxwell-Boltzmann distribution, the ratio of the vesicles with ability to penetrate the porous barrier is defined as:

$$P(E_A, E_{ves}) = 1 - \mathrm{erf}\left(\sqrt{\frac{E_A}{E_{ves}}}\right) + \sqrt{\frac{4E_A}{\pi E_{ves}}} \cdot \exp\left[-\frac{E_A}{E_{ves}}\right] \tag{38}$$

erf is the error function.

Alternatively, the penetrability can be expressed as a function of the penetration driving pressure, Δp, with only two fitting parameters: p^*, corresponding to the characteristic pressure at which the average vesicle energy equals the activation energy ($E_A / E_{ves} = 1$) and P_{max}, corresponding to the maximum penetrability of the barrier (at $\Delta p \rightarrow \infty$):

$$P(\Delta p) = P_{max} \cdot \left\{1 - \mathrm{erf}\left(\sqrt{\frac{p^*}{\Delta p}}\right) + \sqrt{\frac{4p^*}{\pi \Delta p}} \cdot \exp\left[-\frac{p^*}{\Delta p}\right]\right\} \tag{39}$$

By adjusting the penetrability curve described by equation (39) to the measured experimental penetrability data P_{exp}, the system specific parameters p^* and P_{max} can be derived.

p^* value is one measure of the average bilayer bending rigidity κ_c. For the simple and mixed lipid bilayer vesicles based on soybean phosphatidylcholine the bending rigidity can be expressed in units of thermal energy, k_BT, using the measured characteristic pressure p^* as is described in detail in chapter 3.4:

$$\kappa_c = \frac{p^* \cdot 3.67}{MPa} \cdot k_B T \tag{40}$$

The characteristic pressure and the vesicle adaptability (in units of inverse pressure), $a^* = 1/p^*$, are the only vesicle characterising parameters, and nearly independent of the other suspension parameters, such as the average vesicle size (Cevc et al. 2003b; Cevc 2004). In contrast, the P_{max} value depends on the filter and sample parameters, such as the filter porosity, filter area, sample viscosity, temperature etc., and can be referenced to the vesicle free suspension medium or to suitable reference suspensions containing aggregates that are smaller than the pore diameter (in that case no activation is necessary) .

In the solubilisation range the total penetrability is the sum of the pore penetration by the saturated mixed lipid vesicles and the resulting mixed lipid micelles.

$$P_{tot}(\Delta p) = \alpha_{mic} \cdot P_{mic}(\Delta p) + (1-\alpha) \cdot P_{ves}(\Delta p) \tag{41}$$

Co-consideration of vesicle and micelle pore penetration abilities allows calculation of the micellar fraction in the mixed suspension, α_{mic}.

5.3. Results

Penetration of nanoporous barriers by simple lipid vesicles can be improved, in concentration dependent fashion, by addition of an amphiphilic surfactant, such as $C_{18:1}EO_{20}$ (cf. chapter 3). The results measured in this study illustrate a diversified view over the effect of additional amphiphats incorporation (uncharged, negatively, and positively charged) into such mixed lipid bilayer membranes, including the influence of *pH* and I_c on the latter.

5.3.1. Concentration dependent influence of uncharged amphiphile ethanol on the bending rigidity of mixed lipid bilayer vesicles

The membrane softening and, as the case may be, destabilising effect of the uncharged excipient ethanol on $C_{18:1}EO_{20}$ saturated SPC mixed bilayer vesicles with R_e = 0.25 mol/mol was analysed, concentration dependent, with series “E” (Table 11).

Ethanol and other short chain alcohols are known to laterally expand, thin and thus reduce the bending rigidity of phosphatidylcholine bilayer membranes (Vierl et al. 1994; Lobbecke et al. 1995; Ly et al. 2002; Ly et al. 2004) including even complete bilayer solubilisation with 45 – 50 w-% ethanol (Touitou et al. 2000).

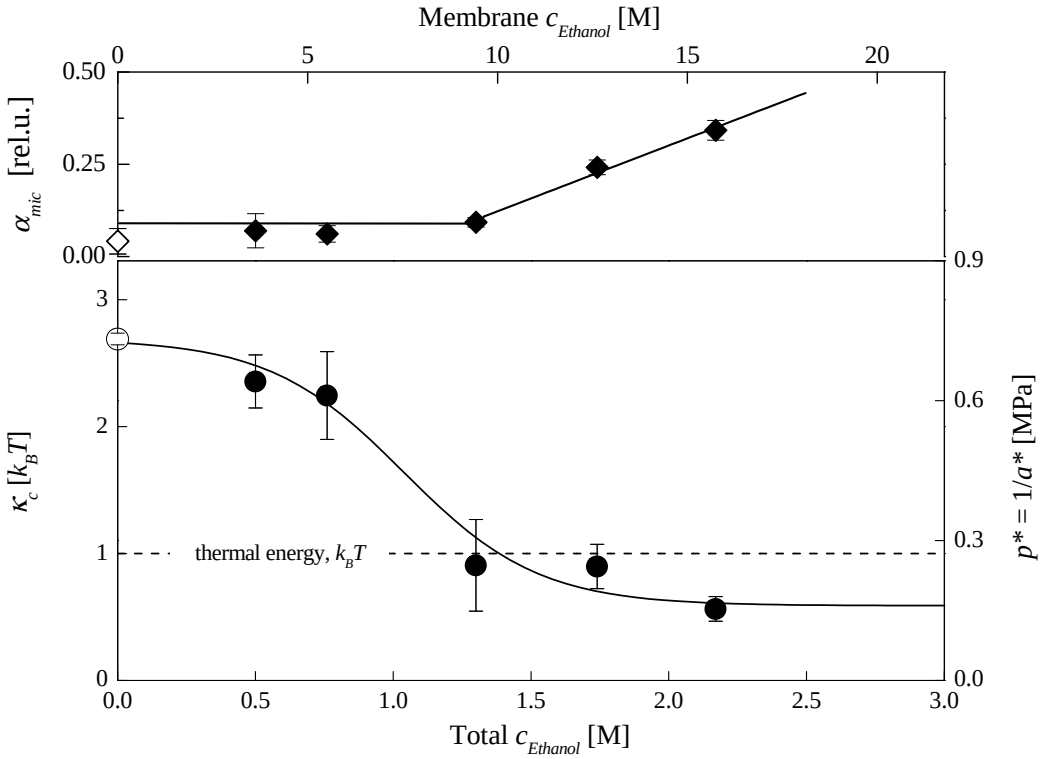

Figure 33: Influence of ethanol (filled symbols) on bending rigidity of mixed lipid bilayers (empty symbols) with $C_{18:1}EO_{20}$ to SPC molar ratio of R_e = 0.25 mol/mol.
The lower panel shows decreasing κ_c with increasing ethanol concentration, highlighted with a sigmoidal ad-hoc fit. Above a total concentration ~ 1.3 M, corresponding to a membrane concentration ~ 9.5 M, the bilayer membrane becomes instable, with a bending rigidity $\kappa_c < k_BT$, causing mixed micelles formation (upper panel).

Adaptability measurements in the lower panel of Figure 33 with polyoxyethylene (20) oleyl ether saturated soybean phosphatidylcholine membranes (R_e = 0.25 mol/mol) confirm the bilayer softening effect of ethanol. They reveal a quasi-sigmoidal decrease of the bilayer bending rigidity with increasing ethanol concentration. At ~ 1.3 M total ethanol concentration, corresponding to a bilayer membrane concentration of ~ 9.5 M (Ly et al. 2004), the bilayer elasticity is in the range of $\kappa_c \approx k_BT$, and even below the thermal energy at higher concentrations. Bilayer destabilisation above 1.3 M ethanol (7.5 v-%) results in formation of mixed micelles, which represent an increasing fraction of total aggregates (upper panel in Figure 33). This resembles the lysis measurements reported by Ly et al. (2002), which showed a decreasing lysis tension up to 10 v-% ethanol when a steady state is reached, corresponding to SOPC membrane saturation with ethanol. Thereafter, vesicle solubilisation starts and is completed at ~ 55 v-% ethanol.

5.3.2. Bending rigidity of mixed lipid bilayer vesicles containing negatively charged ketoprofen

In analogy to the quasi-sigmoidal dependency of ethanol effect on $C_{18:1}EO_{20}$ saturated SPC mixed bilayer vesicles, the addition of negatively charged ketoprofen (series "K" at pH = 7.2) to such bilayer membranes also decreases the bending rigidity in concentration dependent manner (Figure 34). The bilayer adaptability, a^*, and bending rigidity, κ_c, change after an initial plateau up to a steady state level of $p^* = 1/a^* \approx 0.28$ MPa^{-1} and $\kappa_c \approx k_BT$, corresponding to a total ketoprofen concentration $\geq$ 55 mM and a bilayer membrane concentration of $c_{Ketoprofen} \geq 350$ mM (calculated with the partition results derived in chapter 4.4.3.

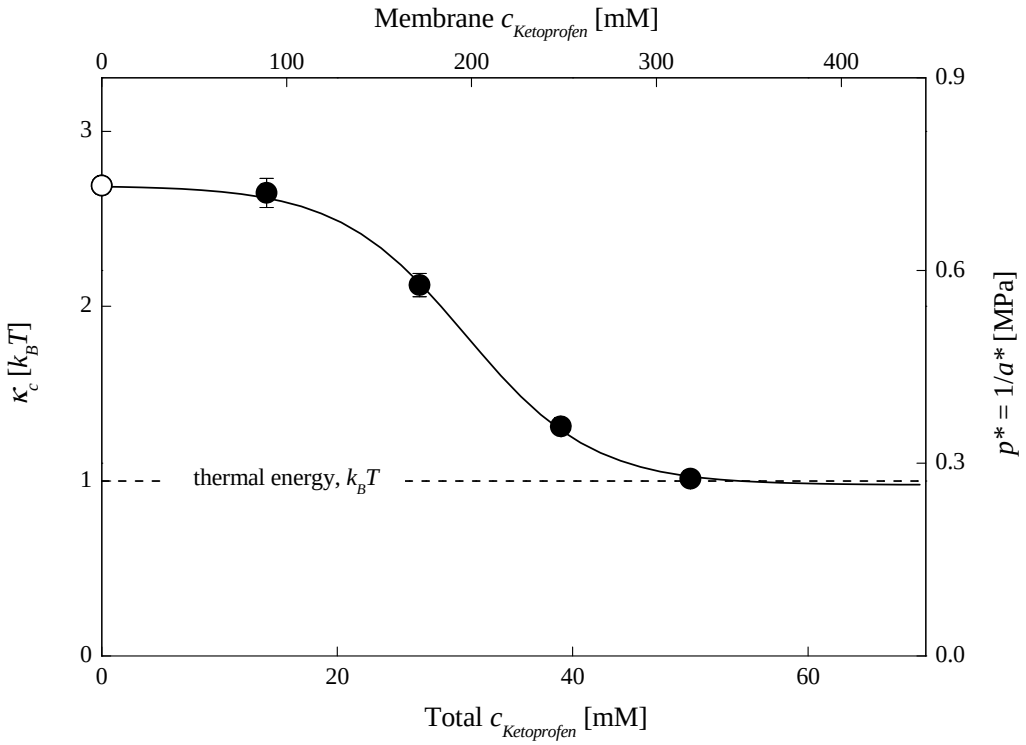

Figure 34: Influence of negatively charged ketoprofen (filled symbols) on bending rigidity of mixed lipid bilayers (empty symbols)) with $C_{18:1}EO_{20}$ to SPC molar ratio of R_e = 0.25 mol/mol. Ketoprofen reduces, concentration dependent, the bending rigidity of $C_{18:1}EO_{20}$/SPC vesicles to $\kappa_c \approx k_BT$, highlighted with a sigmoidal ad-hoc fit.

5.3.3. Effect of positively charged bupivacaine on pore penetration and bending rigidity of simple and mixed lipid bilayers

In addition to testing membrane softening effects of uncharged ethanol and negatively charged ketoprofen in $C_{18:1}EO_{20}$/SPC mixed lipid bilayer vesicles, I studied the related influence of positively charged bupivacaine at constant total drug concentration on mixed bilayer membranes with different surfactant to lipid ratios R_e.

Narrow pore penetration by different $C_{18:1}EO_{20}$/SPC mixed lipid bilayer vesicles (series "S") depends on the surfactant concentration in the bilayer membrane, as is presented in Figure 35 (grey curves). As extensively discussed elsewhere, the pore penetration by such mixed bilayer vesicles increases up to the molar surfactant to lipid saturation limit, R_e^{sat} = 0.25 mol/mol. Adaptability of the corresponding mixed bilayer vesicles containing positively charged bupivacaine at *pH* = 4.7 under constant total drug concentration (series "SB") reveals an additional membrane softening effect resulting in higher pore penetrability (black curves in Figure 35).

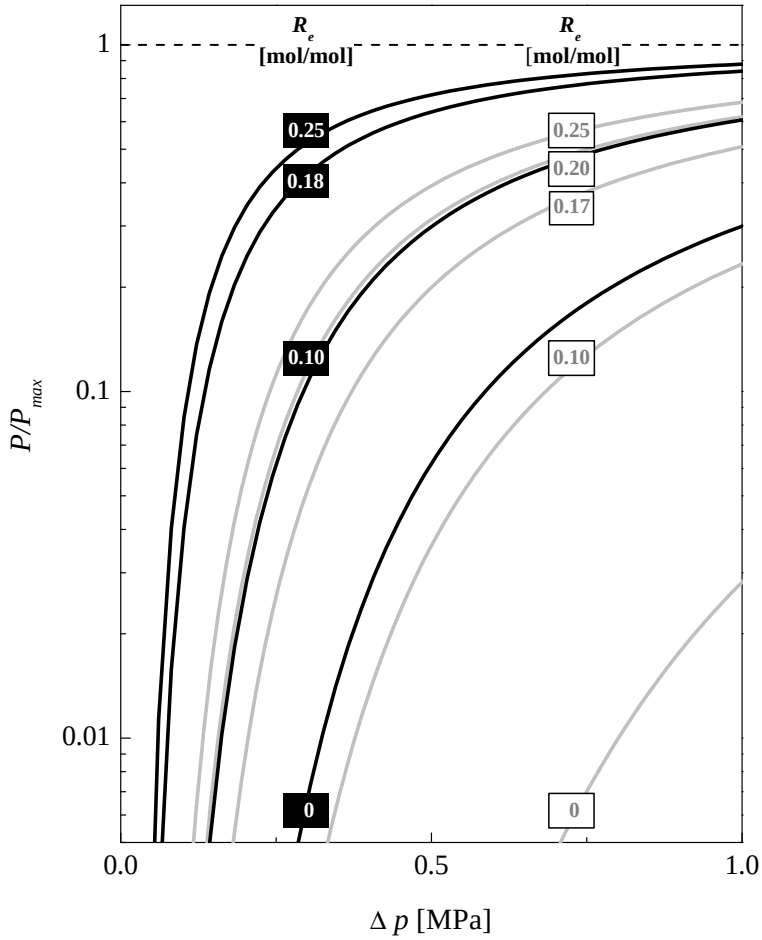

Figure 35: Relative pore penetrability, P/P_{max}, of the mixed bilayer vesicles composed of different $C_{18:1}EO_{20}$/SPC ratios, R_e, with (black) or without (grey) bupivacaine 67 mM

Compared to the drug-free bilayer membranes with similar surfactant concentration, the mixed lipid vesicles comprising positively charged bupivacaine have a lower bilayer rigidity, κ_c, and therefore a lower characteristic pressure, p^*, as is highlighted in Figure 36 with an exponential ad-hoc fit. Interaction of bupivacaine (total $c_{Bupivacaine}$ = 67 mM) with a simple or mixed lipid bilayer membrane reduces the elastic energy of the latter by a factor of 2 – 3, resulting in highly deformable, yet stable vesicles with $\kappa_c \approx 1.2\ k_BT$ for the surfactant-lipid mixture with R_e = 0.25 mol/mol.

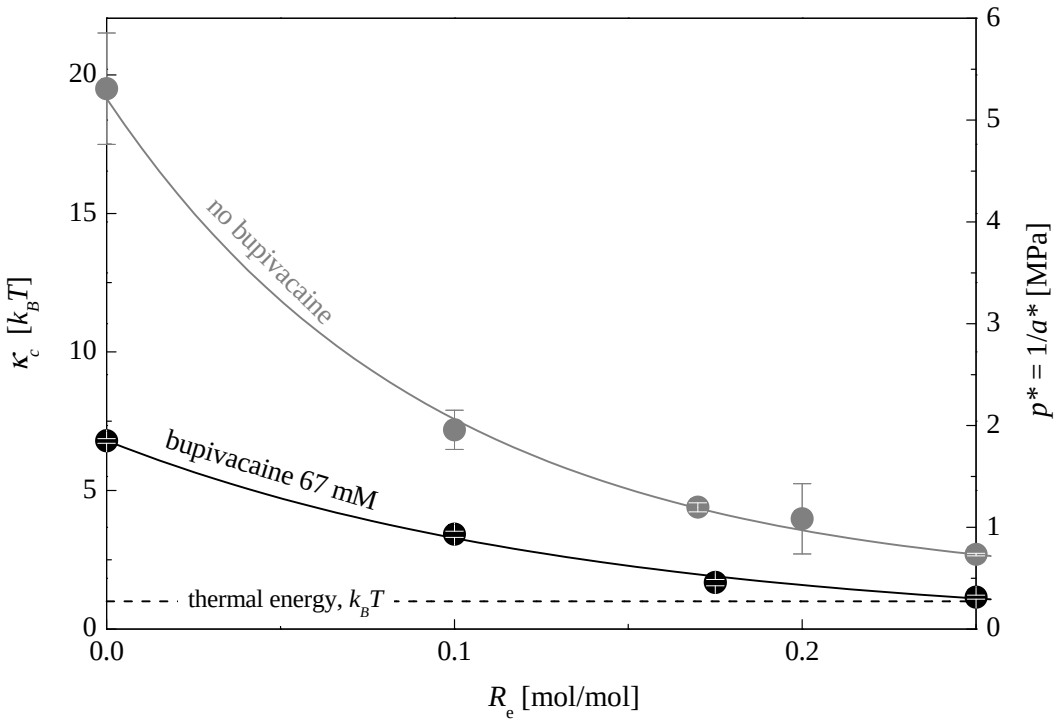

Figure 36: Bilayer rigidity, κ_c, and penetration enforcing characteristic pressure, p^*, as a function of different $C_{18:1}EO_{20}$ to SPC ratios, R_e, with (●) or without (●) added bupivacaine. The positively charged bupivacaine (67 mM) softens simple (R_e = 0 mol/mol) as well as mixed lipid vesicles (R_e > 0 mol/mol) compared to bupivacaine free bilayer membranes. Triple measured data points highlighted by an exponential ad-hoc fit.

5.3.4. Influence of the drug charge state, the bulk *pH*, and the ionic strength on bilayer bending rigidity

A detailed analysis of the bupivacaine mediated bilayer membrane softening, using mixed lipid bvesicles with a constant total bupivacaine concentration and uniform surfactant to lipid ratio, R_e, reveals a *pH* and ionic strength dependent effectiveness of bupivacaine on pore penetration by the resulting vesicles. The same data also document a concomitant decrease of the bilayer bending rigidity (series "*pH*" and series "I_c").

The left panel in illustrates a more or less constant and low bilayer bending rigidity at $pH \leq 6.2$, which increases at $pH > 6.2$; At $pH \approx 7.2$ for example, the bupivacaine containing bilayer is less flexible than the comparable, bupivacaine free bilayer membrane, indicating that only positively charged bupivacaine softens a lipid membrane in contrast to the uncharged drug which stiffens the bilayer.

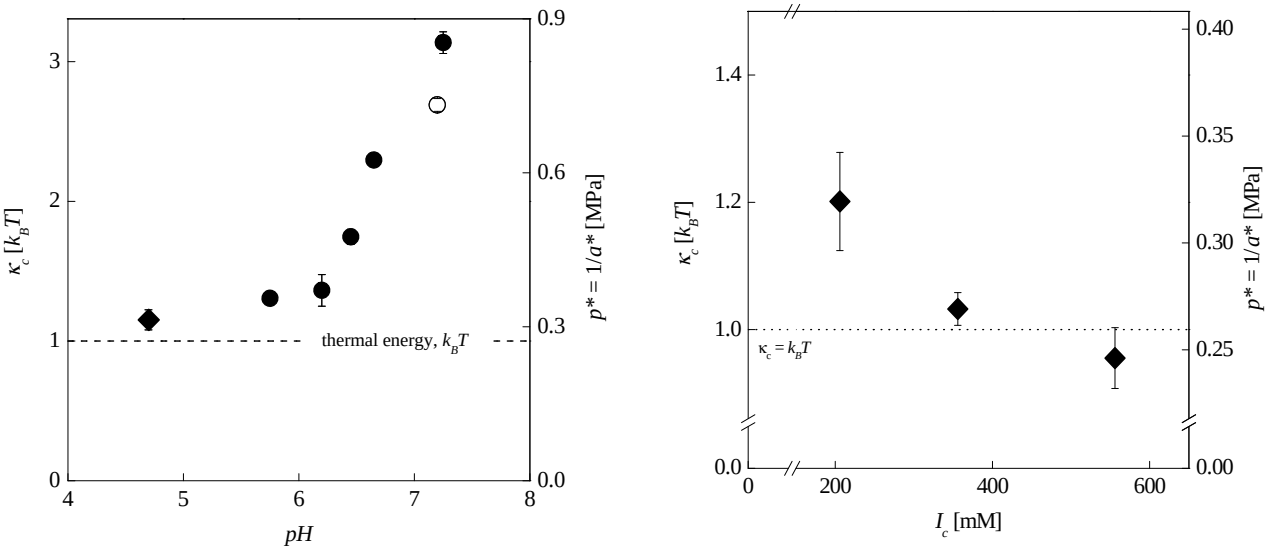

Figure 37: Rigidity of the mixed bilayer vesicles (R_e = 0.25 mol/mol) without (○) or with (● 40 mM; ♦ 53 mM) membrane associated bupivacaine as a function of bulk *pH* and ionic strength, I_c. Left panel illustrates κ_c value decrease with decreasing *pH* whereas the right panel shows a reduced bending rigidity with increasing I_c.

Ionic strength influences bilayer rigidity as well. As is illustrated in the right panel of Figure 37, κ_c decreases with increasing salt concentration reaching, within experimental error, the thermal stability limit at $\kappa_c \approx k_BT$. Both observations are closely related to drug partition into the bilayer membrane and to the resulting changes in membrane electrostatics (cf. chapter 4.4.2), and are intensively discussed later in the text.

5.4. Discussion

Polyoxyethylene (20) oleyl ether is a non-ionic surfactant, which forms, in combination with certain lipids and composition dependent, fluctuating and adaptable bilayer membranes. The most deformable vesicle with such a bilayer, Transfersome®, is a carrier suitable for non-invasive transdermal drug delivery of low and high molecular active agents owing to its ability to cross even very narrow pores in the skin barrier (Cevc 1997; 2004). The membrane softening activity of $C_{18:1}EO_{20}$ at an effective surfactant to lipid ratio $R_e \leq 0.25$ mol/mol was analysed in this study in presence of positively and negatively charged drug molecules and of the uncharged ethanol, which is known to interact with natural and artificial membranes.

Ethanol in mixed lipid vesicles

Ethanol is a small amphiphilic molecule that has been used, as a solvent, in the preparation of lipid bilayer vesicles for years using the so-called injection method (Batzri et al. 1973; Lasic 1993). The influence of ethanol on phospholipids has been investigated independently with structural questions and objectives in mind (Rowe et al. 1990; Nagel et al. 1992; Vierl et al. 1994). In this work, I studied the interaction of ethanol with ultradeformable vesicles, comprising SPC and $C_{18:1}EO_{20}$, with the focus on its ability to change the mechanical properties of lipid bilayers like membrane bending rigidity and thus the resulting vesicle adaptability for skin pore penetration.

Ethanol reduces bending rigidity of surfactant saturated phosphatidylcholine membranes (R_e = 0.25 mol/mol) in concentration dependent fashion as is shown in Figure 33. In a suspension with ~ 1.3 M ethanol, the bilayer elasticity energy decreases up to $\kappa_c \approx k_BT$ (Figure 38). Micropipette aspiration measurements of Ly et al. (2002; 2004), done with SOPC membranes, also confirm κ_c reduction in dependency on ethanol concentration. The addition of 1.3 M ethanol to $C_{18:1}EO_{20}$/SPC vesicles diminishes κ_c by a factor of ~ 2.5 whereas the same alcohol amount in SOPC reduces the bilayers elasticity energy by only ~ 14 %. Such decrease, 13 % and 16 %, was found in this work at lower ethanol concentrations, 0.5 M and 0.76 M, respectively. The most likely reasons for the difference are disparate lipid concentrations used in this study and by Ly, being 10 w-% and 0.05 w-%, respectively.

For more detailed interpretation of the observation one has to consider the membrane/water interface in detail. The phosphatidylcholine headgroup is well hydrated with multiple hydrogen bonds between water and the lipid phosphate and choline group, and for fewer water molecules around the fatty acid carbonyl group. FT-IR results (Chiou et al. 1992),

NMR measurements (Barry et al. 1994; Holte et al. 1997) and microscopic molecular dynamic simulations (Patra et al. 2006) all show that ethanol competes with water for hydrogen bonding with the phosphate group and the fatty acid carbonyl group. However, the alcohol has an advantage over water owing to its slight hydrophobicity. Competition plus an additional interaction of the ethanolic hydrophobic part and the upper segments of lipid tails also favours alcohol binding and dehydrates the bilayer membrane. As a consequence, the bound ethanol increases interfacial solvation and thus the surface area per molecule, while reducing interfacial hydration. This increases membrane disorder and decreases the bilayer thickness. All these modifications lead to a reduced bilayer bending rigidity and increased membrane flexibility (Winterhalter 1995; Ly et al. 2002; 2004).

Nevertheless, ethanol has only a slight effect on the bending rigidity of ultradeformable, $C_{18:1}EO_{20}$ based, mixed lipid vesicles ($TL \approx 10$ w-%) at concentrations < 0.75 M. For the manufacturing of such mixed lipid vesicles by the widely used injection method this solvent concentration is sufficient to manufacture the ethanolic intermediate product nonseriously influencing κ_c in the final product. However, at higher ethanol values, the mixed lipid vesicles become highly flexible at c = 1.3 M and presumably instable above this concentration as reported in 5.3.1.

Negatively and positively charged drug substances in mixed lipid vesicles

Interaction of drug substances with biological membranes is a broad topic analysed and intensively discussed in pharmaceutical research; this relates to drug resorption, distribution, mode of action, and excretion.

The influence of neutral, negatively, and positively charged amphiphilic active agents on membrane mechanics, such as lipid cohesion and bilayer elasticity, is far less well studied and understood. It can be determined with different methods, and is among other factors important in development of highly fluctuating, ultradeformable lipid carriers for transdermal drug delivery. Computer simulations and micropipette aspirations are common methods to determine bending rigidity, κ_c, of phosphatidylcholine bilayers. Examples include an NSAID, salicylate (Zhou et al. 2005), a local anaesthetic, lidocaine (Hogberg et al. 2007), and an antibiotic, azithromycin (Fa et al. 2007). The positively charged lidocaine, the negatively charged salicylate, and the amphiphilic azithromycin reduce κ_c in concentration dependent fashion by up to ~ 50 %.

Figure 38 illustrates the adaptability measurements done with ketoprofen and bupivacaine containing mixed lipid vesicles. The influence of these drugs on the rigidity of $C_{18:1}EO_{20}$ saturated SPC bilayer vesicles (R_e = 0.25 mol/mol) is obvious. Both, the negatively charged ketoprofen and the positively charged bupivacaine lower the bending rigidity of drug-free, deformable mixed lipid vesicles down to the level of thermal energy, $\kappa_c \approx 1$ - 1.2 k_BT, where highly fluctuating vesicles prevail (Safinya et al. 1989; Gompper et al. 1995; Cevc et al. 1998). To understand their influence on membrane mechanics, one has to take a detailed look on bilayer composition and membrane-drug interactions.

All tested drug molecules partition into and interact with the mixed bilayer membrane. As has been shown with partition coefficient measurements in chapter 4.4.3, the partitioning of uncharged molecules is stronger than of charged ones.

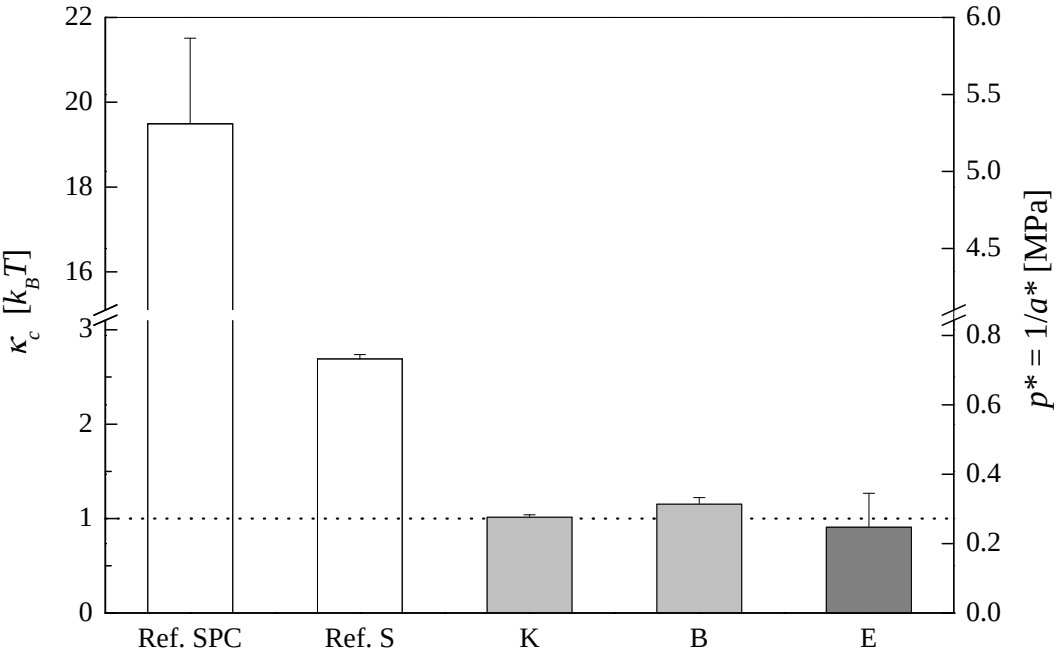

Figure 38: Bending rigidity of simple lipid bilayer vesicles (Ref. SPC) and different, surfactant based mixed lipid bilayer.
Interaction of an amphiphilic molecule with $C_{18:1}EO_{20}$ saturated mixed vesicles (Ref. S with R_e = 0.25 mol/mol) softens the mixed lipid bilayer membrane concentration dependent up to $\kappa_c \approx 1$ - 1.2 k_BT. (K = ketoprofen 50 mM ; B = bupivacaine 53 mM ; E = ethanol 1.3 M)

Nevertheless, the charged molecules reduce κ_c, as is discussed later in the text. Charged bupivacaine interacts with the polar lipid headgroups via hydrogen bonds between the positively charged NH-group and the phosphate oxygens or the fatty acid carbonyl oxygen, similar to the interaction of ethanol with phosphatidylcholines. The positively charged NH-group is additionally attracted by the electrostatic forces to the negatively charged phosphate

group. Similar electrostatic attraction potentially exists between the negatively charged ketoprofen and the positively charged choline nitrogen. As a consequence, the surface area per lipid molecule interacting with the drug increases, and membrane cohesion decreases, as has been reported for the amphiphilic drug molecule azithromycin (Fa et al. 2007).

The increased and measured membrane adaptability for all the tested drug substances in $C_{18:1}EO_{20}$ saturated SPC vesicles is therefore a result of the reduced bending rigidity. Furthermore an additional, supporting mechanism of action is possible. Amphiphilic small charged molecules, like salicylate (Zhou et al. 2005), larger charged amphiphiles, like sodium cholate (Schubert et al. 1986), or the non-ionic surfactants polysorbate 20 (Karatekin et al. 2003) and octyl-β-D-glucopyranoside (Schubert et al. 1988) are all able to form and stabilise membrane holes, formed inter alia spontaneously due to decreased lipid cohesion. The holes help the ultradeformable vesicles to react to deformations by permitting an easy exchange of water between the vesicle interior and the vesicle surroundings, and vice versa. The improved water permeability plus the higher membrane flexibility make a vesicle adaptable enough to enter the skin pores smaller than its average vesicle size, and allows the vesicle to act as a carrier for transdermal drug delivery (Cevc et al. 2003b).

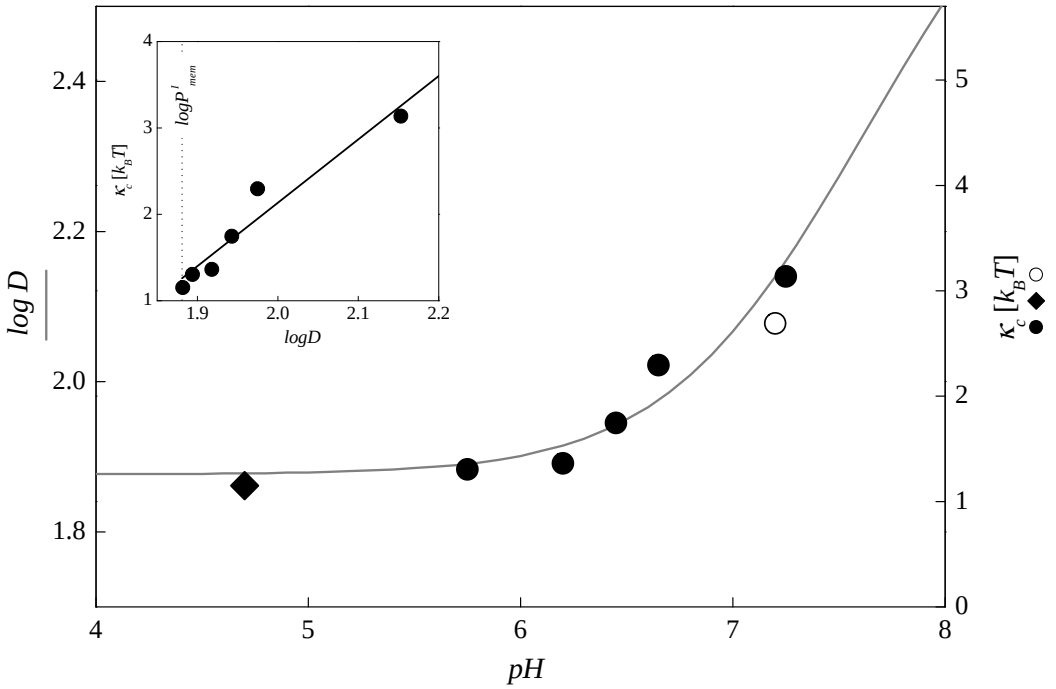

Figure 39: *pH*-dependent bupivacaine distribution log*D* in lipid membranes (——) and *pH*-controlled bending rigidity κ_c of bupivacaine containing (● 40 mM; ♦ 53 mM) and drug-free (○) mixed lipid bilayer vesicles (R_e = 0.25 mol/mol).
The small panel illustrates increasing bilayer elasticity with increasing amounts of charged bupivacaine in the membrane. P^I_{mem} is the partition coefficient for the ionized form.

Amphiphilic, basic, or acidic drug substances interact with the lipid bilayer membranes differently at various *pH* values, dependent on their charge state. This is also reflected in Figure 39, which illustrates *pH*-dependent bupivacaine effect on partitioning into and rigidity of mixed lipid bilayers. Bupivacaine possesses a *pH*-dependent membrane distribution with ~ 8 times higher affinity for the lipid at $pH > 8.5$ compared to $pH < 6$, i.e. above and below the apparent $pK_{app} \approx 7.25$, when uncharged and positively charged bupivacaine prevail. In parallel to increasing membrane partitioning of uncharged drug above pH ≈ 6.2, the mixed bilayer stiffens and bending rigidity, κ_c, increases. The uncharged bupivacaine thus seems to stiffen rather than soften the lipid bilayer. Compared to the drug-free $C_{18:1}EO_{20}$/SPC mixed lipid vesicles (open symbol in Figure 39), the charged drug, conversely, softens the mixed bilayer membrane at lower *pH* values. Despite its reduced membrane affinity, the positively charged bupivacaine increases the elasticity of $C_{18:1}EO_{20}$ saturated phosphatidylcholine bilayer vesicles to $\kappa_c \approx 1.2\ k_BT$.

Such a stiffening and softening effect of molecules on bilayer membranes has been reported by different authors. Hogberg et al. (2007) determined the charge specific location of lidocaine, also a anilide local anaesthetic like bupivacaine, in a lipid bilayer. The uncharged lidocaine is inserted in the bilayer near the fatty acid ester group and the upper part of the lipid tail whereas the positively charged lidocaine is located at the polar headgroup level. The charged form also interacts more strongly with water and the lipid headgroup. Charged anaesthetics thus displace hydration water of the lipid bilayer resulting in a positive membrane curvature, whilst also reducing bending rigidity. In contrast, the deeper located uncharged local anaesthetics stiffen the bilayer membrane, as does cholesterol. The latter is located deeper in the bilayer membrane and promotes negative membrane curvature and thus higher bending rigidity (Evans et al. 1987; Duwe et al. 1990; Evans et al. 1990; Winterhalter 1995; Lundbaek et al. 2004).

Owing to partially electrostatic interaction between the drug molecule and the mixed lipid bilayer, the ionic strength, I_c, influences the bending rigidity, κ_c, as well. Electrostatic contribution to the bending rigidity of a lipid membrane has been reported preciously based on simulations (Winterhalter et al. 1988; 1992) or experiments (Delorme et al. 2007; Zhou et al. 2007) due to the fact that the bilayer bending rigidity is the sum of mechanical and electrostatic terms:

$$\kappa_c = \kappa_c^{\,m} + \kappa_c^{\,el} \tag{42}$$

The electric contribution was calculated by Winterhalter et al (1988) to be proportional to the square of the Debye screening length $\kappa_c^{el} \propto \lambda_D^2$. The Debye screening length, λ_D, in electrolytes or colloidal dispersions can be calculated with the ionic strength as follows (Cevc 1990):

$$\lambda_D = \sqrt{\frac{\varepsilon \cdot \varepsilon_0 \cdot k_B T}{2 \cdot N_A \cdot e^2 \cdot I_c}} \qquad \Rightarrow \qquad \lambda_D{}^2 \propto I_c{}^{-1} \tag{43}$$

ε and ε_0 are the dielectric constant of the aqueous phase and the permittivity of free space, respectively. The remaining parameters are thermal energy k_BT, the Avogadro number $N_{A,}$ and the elementary electronic charge e.

Therefore it is not surprising that Figure 40 suggest a linear correlation (r = 0.9998) between κ_c and the reciprocal ionic strength, I_c^{-1}. This observation confirms the calculations of Winterhalter due to proportionality between $\kappa_c^{el} \propto \lambda_D^2 \propto I_c^{-1}$ (cf. Equation (43) and supports my findings in chapter 4, where a strong relationship between electrostatics and bilayer membrane partitioning was intensively discussed.

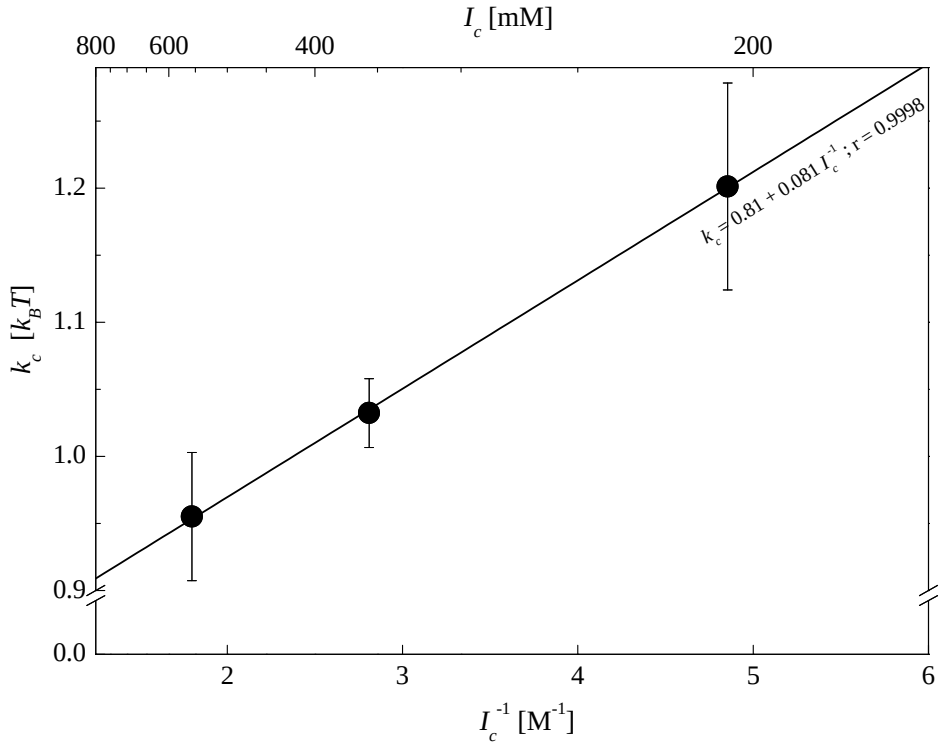

Figure 40: Partitioning, *P*, of positively charged bupivacaine in lipid membrane (—) and the bending rigidity κ_c of bupivacaine containing mixed vesicles (—●—) as a function of reciprocal ionic strength, I_c^{-1}.
(c_d = 53 mM ; *pH* = 4.7 ; R_e = 0.25 mol/mol)

.

Synergy in reducing bilayer bending rigidity

It is worth to ask one final question: Do amphiphilic drug substances soften lipid membranes separately or jointly with the surfactant, which co-forms the basic deformable bilayer in combination with phosphatidylcholine? In other words, is there a synergistic effect between the two amphiphiles?

Synergy between two amphiphilic, membrane softening components has been described by Cevc et al. (2004b) for the negatively charged ketoprofen and the non-ionic surfactant polysorbate 80. Regarding Figure 36 and considering prior results and discussions, it is obvious that both components employed in this study, the positively charged bupivacaine and the non-ionic surfactant polyoxyethylene (20) oleyl ether can individually reduce the lipid bilayer rigidity.

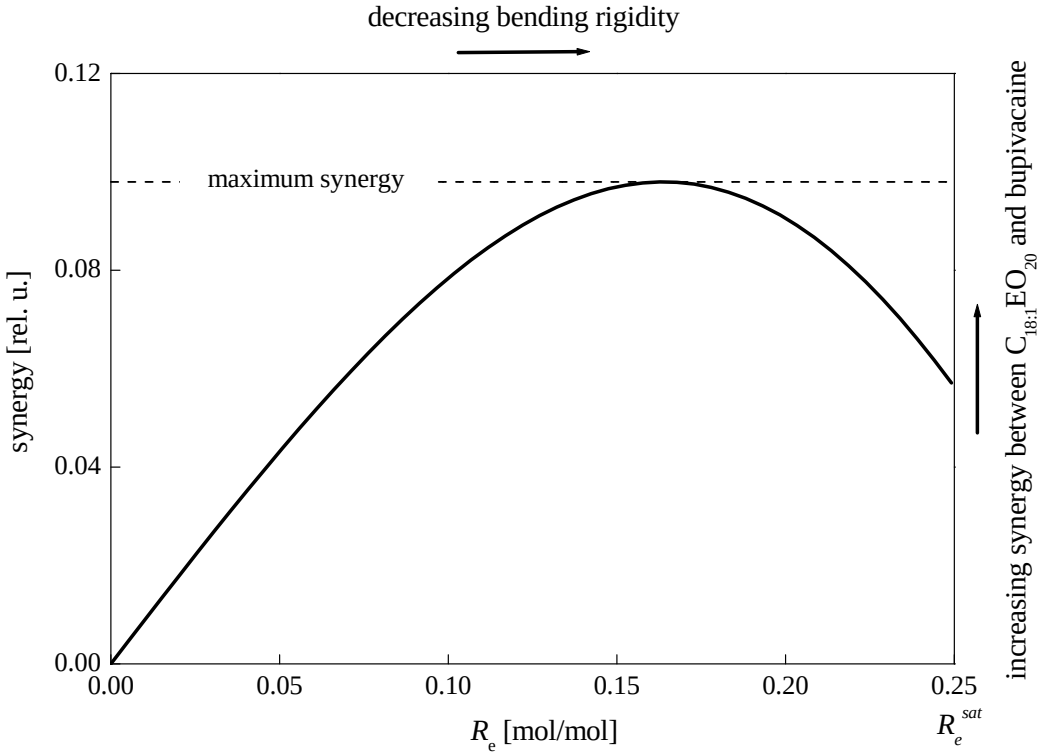

Figure 41: Synergy of $C_{18:1}EO_{20}$ and bupivacaine in softening lipid bilayers with a maximum at effective surfactant to lipid ratio R_e = 0.16 mol/mol.

Based on Figure 36, which shows for both series ("SB" with a constant bupivacaine concentration and an increasing surfactant concentration; "S" without bupivacaine) a R_e – dependent decrease in bilayer's relative bending rigidity

$$\kappa_{c,rel} = \frac{\kappa_c^{SB}}{\kappa_c^{S}} \tag{44}$$

One can quantify the synergistic, bilayer softening effect of the two studied membrane softeners as follows:

$$\text{synergy} = \kappa_{c,rel} - \kappa^{0}_{c,rel} \tag{45}$$

i.e. the difference between relative bending rigidities of the formulations with $R_e > 0$ mol/mol and $R_e = 0$ mol/mol.

Figure 41 illustrates the resulting synergy parameter pertaining to the membranes containing positively charged bupivacaine and non-ionic polyoxyethylene (20) oleyl ether; the data are shown as a function of the effective $C_{18:1}EO_{20}$ to SPC molar ratio. Synergy is evidently maximum at $R_e \approx 0.16$ mol/mol but persists up to the surfactant saturation limit $R_e^{sat} = 0.25$ mol/mol. Below the maximum, additional surfactant progressively improves the drug's membrane-softening potency whereas above the maximum the two kinds of amphiphiles seem to start hindering each other in their bilayer softening activity, without completely loosing their synergistic ability.

5.5. Conclusions and outlook

The development of new medicinal products for non-invasive transdermal drug delivery is a topic of public interest. Availability of such products could improve local efficacy without systemic, and in the ideal case, no local adverse effects. In contrast to conventional TDDS, ultra-adaptable Transfersome® carriers are able to transport active drug substances in a targeted fashion through the skin and even into deeper peripheral tissue regions (Cevc et al. 2001; Cevc 2003; Cevc et al. 2004a; Rother et al. 2007). The results obtained in this study with Transfersome® vesicles, based on a bilayer forming lipid (soybean phosphatidylcholine), the membrane softening surfactant polyoxyethylene (20) oleyl ether, and several drugs, all show excellent in vitro adaptability and pore penetrability. However, the suitability of such highly fluctuating and deformable lipid carriers for practical usage depends on suspension parameters, such as amphiphiles concentration, formulation *pH*, and ionic strength. The latter parameters and the concentration of the excipient ethanol have all to be adjusted during formulation development to optimise the carrier adaptability in terms of bilayer bending rigidity, whilst maintaining carrier integrity ($\kappa_c \geq k_B T$). Future preclinical and clinical studies will be necessary to confirm the good in vitro pore penetrability of the ketoprofen and bupivacaine loaded ultra-adaptable lipid carriers, and their suitability for in vivo treatment of pain and inflammation.

6. SUMMARY

Transfersome® are ultradeformable lipid bilayer vesicles for the local treatment of diseases in superficial and deeper peripheral tissues. The non-invasive dermal and transdermal drug delivery is mediated by these carrier vesicles, which consist of a bilayer forming lipid, such as phosphatidylcholines, and a membrane softening component, like surfactants or amphiphilic drugs. Their high vesicle shape adaptability is the result of the flexible bilayer membrane and the capability of water exchange across the bilayer. Both properties enable the bilayer vesicle to cross the narrow hydrophilic pores in the skin barrier, i.e. the stratum corneum. The driving force for the pore penetration by a Transfersome® is the transepidermal water gradient within the stratum corneum. After non-occlusive application, the bilayer vesicle tries to avoid local dehydration on the skin by penetrating the hydrophilic intercellular pathways in the horny layer.

The major objective in this thesis was the development and characterization of such a new all-purpose Transfersome® formulation using the bilayer softening amphiphile polyoxyethylene (20) oleyl ether, $C_{18:1}EO_{20}$. The low critical micelle concentration, *CMC* = 25 µM, the high membrane partition coefficient, log *K* = 4.3 M^{-1}, the suitable hydrophile-lipophile balance, *HLB* = 15.3, and the cone-shaped geometry made this surfactant worth studying its influence on bilayer membranes in combination with the bilayer forming phospholipid soybean phosphatidylcholine, SPC.

SPC bilayer membrane saturation and solubilisation measurements with and by $C_{18:1}EO_{20}$, respectively, were performed using the static and the dynamic light scattering. Both methods yielded a concordant bilayer saturation limit at an effective surfactant to lipid molar ratio of R_e^{sat} = 0.25 mol/mol, a result comparable to other surfactants with the same polar head group length of 20 ethylenoxide units (Octylphenyl-EO_{20} R_e^{sat} = 0.20 mol/mol; $C_{16}EO_{20}$ R_e^{sat} = 0.28 mol/mol). This low value and the low molar solubilisation ratio of R_e^{sol} = 3 mol/mol allows to classify polyoxyethylene (20) oleyl ether as a rather strong surfactant. In this work I could also show that the time-resolved dynamic light scattering is a suitable and alternative method to analyse the biphasic solubilisation kinetics of such type of surfactants as function of R_e. With the results of kinetic solubilisation measurements I could moreover provide information on molecule properties like the effective diffusion constant, D_{eff} = 2.8 x 10^{-10} m^2s^{-1}, or the surface excess $\Gamma \sim 0.1$ nm^2.

The influence of $C_{18:1}EO_{20}$ on the vesicles shape adaptability was then measured with the recent continuous membrane adaptability assay by analysing different effective molar ratios R_e ranging from surfactant-free SPC liposomes (R_e = 0 mol/mol; $d_{ves} \approx 120$ nm), to $C_{18:1}EO_{20}$ saturated mixed bilayer vesicles (R_e^{sat} = 0.25 mol/mol; $d_{ves} \approx 110$ nm), and finally to solubilised bilayers, i.e. mixed amphiphat micelles (R_e^{sol} = 3 mol/mol; $d_{mic} \leq 15$ nm). The aggregates deformability is measured in that assay as pore penetrability P by the studied aggregates and yields P vs. pressure data similar to those generated by a computer model of ultradeformable vesicle penetration through a constriction. The penetrability of the measured bilayer vesicles through narrow pores (d_p = 20 nm << d_{ves}) increased non-linearly and size independent with R_e and reached maximum value plateau for a surfactant saturated bilayer at R_e^{sat} = 0.25 mol/mol. The flexibility of the saturated membrane remained constant for $R_e > R_e^{sat}$ until complete bilayer solubilisation was reached and mixed micelles were the only aggregates, which passed the obstacle easily due to $d_{mic} < d_p$. With this study I could moreover show that the adaptability a^* of such vesicles can be assessed and translated into bilayer bending rigidity κ_c using a suitable phenomenological theoretical model. The bending rigidity of surfactant-free SPC liposomes could be reduced using $C_{18:1}EO_{20}$ by a factor of ~ 8 from κ_c = 19.5 k_BT to κ_c = 2.5 k_BT for the mixed bilayer vesicles having R_e^{sat} = 0.25 mol/mol. The latter mixed vesicles were demonstrably capable of crossing even very narrow pores, and thus should be suitable for targeted drug delivery across intact skin, which also contains hydrophilic pores with an “open diameter” around 20-30 nm.

The payload of bilayer membrane vesicles with a drug substance was studied in another set of experiments in dependency on the drug’s charge state, bulk *pH*, bilayer electrostatics, and polarity. The bilayer membrane partitioning of the uncharged, neutral drugs, P^N_{mem}, was found to be comparable to reported partition values between 1-octanol and water, being log P^N_{mem} = 3.0 - 3.3 for ketoprofen and log P^N_{mem} = 2.1 – 2.4 for bupivacaine. In contrast, the membrane partition coefficients for the negatively or positively charged active agents were significantly higher compared to the 1-octanol/water partitioning. In dependency on the bulk salt concentration the partition coefficient for ionized ketoprofen ranged from log P^I_{mem} = 0.15 to 1.18 whereas for ionized bupivacaine higher values between log P^I_{mem} = 1.2 and 1.6 were measured. Knowledge and evaluation of the electrostatic influence on the drug partitioning as a function of the membrane surface charge density, the bulk ions concentration, and the polarity of the membrane-water interface enabled me to estimate the drug’s location in the membrane-water interface. Negatively charged ketoprofen is therefore located in the

zwitterionic phosphatidylcholine bilayer membrane between the choline and phosphate group, whereas positively charged bupivacaine is distributed somewhat deeper in the bilayer membrane, between the phosphate and fatty acid carbonyl group.

The effect of drug-vesicle interaction on the bilayer bending rigidity and adaptability of $C_{18:1}EO_{20}$ unsaturated and saturated mixed bilayer vesicles was conclusively studied using negatively charged ketoprofen, positively charged bupivacaine and uncharged ethanol; the latter often used as excipient during vesicle manufacturing process. All three amphiphiles could reduce the bending rigidity of $C_{18:1}EO_{20}$ saturated mixed lipid vesicles in concentration dependent manner from $\kappa_c = 2.5\ k_BT$ to the thermal energy level at $\kappa_c \approx k_BT$. Beyond drug concentration, the bulk *pH* influenced membrane mechanics as well. For the tertiary amine bupivacaine I could demonstrate that only the positively charged drug reduces κ_c whereas the neutral form even stiffens the bilayer membrane. Furthermore, polyoxyethylene (20) oleyl ether and positively charged bupivacaine could synergistically reduce the bilayer bending rigidity, having maximum synergistic potency at $R_e = 0.16$ mol/mol and $c_{drug} = 67$ mM for the tested suspensions.

The results obtained in this thesis with Transfersome® vesicles, based on the bilayer forming lipid soybean phosphatidylcholine, the membrane softening surfactant polyoxyethylene (20) oleyl ether, and several drugs, show that specific in vitro studies on membrane adaptability, pore penetrability, bilayer integrity and drug/vesicle interaction are excellent tools to design highly fluctuating and deformable lipid bilayer vesicles with the intended use as drug carriers for non-invasive, transdermal drug delivery. However, future preclinical and clinical studies will be necessary and indispensable to confirm the suitability of this type of Transfersome®, designed and optimised in the present thesis for the application as local anaesthetic, analgetic, or anti-inflammatory pharmaceutical product.

7. ZUSAMMENFASSUNG

Die nicht-invasive, transdermale Behandlung von lokal ausgeprägten Erkrankungen ist ein interessantes Gebiet in der Forschung und Entwicklung neuer Medikamente und Technologien. Transfersome® haben sich dabei schon als eine geeignete neue Technologieform erwiesen. Transfersome® sind Lipidvesikel, welche aus einer flexiblen und ultradeformierbaren Lipiddoppelschicht aufgebaut sind. Im Gegensatz zu konventionellen Liposomen enthalten Transfersome® neben den bei beiden Vesikelarten vorkommenden membranaufbauenden Phospholipiden, z.B. Phosphatidylcholin, ein oder mehrere amphiphile Membranbestandteile, welche die Lipiddoppelschicht flexibel und anpassungsfähig machen. Zu dieser membranerweichenden Substanzklasse gehören sowohl bestimmte Tenside als auch ausgewählte amphiphile Wirkstoffe. Auf Grund ihrer Anpassungsfähigkeit, auch Adaptabilität genannt, können diese gemischten Lipidvesikel als Wirkstoffträger für den gezielten dermalen und transdermalen Wirkstofftransport in oberflächliche aber auch tiefere, periphere Gewebe eingesetzt werden. Transfersome® Vesikel überwinden dabei nach lokaler, nicht-okklusiver Auftragung die Hautbarriere, genauer gesagt das Stratum corneum. Die treibende Kraft für diesen aktiven Transport ist dabei der transkutane Feuchtigkeitsgradient, vor allem innerhalb des Stratum corneums. Die durch die nicht-okklusive Anwendung einhergehende Vesikeldeydration treibt die Wirkstoffträger unter Vesikeldeformation durch die engen hydrophilen interzellularen Poren des Stratum corneums. Diese Porenpenetration findet immer dann statt, wenn der Energiegewinn bezüglich Dehydration/Rehydration größer ist als der energetische Aufwand für die Vesikeldeformation. Mit diesem Hintergrund ist es verständlich und durch veröffentlichte Vergleichsstudien zwischen ultradeformierbaren Transfersome® und herkömmlichen, relativen unflexibeln Liposomen belegt, dass nur erstgenannte für einen effektiven transdermalen Wirkstofftransport in Frage kommen.

Ziel und Aufgabenstellung dieser Doktorarbeit war es, eine für diverse Wirkstoffe geeignete Transfersome® Formulierung zu entwickeln und diese im Hinblick auf Adaptabilität und Stabilität physikomechanisch zu charakterisieren. Als möglicherweise geeignetes membranerweichendes Tensid wurde dabei im Vorfeld Polyoxyethylen-20-oleylether ($C_{18:1}EO_{20}$) identifiziert. Die geringe Mizellbildungskonzentration von *CMC* = 25 µM, ein hoher molarer Membranverteilungskoeffizient, log *K* = 4.3 M^{-1}, ein *HLB*-Wert von *HLB* = 15.3 und die damit verbundenen kegelförmige Molekülgeometrie schienen geeignete Voraussetzungen zu sein, um das Zusammenspiel von $C_{18:1}EO_{20}$ mit einer Lipidmembran

bestehend aus Soja Phosphatidylcholin (SPC) detailliert zu untersuchen und im Hinblick auf Deformierbarkeit der Lipiddoppelschicht zu optimieren.

Mit Hilfe der statischen und dynamischen Lichtstreuung wurden wichtige Parameter bezüglich der Wechselwirkung zwischen Tensid und Lipid ermittelt: die Membransättigung R_e^{sat} und die Vesikelsolubilisierung R_e^{sol}, jeweils als molares Verhältnis R_e von $C_{18:1}EO_{20}$ zu SPC. Beide Methoden lieferten ein übereinstimmendes Sättigungsverhältnis von R_e^{sat} = 0.25 mol/mol, ein Ergebnis das vergleichbar ist mit dem von nicht-ionischen Tensiden derselben Kopfgruppenlänge (Polyoxyethylene-20-octylphenylether: R_e^{sat} = 0.20 mol/mol; Polyoxyethylen-20-cetylether: R_e^{sat} = 0.28 mol/mol). Dieses Ergebnis bedeutet, dass bei einen Molverhältnis von SPC/$C_{18:1}EO_{20}$ = 4/1 die Lipiddoppelschicht mit dem Tensid maximal beladen ist und eine weiter Erhöhung der Tensidkonzentration zur Vesikelauflösung führt, also zur Solubilisierung und Bildung von Mischmizellen. Eine solche kontinuierlich stattfindende Vesikelsolubilisierung und Mischmizellbildung wurde zwischen $0.25 < R_e < 3$ [mol/mol] beobachtet, welche bei R_e^{sol} = 3 mol/mol abgeschlossen war und die dabei entstandenen Mischmizellen die dann einzig verbliebenen Aggregate bildeten. Sowohl das niedrige Sättigungsverhältnis R_e^{sat} als auch das geringe Solubilisierungsverhältnis R_e^{sol} bestätigten die Einstufung von $C_{18:1}EO_{20}$ als „starkes“ Tensid. Zeitlich aufgelöste Solubilisierungsmessungen mit Hilfe der dynamischen Lichtstreuung zeigten und bekrätigten des Weiteren eine schon früher von anderen Autoren veröffentlichte zweiphasige Solubilisierungskinetik. Die in dieser Arbeit durchgeführten kinetischen Messungen in Abhängigkeit von R_e ermöglichten eine indirekte Bestimmung des effektiven Diffusionskoeffizienten von $C_{18:1}EO_{20}$ mit $D_{eff} = 2.8 \cdot 10^{-10}$ m^2s^{-1} und eine Abschätzung seiner Oberflächenausdehnung von $\Gamma \sim 0.1$ nm^2.

Neben den Membransättigungs- und Solubilisierungseigenschaften von Polyoxyethylen-20-oleylether wurde in ergänzenden Experimenten der Einfluss des Tensids auf die Adaptabilität der Lipiddoppelschicht untersucht. Hierbei wurde mit einem Adaptabilitätstest (CMA) das Penetrationsverhalten von Lipidvesikeln mit unterschiedlichem Tensid zu Lipidverhältnis R_e durch Poren mit einem Durchmesser von $d_p \approx 20$ nm untersucht. Das Prinzip einer solchen CMA-Messung beruht darauf, dass deformierbare Lipidvesikel mit einem Vesikeldurchmesser von $d_{ves} > 5\ d_p$ durch angelegten Druck die engen Filterporen penetrieren und anschliessend im Filtrat fast unverändert vorliegen. Steife, unverformbare Lipidvesikel derselben Größe können hingegen die Barriere nicht passieren. Nur bei sehr hohen Energieeinträgen, z.B. in Form von hohem Druck, werden diese Vesikel unter

Fragmentierung durch die Poren gepresst, ein Vorgang, der auch als Extrusion bekannt ist. Die während einer Messung ermittelte Penetrabilität *P* in Abhängigkeit des angelegten Drucks Δp lässt daher Rückschlüsse auf die Membranadaptabilität zu. In den durchgeführten Messungen nahm die Adaptabilität beginnend mit steifen Liposomen (R_e = 0 mol/mol; $d_{ves} \approx 120$ nm) kontinuierlich und nicht-linear mit zunehmender $C_{18:1}EO_{20}$ - Konzentration zu. Die maximale Membranadaptabilität a^* der gemischten Lipidvesikel ($d_{ves} \approx 110$ nm) wurde mit $R_e = R_e^{sat} = 0.25$ mol/mol erreicht und blieb dann für $R_e^{sat} < R_e < R_e^{sol}$ konstant. Oberhalb von $R_e^{sol} = 3$ mol/mol, also dem Bereich, wo nur noch Mischmizellen existieren, nahm die Penetrabilität dann sprunghaft zu, da die entstandenen Mizellen mit einem Durchmesser $d_{mic} < d_p$ die Barriere mehr oder weniger drucklos passieren konnten. Übereinstimmend kann gesagt werden, dass sowohl die Membransättigungsexperimente mit der statischen und dynamischen Lichtstreuung als auch die Adaptabilitätsmessung geeignete Methoden sind, die maximale Beladung, also die maximale Membranflexibilität einer Lipiddoppelschicht durch Einbau von Tensiden zu ermitteln. Unter Zuhilfenahme eines phänomenologischen Modells konnte ferner diese Flexibilität in Form der allgemein bekannten Biegesteifigkeit der Lipiddoppelschicht, κ_c, quantifiziert werden. Die Biegesteifigkeit eines tensidfreien SPC-Vesikels konnte mit $C_{18:1}EO_{20}$ um den Faktor ~ 8 von $\kappa_c = 19.5\ k_BT$ auf $\kappa_c = 2.5\ k_BT$ reduziert werden. Diese optimierten Transfersome® Vesikel scheinen somit geeignet zu sein, beladen mit Wirkstoff diesen gezielt durch die hydrophilen Poren der Hornhautbarriere transportieren zu können. Diese in der interzellularen Lipidmatrix des Stratum corneums vorhandenen Poren sind zwar mit eine Durchmesser von $d_p < 0.7$ nm sehr eng, können aber, wie von anderen Autoren publiziert, durch externe Kräfte wie Vesikeldruck oder ein elektrischen Potential auf bis zu 20 nm geweitet werden, womit sie für Transfersome® Vesikel passierbar sind.

Um die Transfersome® Vesikel als transdermale Wirkstoffträger einsetzen zu können ist es essentiell die Wechselwirkungen zwischen Vesikel und Wirkstoff und deren Beeinflussung zu kennen. Anhand zweier amphiphiler Wirkstoffe wurde die Partition dieser in Abhängigkeit ihres Ladungszustands, des *pH*-Werts, der Membranelektrostatik und Polarität untersucht. *pH*-metrische Titrationsexperimente zeigten dabei, dass die Membranpartition P^N_{mem} eines Wirkstoffs im ungeladenen Zustand vergleichbar ist mit dem Wert, welcher in einem klassischen 1-Octanol/Wasser System ermittelt wird. Für Ketoprofen, ein Proprionsäurederivat, wurde ein Verteilungskoeffizient von log P^N_{mem} = 3.0 - 3.3 und für Bupivacain, ein tertiäres Amin, log P^N_{mem} = 2.1 – 2.4 ermittelt. Für die geladenen Wirkstoffe wurde jedoch ein gegenteiliges Verhalten beobachtet. Sowohl negativ geladenes Ketoprofen

als auch positiv geladenes Bupivacain zeigten eine signifikant höhere Partition in die Lipiddoppelschicht als in eine 1-Octanol Phase. In Abhängigkeit der Ionenstärke wurde für Ketoprofen eine Membranpartition der geladene Form von log P^I_{mem} = 0.15 bis 1.18 und für geladenes Bupivacain ein Wert von log P^I_{mem} = 1.2 bis 1.6 gemessen. Die Kenntnis und die Berücksichtigung eines elektrostatischen Einflusses auf das Verteilungsverhalten von geladenen Wirkstoffen in Abhängigkeit der Oberflächenladungsdichte des Vesikels, der Salzkonzentration und des Polaritätsprofils der Membran-Wasser Grenzschicht ermöglichten es, die Lage der Wirkstoffmoleküle innerhalb der Lipiddoppelschicht abzuschätzen. Negativ geladenes Ketoprofen orientiert sich vermutlich innerhalb der hydrophilen Lipidkopfgruppe zwischen der Cholin- und Phosphatgruppe wohingegen positiv geladenes Bupivacaine ein wenig tiefer in der Membran sitzt, und zwar zwischen der Phosphatgruppe und der Carbonylgruppe der Fettsäuren.

Da es sich bei den untersuchten Wirkstoffen um amphiphile Moleküle handelt, wurde in einer abschließenden Studie der Einfluss von negativ geladenem Ketoprofen und positiv geladenem Bupivacain auf gemischte Lipidvesikel, zusammengesetzt aus SPC und $C_{18:1}EO_{20}$, untersucht. Ergänzt wurde diese Serie um ungeladenes Ethanol, welches während der Herstellung von Transfersome® Formulierungen als Hilfsstoff eingesetzt wird und auf Grund seiner amphiphilen Eigenschaften ebenfalls die Biegesteifigkeit von Lipiddoppelschichten beeinflussen dürfte. Adaptabilitätsmessungen zeigten, dass alle drei Moleküle die Biegesteifigkeit von $C_{18:1}EO_{20}$ gesättigten Lipidvesikel von κ_c = 2.5 k_BT konzentrations-abhängig auf $\kappa_c \approx k_BT$ reduzieren können. Mit andere Worten: thermische Energie ist ausreichend um die Vesikel zu verformen. Neben dem Konzentrationseinfluss wurde exemplarisch bei Bupivacain auch der Einfluss des *pH*-Werts auf die Vesikeladaptabilität untersucht. Dabei konnte nachgewiesen werden, dass nur positiv geladenes Bupivacain bei ausreichend tiefem *pH*-Wert die Lipiddoppelschicht flexibler macht und dass die ungeladene Form letztgenannte kontraproduktiv versteift. Allerdings brachte die Kombination von positiv geladenem Bupivacain und nichtionischem Polyoxyethylen-20-oleylether auch die Erkenntnis, dass beide Moleküle die Biegesteifigkeit der Lipiddoppelschicht synergistisch senken. In den getesteten Formulierungen wurde dabei ein Synergieoptimum bei einem molaren $C_{18:1}EO_{20}$ zu SPC Verhältnis von R_e = 0.16 mol/mol und einer Bupivacainkonzentration von c_{drug} = 67 mM ermittelt.

Die Ergebnisse dieser Doktorarbeit mit Transfersome® Vesikeln zeigen zum einen, dass Polyoxyethylen-20-oleylether ein exzellentes Tensid ist, welches die Lipiddoppelschicht von

Phosphatidylcholinmembranen in geeignetem molaren Mischungsverhältnis ausreichend verformbar macht, und zum anderen, dass spezifische, und dabei trotzdem leicht durchzuführende Methoden wie Adaptabilitätsmessung, Solubilisierungsmessung und *pH*-metrische Partitionsmessung geeignete Werkzeuge sind, um ultraverformbare Wirkstoffträger für den gezielten transdermalen Transport zu entwickeln und zu optimieren. Trotzdem ist es notwendig und unabdingbar, das untersuchte in vitro Verhalten dieser Lipidvesikel in zukünftigen präklinischen und klinischen Studien zu bestätigen, um die in dieser Doktorarbeit verwendeten Wirkstoffe Bupivacain und Ketoprofen Transfersome® dann gezielt und effektiv zur Lokalanästhesie beziehungsweise zur Analgesie und Entzündungshemmung einsetzen zu können.

LIST OF REFERENCES

Aguilella, V., Kontturi, K., Murtomäki, L. and Ramirez, P. (1994). "Estimation of the pore size and charge density in human cadaver skin." J Control Release. 32: 249-257.

Alcorn, C. J., Simpson, R. J., Leahy, D. E. and Peters, T. J. (1993). "Partition and distribution coefficients of solutes and drugs in brush border membrane vesicles." Biochem Pharmacol. 45: 1775-1782.

Allison, S. D. (2007). "Liposomal drug delivery." J Infus Nurs. 30: 89-95.

Almgren, M. (2000). "Mixed micelles and other structures in the solubilization of bilayer lipid membranes by surfactants." Biochim Biophys Acta. 1508: 146-163.

Arora, A., Hakim, I., Baxter, J., Rathnasingham, R., Srinivasan, R., Fletcher, D. A. and Mitragotri, S. (2007). "Needle-free delivery of macromolecules across the skin by nanoliter-volume pulsed microjets." Proc Natl Acad Sci U S A. 104: 4255-4260.

Ash, M. and Ash, I. (1980). "Encyclopedia of Surfactants". New York. Chemical Publishing Co. 468.

Austin, R. P., Davis, A. M. and Manners, C. N. (1995). "Partitioning of ionizing molecules between aqueous buffers and phospholipid vesicles." J Pharm Sci. 84: 1180-1183.

Austin, R. P., Barton, P., Davis, A. M., Manners, C. N. and Stansfield, M. C. (1998). "The effect of ionic strength on liposome-buffer and 1-octanol-buffer distribution coefficients." J Pharm Sci. 87: 599-607.

Avanti Polar Lipids, I. (2006). "Fatty acid content of tissue-derived phosphatidylcholine." Product Catalog Edition VI Revised. 1201.

Avdeef, A. (1992). "pH-metric log P. Part 1. Difference plots for determining ion-pair octanol-water partition coefficients of multiprotic substances." Quant. Struct. - Act. Relat. 11: 510-517.

Avdeef, A., Box, K. J., Comer, J. E., Hibbert, C. and Tam, K. Y. (1998). "pH-metric logP. Part 10. Determination of liposomal membrane-water partition coefficients of ionizable drugs." Pharm Res. 15: 209-215.

Avdeef, A. (2003). "Absorption and Drug Development: Solubility, Permeability and Charge State". New York. Wiley-Interscience. 312.

Balgavy, P., Dubnickova, M., Kucerka, N., Kiselev, M. A., Yaradaikin, S. P. and Uhrikova, D. (2001). "Bilayer thickness and lipid interface area in unilamellar extruded 1,2-diacylphosphatidylcholine liposomes: a small-angle neutron scattering study." Biochim Biophys Acta. 1512: 40-52.

Balon, K., Riebesehl, B. U. and Muller, B. W. (1999). "Determination of liposome partitioning of ionizable drugs by titration." J Pharm Sci. 88: 802-806.

Bangham, A. D., Standish, M. M. and Watkins, J. C. (1965). "Diffusion of univalent ions across the lamellae of swollen phospholipids." J Mol Biol. 13: 238-252.

Barry, B. (1987). "Penetration enhancers mode of action in human skin". Skin pharmacokinetics. H. Schaefer (eds.). Basel. Karger. 121-137.

Barry, J. A. and Gawrisch, K. (1994). "Direct NMR evidence for ethanol binding to the lipid-water interface of phospholipid bilayers." Biochemistry. 33: 8082-8088.

Batzri, S. and Korn, E. D. (1973). "Single bilayer liposomes prepared without sonication." Biochim Biophys Acta. 298: 1015-1019.

Bauer, K. H., Frömming, K. H. and Führer, C. (2006). "Lehrbuch der Pharmazeutischen Technologie. Mit einer Einführung in die Biopharmazie". Stuttgart. WVG. 478.

Bauerle, H. D. and Seelig, J. (1991). "Interaction of charged and uncharged calcium channel antagonists with phospholipid membranes. Binding equilibrium, binding enthalpy, and membrane location." Biochemistry. 30: 7203-7211.

Beblik, G., Servuss, R.-M. and Helfrich, W. (1985). "Bilayer bending rigidity of some synthetic lecithins." J Phys (Paris). 46: 1773-1778.

Bermudez, H., Hammer, D. A. and Discher, D. E. (2004). "Effect of bilayer thickness on membrane bending rigidity." Langmuir. 20: 540-543.

Biondi, A. C., Senisterra, G. A. and Disalvo, E. A. (1992). "Permeability of lipid membranes revised in relation to freeze-thaw processes." Cryobiology. 29: 323-331.

Bommannan, D., Okuyama, H., Stauffer, P. and Guy, R. H. (1992). "Sonophoresis. I. The use of high-frequency ultrasound to enhance transdermal drug delivery." Pharm Res. 9: 559-564.

Boonme, P., Krauel, K., Graf, A., Rades, T. and Junyaprasert, V. B. (2006). "Characterization of microemulsion structures in the pseudoternary phase diagram of isopropyl palmitate/water/Brij 97:1-butanol." AAPS PharmSciTech. 7: E45.

Bouchard, G., Carrupt, P. A., Testa, B., Gobry, V. and Girault, H. H. (2002). "Lipophilicity and solvation of anionic drugs." Chemistry. 8: 3478-3484.

Boufendi, L., Stoffels, E. and de Giorgi, M. (1994). "Study of initial dust formation in an Ar-SiH4 discharge by laser induced particle explosive evaporation." J Appl Phys. 76: 148-153.

Bouwstra, J. A., Gooris, G. S., van der Spek, J. A. and Bras, W. (1991). "Structural investigations of human stratum corneum by small-angle X-ray scattering." J Invest Dermatol. 97: 1005-1012.

Bouwstra, J. A., De Graaff, A., Groenink, W. and Honeywell, L. (2002). "Elastic vesicles: interaction with human skin and drug transport." Cell Mol Biol Lett. 7: 222-223.

Bouwstra, J. A., Honeywell-Nguyen, P. L., Gooris, G. S. and Ponec, M. (2003). "Structure of the skin barrier and its modulation by vesicular formulations." Prog Lipid Res. 42: 1-36.

Casey, G. (2002). "Physiology of the skin." Nurs Stand. 16: 47-51.

Caspers, P. J., Lucassen, G. W., Carter, E. A., Bruining, H. A. and Puppels, G. J. (2001). "In vivo confocal Raman microspectroscopy of the skin: noninvasive determination of molecular concentration profiles." J Invest Dermatol. 116: 434-442.

Cevc, G., Watts, A. and Marsh, D. (1981). "Titration of the phase transition of phosphatidylserine bilayer membranes. Effects of pH, surface electrostatics, ion binding, and head-group hydration." Biochemistry. 20: 4955-4965.

Cevc, G. and Marsh, D. (1987). "Phospholipid Bilayers, Physical Principles and Models". New York. Wiley-Interscience. 442.

Cevc, G. (1990). "Membrane electrostatics." Biochim Biophys Acta. 1031: 311-382.

Cevc, G. and Blume, G. (1992). "Lipid vesicles penetrate into intact skin owing to the transdermal osmotic gradients and hydration force." Biochim Biophys Acta. 1104: 226-232.

Cevc, G. (1995). "Material transport across permeability barriers by means of lipid vesicles". Handbook of Biological Physics. E. Sackmann (eds.). Amsterdam. Elsevier. 465-490.

Cevc, G. (1996). "Transfersomes, liposomes and other lipid suspensions on the skin: permeation enhancement, vesicle penetration, and transdermal drug delivery." Crit Rev Ther Drug Carrier Syst. 13: 257-388.

Cevc, G., Blume, G., Schätzlein, A., Gebauer, D. and Amla, P. (1996). "The skin: a pathway for systemic treatment with patches and lipid-based agent carriers." Adv Drug Deliv Rev. 18: 349-378.

Cevc, G. (1997). "Drug delivery across the skin." Exp Opin Invest Drugs. 6: 1887-1937.

Cevc, G., Gebauer, D., Stieber, J., Schatzlein, A. and Blume, G. (1998). "Ultraflexible vesicles, Transfersomes, have an extremely low pore penetration resistance and transport therapeutic amounts of insulin across the intact mammalian skin." Biochim Biophys Acta. 1368: 201-215.

Cevc, G. (1999). "Overcoming the skin barrier with artificial smart carriers of drugs". Intelligent materials for controlled release. A. R. Comfort (eds.). Washington, DC. American Chemical Society. 70-86.

Cevc, G. and Blume, G. (2001). "New, highly efficient formulation of diclofenac for the topical, transdermal administration in ultradeformable drug carriers, Transfersomes." Biochim Biophys Acta. 1514: 191-205.

Cevc, G. (2003). "Transdermal drug delivery of insulin with ultradeformable carriers." Clin Pharmacokinet. 42: 461-474.

Cevc, G. and Gebauer, D. (2003a). "Hydration-driven transport of deformable lipid vesicles through fine pores and the skin barrier." Biophys J. 84: 1010-1024.

Cevc, G., Schätzlein, A., Richardsen, H. and Vierl, U. (2003b). "Overcoming Semipermeable Barriers, Such as the Skin, with Ultradeformable Mixed Lipid Vesicles, Transfersomes, Liposomes, or Mixed Lipid Micelles." Langmuir. 19: 10753 -10763.

Cevc, G. (2004). "Lipid vesicles and other colloids as drug carriers on the skin." Adv Drug Deliv Rev. 56: 675-711.

Cevc, G. and Blume, G. (2004a). "Hydrocortisone and dexamethasone in very deformable drug carriers have increased biological potency, prolonged effect, and reduced therapeutic dosage." Biochim Biophys Acta. 1663: 61-73.

Cevc, G. and Vierl, U. (2004b). "Aggregates with increased deformability, comprising at least three amphipats, for improved transport through semi-permeable barriers and for the non-invasive drug application in vivo, especially through the skin." PCT/EP2003/011202 ; WO/2004/032900.

Chanturiya, A., Leikina, E., Zimmerberg, J. and Chernomordik, L. V. (1999). "Short-chain alcohols promote an early stage of membrane hemifusion." Biophys J. 77: 2035-2045.

Chapman, D. L. (1913). "A contribution to the theory of electrocapillarity." Philos. Mag. 25: 475-481.

Chen, B. H. and Miller, C. A. (2000). "Dissolution Rates of Pure Nonionic Surfactants." Langmuir. 16: 5276-5283.

Chernoff, D. M. and Strichartz, G. R. (1990). "Kinetics of local anesthetic inhibition of neuronal sodium currents. pH and hydrophobicity dependence." Biophys J. 58: 69-81.

Chidambaram, N. and Burgess, D. J. (2000). "Effect of nonionic surfactant on transport of surface-active and non-surface-active model drugs and emulsion stability in triphasic systems." AAPS PharmSci. 2: E30.

Chiou, J. S., Krishna, P. R., Kamaya, H. and Ueda, I. (1992). "Alcohols dehydrate lipid membranes: an infrared study on hydrogen bonding." Biochim Biophys Acta. 1110: 225-233.

Davies, J. T. (1957). "A quantitative kinetic theory of emulsion type, I. Physical chemistry of the emulsifying agent." Proc. 2nd Int. Congr. Surface Activity. 1: 426.

Delorme, N., Bardeau, J. F., Carriere, D., Dubois, M., Gourbil, A., Mohwald, H., Zemb, T. and Fery, A. (2007). "Experimental evidence of the electrostatic contribution to the bending rigidity of charged membranes." J Phys Chem B. 111: 2503-2505.

Duwe, H. T., Kaes, J. and Sackmann, E. (1990). "Bending elastic moduli of lipid bilayers: modulation by solute." J Phys (Paris). 51: 945-962.

Eastoe, J. and Dalton, J. S. (2000). "Dynamic surface tension and adsorption mechanisms of surfactants at the air-water interface." Adv Colloid Interface Sci. 85: 103-144.

Edwards, K. and Almgren, M. (1991). "Solubilization of Lecithin Vesicles by C12E8." J Colloid Interf Sci. 147: 1-21.

Ehsan, S., Prasher, S. O. and Marshall, W. D. (2006). "A washing procedure to mobilize mixed contaminants from soil: I. Polychlorinated biphenyl compounds." J Environ Qual. 35: 2146-2153.

Elias, P. M., Menon, G. K., Grayson, S., Brown, B. E. and Rehfeld, S. J. (1987). "Avian sebokeratocytes and marine mammal lipokeratinocytes: structural, lipid biochemical, and functional considerations." Am J Anat. 180: 161-177.

Evans, E. and Needham, D. (1987). "Physical properties of surfactant bilayer membranes: thermal transitions, elasticity, rigidity, cohesion, and colloidal interactions." J Phys Chem. 91: 4219-4228.

Evans, E. and Rawicz, W. (1990). "Entropy-driven tension and bending elasticity in condensed-fluid membranes." Phys Rev Lett. 64: 2094-2097.

Evans, E., Rawicz, W. and Hofmann, A. F. (1994). "Lipid bilayer expansion and mechanical disruption in solutions of water-soluble bile acids". Bile Acids in Gastroenterology: Basic & Clinical Advances. A. Stiehl (eds.). Boston. Kluwer Academic. 59-68.

Evans, E. A. (1974). "Bending resistance and chemically induced moments in membrane bilayers." Biophys J. 14: 923-931.

Fa, N., Lins, L., Courtoy, P. J., Dufrene, Y., Van Der Smissen, P., Brasseur, R., Tyteca, D. and Mingeot-Leclercq, M. P. (2007). "Decrease of elastic moduli of DOPC bilayers induced by a macrolide antibiotic, azithromycin." Biochim Biophys Acta. 1768: 1830-1838.

Fainerman, V. B., Makievskia, A. V. and Miller, R. (1994). "The analysis of dynamic surface tension of sodium alkyl sulphate solutions, based on asymptotic equations of adsorption kinetic theory." Colloids and Surfaces A. 87: 61-75.

Fernandez, M. S. and Fromherz, P. (1977). "Lipoid pH indicators as probes of electrical potential and polarity in micelles." J Phys Chem. 81: 1755-1761.

Friberger, P. and Aberg, G. (1971). "Some physiochemical properties of the racemates and the optically active isomers of two local anaesthetic compounds." Acta Pharm Suec. 8: 361-364.

Gabizon, A. and Martin, F. (1997). "Polyethylene glycol-coated (pegylated) liposomal doxorubicin. Rationale for use in solid tumours." Drugs. 54 Suppl 4: 15-21.

Giraud, M. N., Motta, C., Romero, J. J., Bommelaer, G. and Lichtenberger, L. M. (1999). "Interaction of indomethacin and naproxen with gastric surface-active phospholipids: a possible mechanism for the gastric toxicity of nonsteroidal anti-inflammatory drugs (NSAIDs)." Biochem Pharmacol. 57: 247-254.

Godin, B. and Touitou, E. (2003). "Ethosomes: new prospects in transdermal delivery." Crit Rev Ther Drug Carrier Syst. 20: 63-102.

Gompper, G. and Kroll, D. M. (1995). "Driven transport of fluid vesicles through narrow pores." Phys Rev E Stat Phys Plasmas Fluids Relat Interdiscip Topics. 52: 4198-4208.

Gouy, G. (1910). "Sur la constitution de la charge electrique a la surface d´un electrolyte." J. Phys. Radium. 9: 457-468.

Grant, G. J., Barenholz, Y., Piskoun, B., Bansinath, M., Turndorf, H. and Bolotin, E. M. (2001). "DRV liposomal bupivacaine: preparation, characterization, and in vivo evaluation in mice." Pharm Res. 18: 336-343.

Grant, G. J., Barenholz, Y., Bolotin, E. M., Bansinath, M., Turndorf, H., Piskoun, B. and Davidson, E. M. (2004). "A novel liposomal bupivacaine formulation to produce ultralong-acting analgesia." Anesthesiology. 101: 133-137.

Gregoriadis, G. and Dean, M. F. (1979). "Enzyme therapy in genetic diseases." Nature. 278: 603-604.

Griffin, W. T. (1949). "Classification of Surface-Active Agents by 'HLB." Journal of the Society of Cosmetic Chemists. 1: 311.

Guo, X., Rong, Z. and Ying, X. (2006). "Calculation of hydrophile-lipophile balance for polyethoxylated surfactants by group contribution method." J Colloid Interface Sci. 298: 441-450.

Hadgraft, J. (2001). "Skin, the final frontier." Int J Pharm. 224: 1-18.

Hadgraft, J. (2004). "Skin deep." Eur J Pharm Biopharm. 58: 291-299.

Heerklotz, H., Binder, H., Lantzsch, G. and Klose, G. (1994). "Membrane/water partition of oligo(ethylene oxide) dodecyl ethers and its relevance for solubilization." Biochim Biophys Acta. 1196: 114-122.

Heerklotz, H., Binder, H., Lantzsch, G. and Klose, G. (1997). "Lipid/Detergent Interaction Thermodynamics as a Function of Molecular Shape." J Phys Chem B. 101: 639-645.

Heerklotz, H. and Seelig, J. (2000a). "Correlation of membrane/water partition coefficients of detergents with the critical micelle concentration." Biophys J. 78: 2435-2440.

Heerklotz, H. and Seelig, J. (2000b). "Titration calorimetry of surfactant-membrane partitioning and membrane solubilization." Biochim Biophys Acta. 1508: 69-85.

Helenius, A. and Simons, K. (1975). "Solubilization of membranes by detergents." Biochim Biophys Acta. 415: 29-79.

Helfrich, W. (1973). "Elastic properties of lipid bilayers: Theory and possible experiments." Z Naturforsch. 28c: 693-703.

Helfrich, W. (1986). "Size distributions of vesicles: The role of the effective rigidity of membranes." J Phys (Paris). 47: 321-329.

Heuschkel, S., Goebel, A. and Neubert, R. H. (2007). "Microemulsions-modern colloidal carrier for dermal and transdermal drug delivery." J Pharm Sci. 97: 603 - 631.

Hofland, H. E., Bouwstra, J. A., Bodde, H. E., Spies, F. and Junginger, H. E. (1995). "Interactions between liposomes and human stratum corneum in vitro: freeze fracture electron microscopical visualization and small angle X-ray scattering studies." Br J Dermatol. 132: 853-866.

Hogberg, C. J., Maliniak, A. and Lyubartsev, A. P. (2007). "Dynamical and structural properties of charged and uncharged lidocaine in a lipid bilayer." Biophys Chem. 125: 416-424.

Holte, L. L. and Gawrisch, K. (1997). "Determining ethanol distribution in phospholipid multilayers with MAS-NOESY spectra." Biochemistry. 36: 4669-4674.

Honeywell-Nguyen, P. L., de Graaff, A. M., Groenink, H. W. and Bouwstra, J. A. (2002). "The in vivo and in vitro interactions of elastic and rigid vesicles with human skin." Biochim Biophys Acta. 1573: 130-140.

Horozov, T. and Joos, P. (1995). "Dynamic Surface-Tension of Surfactant Solutions Studied by Peaktensiometry." J Colloid Interface Sci. 173: 334-342.

Hunter, D. G. and Frisken, B. J. (1998). "Effect of extrusion pressure and lipid properties on the size and polydispersity of lipid vesicles." Biophys J. 74: 2996-3002.

Iizuka, H. (1994). "Epidermal turnover time." J Dermatol Sci. 8: 215-217.

Inoue, T., Nakashima, K. and Suzuki, M. (2002). "Surface tension study on aqueous solution of nonionic surfactant with unsaturated hydrocarbon chain." J Oleo Sci. 51: 753-760.

Inouye, H. and Kirschner, D. A. (1988). "Membrane interactions in nerve myelin: II. Determination of surface charge from biochemical data." Biophys J. 53: 247-260.

Israelachvili, J. N., Mitchell, D. J. and Ninham, B. W. (1977). "Theory of self-assembly of lipid bilayers and vesicles." Biochim Biophys Acta. 470: 185-201.

Israelachvili, J. N. (1985). "Thermodynamic and geometric aspects of amphiphile aggregation into micelles, vesicles and bilayers, and the interactions between them". Physics of Amphiphiles: Micelles, Vesicles and Microemulsions. M. Corti (eds.). Amsterdam. North-Holland Physics Publishing. 23-58.

Israelachvili, J. N. (1992). "Intermolecular and surface forces with applications to colloidal and biological systems". New York. Academic Press Inc. 450.

Jenning, V., Gysler, A., Schafer-Korting, M. and Gohla, S. H. (2000). "Vitamin A loaded solid lipid nanoparticles for topical use: occlusive properties and drug targeting to the upper skin." Eur J Pharm Biopharm. 49: 211-218.

Joos, P. and Rillaerts, E. (1982). "Rate of demicellization from the dynamic surface tensions of micellar solutions." J Phys Chem. 86: 3471-3478.

Junyapraserta, V. B., Boonmea, P., Songkrob, S., Krauelc, K. and Radesc, T. (2007). "Transdermal delivery of hydrophobic and hydrophilic local anesthetics from o/w and w/o Brij 97-based microemulsions." J Pharm Pharmaceut Sci. 10: 319-329.

Karatekin, E., Sandre, O., Guitouni, H., Borghi, N., Puech, P. H. and Brochard-Wyart, F. (2003). "Cascades of transient pores in giant vesicles: line tension and transport." Biophys J. 84: 1734-1749.

Kennedy, R. A. and Kennedy, M. L. (2007). "Effect of selected non-ionic surfactants on the flow behavior of aqueous veegum suspensions." AAPS PharmSciTech. 8: 25.

Kim, J. G. and Kim, J. D. (1991). "Vesicle to micelle transitions of egg phosphatidylcholine liposomes induced by nonionic surfactants, poly(oxyethylene) cetyl ethers." J Biochem (Tokyo). 110: 436-442.

Kirjavainen, M., Urtti, A., Jaaskelainen, I., Suhonen, T. M., Paronen, P., Valjakka-Koskela, R., Kiesvaara, J. and Monkkonen, J. (1996). "Interaction of liposomes with human skin in vitro--the influence of lipid composition and structure." Biochim Biophys Acta. 1304: 179-189.

Kiselev, M. A., Ryabova, N. Y., Balagurov, A. M., Dante, S., Hauss, T., Zbytovska, J., Wartewig, S. and Neubert, R. H. (2005). "New insights into the structure and hydration of a stratum corneum lipid model membrane by neutron diffraction." Eur Biophys J. 34: 1030-1040.

Klammt, C., Schwarz, D., Fendler, K., Haase, W., Dotsch, V. and Bernhard, F. (2005). "Evaluation of detergents for the soluble expression of alpha-helical and beta-barrel-type integral membrane proteins by a preparative scale individual cell-free expression system." Febs J. 272: 6024-6038.

Ko, C. J., Ko, Y. J., Kim, D. M. and Park, H. J. (2003). "Solution properties and PGSE-NMR self-diffusion study of C18:1/oil/water system." Colloids and Surfaces A. 216: 55-63.

Kragh-Hansen, U., le Maire, M. and Moller, J. V. (1998). "The mechanism of detergent solubilization of liposomes and protein-containing membranes." Biophys J. 75: 2932-2946.

Kramer, S. D., Braun, A., Jakits-Deiser, C. and Wunderli-Allenspach, H. (1998). "Towards the predictability of drug-lipid membrane interactions: the pH-dependent affinity of propanolol to phosphatidylinositol containing liposomes." Pharm Res. 15: 739-744.

Kroll, D. M. and Gompper, G. (1992). "The conformation of fluid membranes: Monte Carlo simulations." Science. 255: 968-971.

Kunieda, H., Shigeta, K. and Ozawa, K. (1997). "Self-Organizing Structures in Poly(oxyethylene) Oleyl Ether-Water System." J Phys Chem B. 101: 7952-7957.

La Rotonda, M.-I.-., Amato, G., Barbato, F., Silipo, C. and Vittoria, A. (1983). "Relationships between octanol-water partition data, chromatographic indices and their dependence on pH in a set of nonsteroidal anti-inflammatory drugs." Quant. Struct. - Act. Relat. 2: 168-173.

Langner, M., Isac, T. and Hui, S. W. (1995). "Interaction of free fatty acids with phospholipid bilayers." Biochim Biophys Acta. 1236: 73-80.

Langner, M. and Kral, T. E. (1999). "Liposome-based drug delivery systems." Pol J Pharmacol. 51: 211-322.

Lantzsch, G., Binder, H. and Heerklotz, H. (1994). "Surface area per molecule in lipid/C12En membranes as seen by fluorescence resonance energy transfer." J Fluorescence. 4: 339-343.

Lasch, J. (1995). "Interaction of detergents with lipid vesicles." Biochim Biophys Acta. 1241: 269-392.

Lasic, D. D. (1993). "Ethanol Injection". Liposomes: From Physics to Application. (eds.). Amsterdam. Elsevier. 88-90.

Lehmann, J. and Rother, M. (2003). "Transfersomes and their application in dermatopharmaceutics". Trends in dermatopharmacy. W. C. Marsch (eds.). Aachen. Shaker Verlag. 260.

Levenberg, K. (1944). "A Method for the Solution of Certain Non-Linear Problems in Least Squares." Quart Appl Math. 2: 164-168.

Levin, G., Gershonowitz, A., Sacks, H., Stern, M., Sherman, A., Rudaev, S., Zivin, I. and Phillip, M. (2005). "Transdermal delivery of human growth hormone through RF-microchannels." Pharm Res. 22: 550-555.

Levy, D., Gulik, A., Seigneuret, M. and Rigaud, J. L. (1990). "Phospholipid vesicle solubilization and reconstitution by detergents. Symmetrical analysis of the two processes using octaethylene glycol mono-n-dodecyl ether." Biochemistry. 29: 9480-9488.

Lichtenberg, D., Robson, R. J. and Dennis, E. A. (1983). "Solubilization of phospholipids by detergents. Structural and kinetic aspects." Biochim Biophys Acta. 737: 285-304.

Lichtenberg, D. (1985). "Characterization of the solubilization of lipid bilayers by surfactants." Biochim Biophys Acta. 821: 470-478.

Lichtenberg, D. (1993). "Micelles and liposomes". Biomembranes: Physical Aspects, Vol. 1. M. Shinitzky (eds.). Weinheim. VCH. 63-95.

Lichtenberg, D., Opatowski, E. and Kozlov, M. M. (2000). "Phase boundaries in mixtures of membrane-forming amphiphiles and micelle-forming amphiphiles." Biochim Biophys Acta. 1508: 1-19.

Lichtenberger, L. M., Wang, Z. M., Romero, J. J., Ulloa, C., Perez, J. C., Giraud, M. N. and Barreto, J. C. (1995). "Non-steroidal anti-inflammatory drugs (NSAIDs) associate with zwitterionic phospholipids: insight into the mechanism and reversal of NSAID-induced gastrointestinal injury." Nat Med. 1: 154-158.

Lichtenberger, L. M. (2001). "Where is the evidence that cyclooxygenase inhibition is the primary cause of nonsteroidal anti-inflammatory drug (NSAID)-induced gastrointestinal injury? Topical injury revisited." Biochem Pharmacol. 61: 631-637.

Loan Honeywell-Nguyen, P., Wouter Groenink, H. W. and Bouwstra, J. A. (2006). "Elastic vesicles as a tool for dermal and transdermal delivery." J Liposome Res. 16: 273-280.

Lobbecke, L. and Cevc, G. (1995). "Effects of short-chain alcohols on the phase behavior and interdigitation of phosphatidylcholine bilayer membranes." Biochim Biophys Acta. 1237: 59-69.

Loth, H. (1986). "Grundlagen des intra. und transdermalen Transports von Arzneistoffen, I." Acta Pharm Technol. 32: 109-114.

Loth, H. (1987). "Grundlagen des intra. und transdermalen Transports von Arzneistoffen, II." Acta Pharm Technol. 33: 3-14.

Lundbaek, J. A., Birn, P., Hansen, A. J., Sogaard, R., Nielsen, C., Girshman, J., Bruno, M. J., Tape, S. E., Egebjerg, J., Greathouse, D. V., Mattice, G. L., Koeppe, R. E., 2nd and Andersen, O. S. (2004). "Regulation of sodium channel function by bilayer elasticity: the importance of hydrophobic coupling. Effects of Micelle-forming amphiphiles and cholesterol." J Gen Physiol. 123: 599-621.

Ly, H. V., Block, D. E. and Longo, M. L. (2002). "Interfacial Tension Effect of Ethanol on Lipid Bilayer Rigidity, Stability, and Area/Molecule: A Micropipet Aspiration Approach." Langmuir. 18: 8988-8995.

Ly, H. V. and Longo, M. L. (2004). "The Influence of Short-Chain Alcohols on Interfacial Tension, Mechanical Properties, Area/Molecule, and Permeability of Fluid Lipid Bilayers." Biophys J. 87: 1013-1033.

MacDonald, R. C., MacDonald, R. I., Menco, B. P., Takeshita, K., Subbarao, N. K. and Hu, L. R. (1991). "Small-volume extrusion apparatus for preparation of large, unilamellar vesicles." Biochim Biophys Acta. 1061: 297-303.

MacDonald, R. C. and MacDonald, R. I. (1993). "Applications of freezing and thawing in liposome technology". Liposome Technology. G. Gregoriadis (eds.). Boca Raton. CRC Press. 209-228.

Marquardt, D. (1963). "An Algorithm for Least-Squares Estimation of Nonlinear Parameters." SIAM J Appl Math. 11: 431-441.

Marsh, D. and King, M. D. (1986). "Prediction of the critical micelle concentrations of mono- and di-acyl phospholipids." Chem Phys Lipids. 42: 271-277.

Marsh, D. (2001). "Polarity and permeation profiles in lipid membranes." Proc Natl Acad Sci U S A. 98: 7777-7782.

Mayer, L. D., Hope, M. J. and Cullis, P. R. (1986). "Vesicles of variable sizes produced by a rapid extrusion procedure." Biochim Biophys Acta. 858: 161-168.

Mezei, M. and Gulasekharam, V. (1980). "Liposomes--a selective drug delivery system for the topical route of administration. Lotion dosage form." Life Sci. 26: 1473-1477.

Miyazaki, J., Hideg, K. and Marsh, D. (1992). "Interfacial ionization and partitioning of membrane-bound local anesthetics." Biochim Biophys Acta. 1103: 62-68.

Moser, K., Kriwet, K., Naik, A., Kalia, Y. N. and Guy, R. H. (2001). "Passive skin penetration enhancement and its quantification in vitro." Eur J Pharm Biopharm. 52: 103-112.

Nagel, N. E., Cevc, G. and Kirchner, S. (1992). "The mechanism of the solute-induced chain interdigitation in phosphatidylcholine vesicles and characterization of the isothermal phase transitions by means of dynamic light scattering." Biochim Biophys Acta. 1111: 263-269.

Needham, D., McIntosh, T. J. and Lasic, D. D. (1992). "Repulsive interactions and mechanical stability of polymer-grafted lipid membranes." Biochim Biophys Acta. 1108: 40-48.

Neubert, R., Wohlrab, W. and Marsch, W. (2001). "Dermatopharmazie: Vehikel – Wirkstoffe - Pharmakologie". Stuttgart. WVG. 178.

Noguchi, H. and Gompper, G. (2006). "Dynamics of vesicle self-assembly and dissolution." J Chem Phys. 125: 164908.

Nomura, F., Nagata, M., Inaba, T., Hiramatsu, H., Hotani, H. and Takiguchi, K. (2001). "Capabilities of liposomes for topological transformation." Proc Natl Acad Sci U S A. 98: 2340-2345.

Olson, F., Hunt, C. A., Szoka, F. C., Vail, W. J. and Papahadjopoulos, D. (1979). "Preparation of liposomes of defined size distribution by extrusion through polycarbonate membranes." Biochim Biophys Acta. 557: 9-23.

Ondrias, K., Stasko, A., Misik, V., Reguli, J. and Svajdlenka, E. (1991). "Comparison of perturbation effect of propranolol, verapamil, chlorpromazine and carbisocaine on lecithin liposomes and brain total lipid liposomes. An EPR spectroscopy study." Chem Biol Interact. 79: 197-206.

Ottiger, C. and Wunderli-Allenspach, H. (1999). "Immobilized artificial membrane (IAM)-HPLC for partition studies of neutral and ionized acids and bases in comparison with the liposomal partition system." Pharm Res. 16: 643-650.

Partearroyo, M. A., Urbaneja, M. A. and Goni, F. M. (1992). "Effective detergent/lipid ratios in the solubilization of phosphatidylcholine vesicles by Triton X-100." FEBS Lett. 302: 138-140.

Patel, H. and Cronin, M. (2001). "Determination of the optimal physico-chemical parameters to use in a QSAR-approach to predict skin permeation rate." Liverpool. Final report. QSAR and Modelling Research Group. European Chemical Industry Council Long-range Research Initiative. 109.

Patra, M., Salonen, E., Terama, E., Vattulainen, I., Faller, R., Lee, B. W., Holopainen, J. and Karttunen, M. (2006). "Under the influence of alcohol: the effect of ethanol and methanol on lipid bilayers." Biophys J. 90: 1121-1135.

Paul, A., Cevc, G. and Bachhawat, B. K. (1995). "Transdermal immunization with large proteins by means of ultradeformable drug carriers." Eur J Immunol. 25: 3521-3524.

Paul, A., Cevc, G. and Bachhawat, B. K. (1998). "Transdermal immunisation with an integral membrane component, gap junction protein, by means of ultradeformable drug carriers, transfersomes." Vaccine. 16: 188-195.

Pauletti, G. M. and Wunderli-Allenspach, H. (1994). "Partition coefficients in vitro: artificial membranes as a standardized distribution model." Eur J Pharm Sci. 1: 273-282.

Pedros, J., Gomez, C. M., Campos, A. and Abad, C. (1997). "A fluorescence spectroscopy study of the interaction of monocationic quinine with phospholipid vesicles. Effect of the ionic strength and lipid composition." Spectrochim Acta A Mol Biomol Spectrosc. 53A: 2219-2228.

Petrov, A. G. (1999). "The lyotropic state of matter: Molecular physics and living matter physics". Amsterdam. Gordon and Breach Science Publishers. 217.

Planas, M. E., Gonzalez, P., Rodriguez, L., Sanchez, S. and Cevc, G. (1992). "Noninvasive percutaneous induction of topical analgesia by a new type of drug carrier, and prolongation of local pain insensitivity by anesthetic liposomes." Anesth Analg. 75: 615-621.

Popescu, G., Ikeda, T., Goda, K., Best-Popescu, C. A., Laposata, M., Manley, S., Dasari, R. R., Badizadegan, K. and Feld, M. S. (2006). "Optical measurement of cell membrane tension." Phys Rev Lett. 97: 218101.

Prausnitz, M. R., Bose, V. G., Langer, R. and Weaver, J. C. (1993). "Electroporation of mammalian skin: a mechanism to enhance transdermal drug delivery." Proc Natl Acad Sci U S A. 90: 10504-10508.

Provencher, S. W. (1982). "CONTIN: A general purpose constrained regularization program for inverting noisy algebraic and integral equations." Comput Phys Commun. 27: 229-242.

Rafols, C., Roses, M. and Bosch, E. (1997). "A comparison between different approaches to estimate the aqueous pKa values of several non-steroidal anti-inflammatory drugs." Anal Chim Acta. 338: 127-134.

Ragsdale, D. S., McPhee, J. C., Scheuer, T. and Catterall, W. A. (1994). "Molecular determinants of state-dependent block of Na+ channels by local anesthetics." Science. 265: 1724-1728.

Rawicz, W., Olbrich, K. C., McIntosh, T., Needham, D. and Evans, E. (2000). "Effect of chain length and unsaturation on elasticity of lipid bilayers." Biophys J. 79: 328-339.

Razak, J. L., Cutak, B. J., Larive, C. K. and Lunte, C. E. (2001). "Correlation of the capacity factor in vesicular electrokinetic chromatography with the octanol:water partition coefficient for charged and neutral analytes." Pharm Res. 18: 104-111.

Rhee, Y. S., Choi, J. G., Park, E. S. and Chi, S. C. (2001). "Transdermal delivery of ketoprofen using microemulsions." Int J Pharm. 228: 161-170.

Ribosa, I. G. M. T., Parra, J. L., de la Maza, A., Sanchez-Leal, J., Trullas, C., Tsi, A., Balaguer, F. and Pelejero, C. (1992). "Physico-chemical modifications of liposome structures through interaction with surfactants." Int J Cosmetic Sci. 14: 131-149.

Rösch, M. (1971). "Tenside." 8: 302.

Rother, M., Lavins, B. J., Kneer, W., Lehnhardt, K., Seidel, E. J. and Mazgareanu, S. (2007). "Efficacy and safety of epicutaneous ketoprofen in Transfersome (IDEA-033) versus oral celecoxib and placebo in osteoarthritis of the knee: multicentre randomised controlled trial." Ann Rheum Dis. 66: 1178-1183.

Rowe, E. S. and Cutrera, T. A. (1990). "Differential scanning calorimetric studies of ethanol interactions with distearoylphosphatidylcholine: transition to the interdigitated phase." Biochemistry. 29: 10398-10404.

Ruddy, S. B. and Hadzija, B. W. (1992). "Iontophoretic permeability of polyethylene glycols through hairless rat skin: application of hydrodynamic theory for hindered transport through liquid-filled pores." Drug Des Discov. 8: 207-224.

Ruetsch, Y. A., Boni, T. and Borgeat, A. (2001). "From cocaine to ropivacaine: the history of local anesthetic drugs." Curr Top Med Chem. 1: 175-182.

Safinya, C. R., Sirota, E. B., Roux, D. and Smith, G. S. (1989). "Universality in interacting membranes: The effect of cosurfactants on the interfacial rigidity." Phys Rev Lett. 62: 1134-1137.

Schätzlein, A. and Cevc, G. (1998). "Non-uniform cellular packing of the stratum corneum and permeability barrier function of intact skin: a high-resolution confocal laser scanning microscopy study using highly deformable vesicles (Transfersomes)." Br J Dermatol. 138: 583-592.

Schneider, M. B., Jenkins, J. T. and Webb, W. W. (1984). "Thermal fluctuations of large cylindrical phospholipid vesicles." Biophys J. 45: 891-899.

Schubert, R., Beyer, K., Wolburg, H. and Schmidt, K. H. (1986). "Structural changes in membranes of large unilamellar vesicles after binding of sodium cholate." Biochemistry. 25: 5263-5269.

Schubert, R. and Schmidt, K. H. (1988). "Structural changes in vesicle membranes and mixed micelles of various lipid compositions after binding of different bile salts." Biochemistry. 27: 8787-8794.

Schwarz, W., Palade, P. T. and Hille, B. (1977). "Local anesthetics. Effect of pH on use-dependent block of sodium channels in frog muscle." Biophys J. 20: 343-368.

Shigeta, Suzuski and Kunieda (1997). "Phase behavior of polyoxyethylene oleyl ether in water." Progr Colloid Polym Sci. 106: 49-54.

Simoes, S. I., Tapadas, J. M., Marques, C. M., Cruz, M. E., Martins, M. B. and Cevc, G. (2005). "Permeabilisation and solubilisation of soybean phosphatidylcholine bilayer vesicles, as membrane models, by polysorbate, Tween 80." Eur J Pharm Sci. 26: 307-317.

Singh, J. and Roberts, M. S. (1989). "Transdermal delivery of drugs by iontophoresis: a review." Drug Des Deliv. 4: 1-12.

Skrdla, P. J. and Robertson, R. T. (2005). "Semiempirical equations for modeling solid-state kinetics based on a Maxwell-Boltzmann distribution of activation energies: applications to a polymorphic transformation under crystallization slurry conditions and to the thermal decomposition of AgMnO4 crystals." J Phys Chem B. 109: 10611-10619.

Takegami, S., Kitamura, K., Kitade, T., Takashima, M., Ito, M., Nakagawa, E., Sone, M., Sumitani, R. and Yasuda, Y. (2005). "Effects of phosphatidylserine and phosphatidylethanolamine content on partitioning of triflupromazine and chlorpromazine between phosphatidylcholine-aminophospholipid bilayer vesicles and water studied by second-derivative spectrophotometry." Chem Pharm Bull (Tokyo). 53: 147-150.

Tanford, C. (1973). "Micelle shape and size." J Phys Chem. 76: 3020-3024.

Thomas, P. G. and Seelig, J. (1993). "Binding of the calcium antagonist flunarizine to phosphatidylcholine bilayers: charge effects and thermodynamics." Biochem J. 291 (Pt 2): 397-402.

Touitou, E., Dayan, N., Bergelson, L., Godin, B. and Eliaz, M. (2000). "Ethosomes - novel vesicular carriers for enhanced delivery: characterization and skin penetration properties." J Control Release. 65: 403-418.

Trommer, H. and Neubert, R. H. (2006). "Overcoming the stratum corneum: the modulation of skin penetration. A review." Skin Pharmacol Physiol. 19: 106-121.

Tsai, M. A., Frank, R. S. and Waugh, R. E. (1993). "Passive mechanical behavior of human neutrophils: power-law fluid." Biophys J. 65: 2078-2088.

Umbreit, J. N. and Strominger, J. L. (1973). "Relation of detergent HLB number to solubilization and stabilization of D-alanine carboxypeptidase from Bacillus subtilis membranes." Proc Natl Acad Sci U S A. 70: 2997-3001.

Uniqema (2008). "Product information Brij 98V." 3.

van den Bergh, B. A., Vroom, J., Gerritsen, H., Junginger, H. E. and Bouwstra, J. A. (1999). "Interactions of elastic and rigid vesicles with human skin in vitro: electron microscopy and two-photon excitation microscopy." Biochim Biophys Acta. 1461: 155-173.

Vierl, U., Lobbecke, L., Nagel, N. and Cevc, G. (1994). "Solute effects on the colloidal and phase behavior of lipid bilayer membranes: ethanol-dipalmitoylphosphatidylcholine mixtures." Biophys J. 67: 1067-1079.

Vollhardt, K. P. C. and Schore, N. E. (1998). "Organic chemistry: structure and function". New York. W H Freeman & Co. 1203.

Wang, J. J., Sung, K. C., Hu, O. Y., Yeh, C. H. and Fang, J. Y. (2006). "Submicron lipid emulsion as a drug delivery system for nalbuphine and its prodrugs." J Control Release. 115: 140-149.

Ward, A. F. M. and Tordai, L. (1946). "Time-Dependence of Boundary Tensions of Solutions I. The Role of Diffusion in Time-Effects." J Chem Phys. 14: 453.

Warner, R. R., Myers, M. C. and Taylor, D. A. (1988). "Electron probe analysis of human skin: determination of the water concentration profile." J Invest Dermatol. 90: 218-224.

Wartewig, S. and Neubert, R. H. (2007). "Properties of ceramides and their impact on the stratum corneum structure: a review. Part 1: ceramides." Skin Pharmacol Physiol. 20: 220-229.

Williams, R. O., 3rd and Liu, J. (1999). "Formulation of a protein with propellant HFA 134a for aerosol delivery." Eur J Pharm Sci. 7: 137-144.

Winterhalter, M. and Helfrich, W. (1988). "Effect of Surface Charge on the Curvature Elasticity of Membranes." J. Phys. Chem. 92: 6865-6867.

Winterhalter, M. and Helfrich, W. (1992). "Bending elasticity of electrically charged bilayers: coupled monolayers, neutral surfaces and balancing stress." J. Phys. Chem. 96: 327-330.

Winterhalter, M. (1995). "On the molecular origin of the bending elastic moduli." Progr Colloid Polym Sci. 98: 271-275.

Yorek, M. (1993). "Biological Distribution". Phospholipids Handbook. G. Cevc (eds.). New York. Marcel Dekker Inc. 745-776.

Yoshida, N. H. and Roberts, M. S. (1993). "Solute molecular size and transdermal iontophoresis across excised human skin." J Control Release. 25: 177-195.

Zhelev, D. V. (1998). "Material property characteristics for lipid bilayers containing lysolipid." Biophys J. 75: 321-330.

Zhou, Y. and Raphael, R. M. (2005). "Effect of salicylate on the elasticity, bending stiffness, and strength of SOPC membranes." Biophys J. 89: 1789-1801.

Zhou, Y. and Raphael, R. M. (2007). "Solution pH alters mechanical and electrical properties of phosphatidylcholine membranes: relation between interfacial electrostatics, intramembrane potential, and bending elasticity." Biophys J. 92: 2451-2462.

APPENDIX I: LIST OF TABLES

APPENDIX II: LIST OF FIGURES

APPENDIX III: ABBREVIATIONS

ADME	Absorption, distribution, metabolism, excretion
B	Bupivacaine
$C_{18:1}EO_{20}$	Polyoxyethylene (20) oleyl ether
CAC	Critical aggregate concentration
CMA	Membrane adaptability measurement
CMC	Critical micelle concentration
COX	Cyclooxygenase
Cryo-TEM	Cryo transmission electron microscopy
CUM2	Cumulant analysis of second order
DLS	Dynamic light scattering
ECL	Effective chain length
EO	Polyoxyethylene
EP	European Pharmacopoeia
EPC	Egg-yolk phosphatidylcholine
EtOH	Ethanol
HLB	Hydrophile-lipophile balance
IAM	Immobilized artificial membrane
K	Ketoprofen
LUV	Large unilamellar vesicles
n.a.	Not available
NSAID	Non-steroidal anti-inflammatory drug
PC	Phosphatidylcholine
PCS	Photon correlation spectroscopy
PCTE	Track etched polycarbonate membranes
POPC	Palmitoyl oleyl phosphatidylcholine
QSAR	Quantitative structure activity relationship
S	Surfactant
SDS	Sodium dodecyl sulphate

S_{kin}	Kinetic measurement of lipid bilayer solubilisation
SLS	Static light scattering
SOPC	Stearly-oleyl-phosphatidylcholine
SPC	Soy bean phosphatidylcholine
S_{step}	Stepwise measurement of lipid bilayer solubilisation
SUV	Small unilamellar vesicles
TDDS	Transdermal drug delivery systems
TL	Total lipid mass (w-%)